Deterministic modelling of kinetics and radiobiology of radiation-cisplatin interaction in the treatment of head and neck cancers

Loredana G. Marcu

A thesis submitted for the degree of
Doctor of Philosophy
in the School of Chemistry and Physics
University of Adelaide

September 2004

Table of Contents

List of Figures

List of Pictures

List of Tables

Abstract

One of the main objectives of combining radiation treatment and chemotherapy is to obtain a therapeutic gain by an improved tumour control with less or no enhancement of normal tissue toxicity. The optimal schedule for the combined treatment of cisplatin-radiation is still under investigation. Neither the optimal time interval, nor the most adequate sequence of administration of cisplatin and radiation are known. The results of the trials are also inconclusive. Some trials showed a supra-additive effect from the administration of cisplatin before radiotherapy, others, on contrary, from the injection of drug after radiotherapy.

The present work encompasses the major challenges brought by the combined modality treatment: cisplatin-radiotherapy. The major goal of this work was to investigate the optimal treatment sequencing between cisplatin and radiotherapy and also the optimal schedule for head and neck carcinomas. Therefore, a computer-based tumour model with literature-given biological parameters has been developed which has allowed the simulation of treatment with radiation and chemotherapy. Radiotherapy has been simulated on the virtual tumour and the effects of radiotherapy on tumour regression and regrowth have been analyzed. Also, the mechanisms of cisplatin's action on tumour have been implemented, and the phenomena of drug resistance and tumour repopulation during chemotherapy studied. Finally, the combined modality treatment has been simulated, and the effect of drug-radiation interaction on tumour behaviour evaluated.

The current investigation has shown that cisplatin administered immediately before radiation gives similar tumour control to the post-radiation sequencing of the drug. Furthermore, the killing effect of the combined modality treatment on tumour increases with the increase in cell recruitment. The individual cell kill produced by cisplatin and radiation leads to an additive-only tumour response when the treatments are given concurrently, and for a synergistic effect cisplatin must potentiate the effect of radiation. The final conclusion, by which cisplatin

administered on a daily basis leads to a better tumour control than cisplatin administered weekly, is in accordance with the latest trial results on head and neck cancers. Therefore, treatment regimens that correlate better with the pharmacokinetics and the radiobiological properties of the therapeutic agents result in better outcomes.

Thesis Statement

This work contains no material which has been accepted for the award of any other degree or diploma in any university or other institution and, to the best of my knowledge and belief, contains no material previously published or written by another person, except where due reference has been made in the text.

I give consent to this copy of my thesis, when deposited in the University Library, being available for loan and photocopying.

Signed:

……..

Dated:

……..

Acknowledgements

I am totally indebted to Dr. Rod Crewther, who supported my scholarship application to undertake this PhD with the University of Adelaide. This meant the world to me.

I am equally obliged to the Royal Adelaide Hospital, who has accepted me as a doctoral candidate, especially to Assoc/Prof Tim van Doorn, who was also my principal supervisor during these years. First of all, I have to thank you for giving me the opportunity to undertake my research in such an exciting area as radiobiology. I am grateful for your support during my work, for your guidance, for the valuable meetings we had, for being patient while going through my manuscripts, over and over again. I have learnt a lot from you and I thank you, Tim, for that.

During my candidature, I had the chance to work with Dr Sergei Zavgorodni (now at British Columbia Cancer Agency, Canada), one of the most knowledgeable physicists I have ever met. Thank you, Sergei, for your encouragements, for always making time for discussions, and for all the help you gave me in those two years. For the second half of my candidature I had Dr Eva Bezak as a co-supervisor, and I am grateful for that. Thank you, Eva, from my heart, for being a precious adviser, a truthful colleague, and a great friend. I am also indebted to Professor Ian Olver, who put me on the right path, giving me valuable information, and sharing his precious time whenever I needed his help.

Thank you, Ralph, for the folder with the chemo-papers you generously gave me at the very beginning when I was still confused about the avenue I was going to follow in my research. Those few papers were worth more than anyone would think.

I would have never thought that I'll have the opportunity to learn and work independently with cell line cultures in such a short time. I am fully obliged to Dr Bruce Lyons, who made this possible, and I am thanking him for being such a patient teacher, and such a great friend.

I wish to express my gratitude to Dr Eric Yeoh for being part of our radiobiology group and for his contribution to my research. I also wish to thank Dr John Patterson for sharing the office with me, and for the enormous support he gave me during my candidature. John, you were my guardian angel.

I am thankful to the whole Department of Medical Physics for being so friendly, especially to Christine, the greatest secretary I have ever met, and to Kurt for sharing his knowledge of TLD's with me. Thank you, Margaret, for providing continuous IT assistance, enabling the smooth run of my program and data processing.

I wish to acknowledge the friendly staff from the School of Chemistry and Physics, particularly Dr Judith Pollard for her dedication as a teacher, also Irene and Dallas for their continuous support and friendship which I highly appreciate. Thank you, Setayesh, for your encouraging words and for the constructive discussions we had in these years.

Dave, you are my hero. It is hard to express in words how grateful I am for you being my pillar all this time. Without you, this work would not have seen the light of day. Alex, my little love, you were Mummy's mental break, keeping me entertained all the way through, while watching you grow along with my work. Although from far away, I was constantly encouraged and supported by my Mother and Brother. I thank God for having you all. Love you always.

Adelaide

13th of September 2004

Publications and presentations

Publications in refereed journals

L. Marcu, E. Bezak, I. Olver, T van Doorn, Tumour resistance to cisplatin: a modelling approach, *Physics in Medicine and Biology* 2005; 50:93-102.

L. Marcu, AB Lyons, E. Bezak, T van Doorn, The mechanisms and the onset of accelerated repopulation of radiotherapy stimulated squamous cell carcinoma, *Austral-Asian Journal of Cancer* 2004; 3:167-171.

L. Marcu, T van Doorn, I. Olver, Modelling of post irradiation accelerated repopulation in squamous cell carcinomas, *Physics in Medicine and Biology* 2004; 49:3767-3779.

L. Marcu, T van Doorn, I. Olver, Cisplatin and radiotherapy in the treatment of locally advanced head and neck cancer: a review of their cooperation, *Acta Oncologica* 2003; 42:315-325.

L. Marcu, T van Doorn, I. Olver, S. Zavgorodni, Growth of a virtual tumour using probabilistic methods of cell generation, *Australasian Physical and Engineering Sciences in Medicine* 2002; 25:155-161.

Submitted papers in refereed journals

L. Marcu, T van Doorn, E. Bezak, Determination of cell cycle phase-specific α parameters for squamous cell carcinomas of the head and neck, *International Journal of Radiation Oncology Biology Physics*, 2004.

L. Marcu, E. Bezak, I. Olver, T van Doorn, Scheduling cisplatin and radiotherapy in the treatment of squamous cell carcinomas of the head and neck: a modelling approach, *International Journal of Radiation Biology*, 2004.

Conference presentations

L. Marcu, T van Doorn, E. Bezak, I. Olver, Tumour resistance to cisplatin: a modelling approach, *MOT Meeting, Adelaide,* May 2004.

L. Marcu, AB Lyons, T van Doorn, E. Bezak, The mechanisms and the onset of accelerated repopulation of radiotherapy stimulated squamous cell carcinoma, *MOT Meeting, Adelaide*, May 2004.

L. Marcu, T van Doorn, I. Olver, Cell recruitment in tumour regrowth during radiotherapy: a modelling approach, *WC2003, Sydney*, August 2003.

T van Doorn, **L. Marcu**, I. Olver, S. Zavgorodni, Inter-relation of biological parameters in the computer simulation of the temporal development of a head and neck tumour, *ICTR, Lugano,* Switzerland, March 2003.

L. Marcu, T van Doorn, I. Olver, S. Zavgorodni, Recruitment and stem cell cycle duration in accelerated repopulation of radiotherapy stimulated squamous cell carcinoma, *ICTR, Lugano*, Switzerland, March 2003.

L. Marcu, T van Doorn, I. Olver, S. Zavgorodni, Monte Carlo simulation of the radiotherapy of a virtual head and neck tumour, *EPSM, Rotorua,* New Zealand, November 2002.

L. Marcu, T van Doorn, I. Olver, S. Zavgorodni, Computer simulation of tumour growth and cellular phase distribution prior to chemoradiotherapy, *EPSM, Fremantle,* September-October 2001.

L. Marcu, T van Doorn, I. Olver, Daily versus weekly administration of cisplatin in combined chemoradiotherapy, *AIP Conference, Adelaide*, December 2000.

Other presentations

L. Marcu, Accelerated repopulation of radiotherapy stimulated squamous cell carcinoma, *ACPSEM student night*, October 2003.

"First prize for the best postgraduate paper presentation"

L. Marcu, Radiotherapy treatment of a virtual head and neck tumour by Monte Carlo simulation, *ACPSEM student night*, October 2002.

"Second prize for the best postgraduate paper presentation"

L. Marcu, Computer simulation of tumour growth and cellular phase distribution prior to chemoradiotherapy, *ACPSEM student night*, September 2001.

"First prize for the best postgraduate paper presentation"

In memory of my Father

Chapter 1

General introduction

1.1. Challenges in the combined chemo-radiotherapy

1.1.1. Introduction

One of the main objectives of combining radiation treatment and chemotherapy is to obtain a therapeutic gain by an improved tumour control with less or no enhancement of normal tissue toxicity. Therapeutic gain is defined by Steel (1988) as a combination of drugs and radiation that gives a superior tumour response to either of the components alone, with comparable level of toxicity. Such therapeutic gain may be attained by exploiting one of the following modes of action (Steel 1988):

- Enhancement of tumour response
- Normal tissue protection
- Independent cell kill
- Spatial cooperation.

The majority of experimental studies show that the last two ways of action rather than enhancement of tumour response or normal tissue protection are most likely to lead to a therapeutic gain. Both increased tumour response and better normal tissue control have been observed in experimental studies, but none of them had clinical implications (von der Maase 1994).

Spatial cooperation indicates that the two treatment modalities (chemo and radiotherapy) affect different tumour sites. Usually, radiotherapy is administered to the primary tumour, while chemotherapy affects the metastatic disease. Also, when there is no spread of the cancer, chemotherapy can be efficient on the primary site, complementing the effect of radiation.

With independent cell kill, therapeutic gain can only be achieved if the toxicities resulting from the two treatments do not overlap. For example, several chemotherapeutic agents with cell-cycle specific properties are cytotoxic to the synthetic phase, which is known to be the most radioresistant. Independent cell kill can also be achieved from the cooperation of radiation and drugs which are cytotoxic under hypoxic conditions.

The overall effect expected from the combined modality treatment to achieve therapeutic advantage should be supra-additive. However, in numerous chemo-radiotherapy trials, the results were only additive, or even sub-additive (Dewit 1987), illustrating the crucial role of timing between therapies to achieve better tumour control.

Drug-radiation interactions, both in normal and in cancerous tissues, are very complex. Their interaction depends on several factors, which ultimately dictate the therapeutic ratio:

- Drug regimen
- Radiation schedule
- Timing between chemo and radiotherapy
- Tissue type.

1.1.2. Cisplatin and radiotherapy in combined modality treatments

The first evidence for interaction between cisplatin and radiation originated from Zak and Drobnik (1971) who observed an increase in the probability of tumour control in mice by the drug when combined with whole body irradiation. It was suggested that the outcome resulted in a 'greater-than-additive' tumour cell killing.

In the late seventies, more studies on the combined modality treatment were undertaken on bacteria, followed by experiments in cultured mammalian cells. Despite some inconsistencies in observations among various investigators, even in the same cell line, there was a common observation reflecting the shoulder reduction of the X-ray dose response curve by cisplatin. Some authors have attributed this reduction of the shoulder to an inhibition of sublethal damage repair (Dewit 1987). With the experiments on murine tumours came the first convincing evidence for supra-additive effects of cisplatin and radiation (Douple 1979).

Results from clinical trials, though sometimes inconsistent (Chapter 2), reveal that there are survival benefits from the combined treatment in comparison to radiation alone. However, it is not clarified whether the benefit is primarily due to potentiation of radiation or to additional cell kill by cisplatin.

1.1.3. Scheduling and sequencing cisplatin-radiotherapy

The optimal schedule for the combined treatment of cisplatin-radiation is still under investigation. Neither the optimal time interval, nor the most adequate sequence of administration of cisplatin and radiation are known. Some trials showed a supra-additive effect from the administration of cisplatin before radiotherapy, others, on contrary, from the injection of drug after radiotherapy (Chapter 2). However, it was shown that for the best therapeutic response, the

administration of cisplatin should be immediately before or after radiation (Coughlin 1989).

1.2. The need for modelling in cancer treatment

Pursuit of an enhanced treatment regimen is conventionally performed through a range of controlled clinical trials, each trial potentially isolating a single parameter and evaluating its significance. Clinical trials are indispensable prerequisites to establish novel therapeutic principles. However, trials are lengthy processes which involve several determining factors for their success: trial design, patient selection, patient follow-up, compelling data analysis and interpretation. Furthermore, trials cannot certainly forecast the outcomes, neither can they explore the sensitivity of the outcome to input parameters and covariates.

Models can overcome some of the limitations encountered by trials, by predicting the outcome of a lengthy treatment in short time and also by determining the relationships between the input parameters and the outcome. Beside animal models and cell lines, which are often used for pre-clinical studies, there are models encompassing mathematical, physical and engineering concepts representing the biological world. Such concepts are implemented into mathematical or computer models, artificial neural networks or algorithmic models.

Models in cancer treatment are simplified tools to reproduce the biological world. Therefore they do not reflect accurately the fine details of the real systems. Also, when host response or the presence of tumour microenvironment is needed for particular outcomes, models are operationally limited.

To compensate for some of its deficiencies, the approach of computer modelling has several advantages. Kinetic parameters can be easily changed and results rapidly obtained. Furthermore, various mechanisms can be studied in isolation, determining their impact on specific processes (e.g. cell recruitment and the effect

on tumour repopulation). Extreme values for different parameters may be considered, and limiting factors determined for biologically valid results (e.g. short cell cycle times after radiotherapy).

Computer models can be used to simulate tumour cell kinetics and dynamics, drug pharmacokinetics, therapies, and give similar results to those in experimental tumours. Models are needed to open further research avenues and to suggest relationships between radiobiological parameters.

1.3. Aims of current investigation

This work encompasses the major challenges brought by the combined modality treatment: chemo-radiotherapy. With a particular focus on cisplatin, and on one of the most responsive cancers to the combined cisplatin-radiotherapy – head and neck, the present work simulates the treatment of the squamous cell carcinomas of the head and neck when cisplatin and radiotherapy are used concurrently.

The initial study, which was undertaken on various trials on cisplatin-radiotherapy for head and neck cancers, has shown that many questions concerning the combined modality treatment are unanswered. In order to bring light on some of the challenges encountered, a virtual tumour simulating the biological properties of a head and neck cancer has been developed by computer-based probabilistic methods. The tumour has then been treated with radiotherapy as a sole treatment, and also with cisplatin, followed by the combined modality treatment. The current work brings together the radiobiological properties of radiation and also the major characteristics of cisplatin, in a modelling process which reflects the interaction between drug and radiation.

The aims of the current investigation were the following:

- To uncover the challenges in the combined modality treatment for head and neck cancers

- To develop a computer-based tumour model with realistic biological parameters, that would allow simulation of treatment with radiation and chemotherapy
- To simulate radiotherapy on the virtual tumour and analyse the effects of radiotherapy on tumour regression and regrowth
- To investigate the mechanisms responsible for tumour repopulation after radiotherapy
- To implement the mechanisms of action of cisplatin, to simulate and analyse the effect of cisplatin on the virtual tumour
- To investigate the effect of drug resistance on tumour response
- To examine the process of tumour repopulation after chemotherapy
- To simulate the combined modality treatment: cisplatin-radiotherapy on the virtual tumour and to analyse the effect of the treatment on tumour behaviour
- To investigate the optimal treatment sequencing between cisplatin and radiotherapy and also the optimal schedule for head and neck carcinomas.

1.4. Thesis outline

Chapter 1 presents the challenges encountered by the combined modality treatment and the need to address some of the problems through a modelling approach. The aims of the current investigation are also presented.

An analysis of the existing clinical trials on head and neck carcinomas using cisplatin in combination with radiation is presented in Chapter 2. The main challenge in the combined modality treatment regarding the sequencing and scheduling of drug and radiation is highlighted.

Chapter 3 describes the tumour growth model which has been developed using stochastic methods of cell production. The kinetic properties of the virtual tumour are also described.

A simulation of radiotherapy on the previously grown tumour is undertaken in Chapter 4, and tumour regression and regrowth studied. The onset of repopulation and also the mechanisms responsible for accelerated repopulation after radiotherapy are modelled and discussed.

Chapter 5 presents the effect of cisplatin on tumour regression. The main kinetic properties of cisplatin are implemented into the computer model and drug resistance is also analysed. Tumour repopulation after chemotherapy is discussed and the effect on tumour control compared with drug resistance. Various schedules for cisplatin as a sole treatment are presented and the optimal schedule highlighted.

The combined modality treatment with cisplatin and radiation is modelled in Chapter 6. The optimal timing between drug administration and radiotherapy is investigated and the mechanism of radiation potentiation by cisplatin is also analysed. Daily as well as weekly treatments with cisplatin with concurrent radiotherapy are simulated and the results compared with those given by clinical trials.

The final chapter, Chapter 7, is a compilation of the main conclusions drawn by the current investigation.

Chapter 2

Cisplatin and radiotherapy in the treatment of locally advanced head and neck cancer: a review of their cooperation

2.1. Introduction

Head and neck cancer constitutes approximately 12% of all cancers. Over 95% are squamous cancers and 4-5% are salivary gland carcinomas or melanomas. With locally advanced head and neck cancer the relapse rate is 50-60% within 2 years and 20-30% develop distant metastases (Vikram 1984). Therefore there is scope for improved outcomes of head and neck cancer treatment through consideration of biological responses to combined modality therapies. The current most commonly used treatment is combined chemo/radiotherapy with a single or multiple chemotherapeutic agents.

Early studies of chemotherapy (1960s and 1970s) in head and neck cancers involved mainly patients with recurrent or metastatic disease treated either with a single agent or with multiple chemotherapeutic agents. Chemo-radiotherapy has been used in the 1980s with chemotherapy as a neoadjuvant treatment for advanced stages of the disease. Concurrent chemoradiation has been introduced in the 1990s, with many recently reported trials using the simultaneous treatment as a standard care for advanced head and neck cancer patients (Harari 2003).

However, objective analysis of an optimal treatment regimen is complicated by the multiplicity of drugs and their interactions with the ionising radiations. In an

attempt to provide greater insight, the following treatise focuses on the merits of trials utilising one chemotherapeutic agent: cisplatin (Rosenberg 1965).

As a single therapeutic agent, the clinical results with cisplatin are quite poor in advanced head and neck cancer, despite demonstrated effectiveness *in vitro*. Radiotherapy alone has an impact on the short term prognosis of advanced head and neck cancer but the long-term benefits have been moderate (Jeremic 1997, Tannock 1998).

The majority of the trials using combined chemo-radiotherapy for locally advanced head and neck cancer have presented some promising results. Current trials tend to administer the drug on a daily basis, concurrently with radiation, leading to improved long-term benefits and better tolerated treatment (Choi 1997, Jeremic 2000).
Of the numerous clinical trials examined for this study, only 16 of them combined chemo-radiotherapy and met the following selection criteria:

- cisplatin should be the sole chemotherapeutic agent in combination with radiation,
- the patients should have unresectable squamous cell carcinomas of the head and neck (stage III or IV) with no recurrent disease or distant metastases, and
- the patients should not have received previous treatment for the same malignancy.

These clinical studies indicate that treatment related parameters (drug dose, route of administration, delivery time, radiation dose, fractionation type, timing between radiation and drug delivery, overall treatment time) and the disease related parameters (tumour stage, nodal stage, tumour resistance) are crucial to the success of the treatment.

2.2. Cisplatin as a therapeutic agent

As described in more details in Chapter 5, there are 5 major characteristics that are considered to be responsible for the cytotoxic effects of cisplatin: radiosensitiser - through the inhibition of the repair of potentially lethal damage and sublethal damage, hypoxic cell sensitiser, cell-cycle perturbator, an ability to form DNA adducts and, suppression of tumour neovascularization.

Cisplatin has the ability to form both intrastrand and interstrand adducts with DNA (Prestayko 1980). Although the number of interstrand cross-links is less than 1% of the total adducts, Reed and Kohn (1990) consider this type of adduction responsible for the cytotoxic effect of cisplatin. The *trans* isomer (with the chlorine atoms located across the platinum complex), transplatin, has proved to be inactive on tumour cells (Kohn 1990) as it cannot be linked interstrand to the DNA, but can form intrastrand adducts.

2.2.1. Cisplatin as a single therapeutic agent

The table in Appendix A presents the schedules and results for a number of different trials in which cisplatin was administered alone. Although some of these trials (Creagan 1983, Jacobs 1978, Sako 1978, Veronesi 1986) have shown cisplatin to be equally effective as radiotherapy alone, the trials were undertaken primarily with recurrent diseases and the obtained results were poorer than for some previously untreated tumours. This has led to the administration of this platinum compound mainly for palliation.

Cisplatin has been delivered either in the range 80-120 mg/m^2 or 20-60 mg/m^2. In Veronesi's trial (1986), the tumour response and normal tissue toxicity were compared after high-dose infusion (120 mg/m^2) given every 3 weeks for 2 cycles and also after low dose infusion (60 mg/m^2) following the same schedule. While the tumour response was the same, the higher dose resulted in a greater toxicity and necessitated more extensive patient hydration. Similar overall responses were

achieved by Sako (1978) with 15 minute infusion of 20 mg/m^2 for 5 days, administered every 3 weeks to a group of patients, and a high-dose regimen of 120 mg/m^2 every 3 weeks to another group. In contrast, however, toxicity was found to be minimal (Jacobs 1978), or moderate and better tolerated (Creagan 1983) when low doses of cisplatin were administered by 24 hour infusion. These results are in agreement with the ototoxicity study by Vermorken (1983) and suggest that a daily slow infusion of a low-dose is preferable to a bolus, or fast, high-dose administration.

2.2.2. Cisplatin followed by radiotherapy

A phase II study of weekly high-dose cisplatin and radiotherapy delivery, given in two separate schedules was conducted by Planting (1997) on 59 patients with previously untreated, locally advanced, head and neck tumours. The chemo-treatment time was 6 weeks, with weekly 80 mg/m^2 cisplatin infused over 3 hours. Following the administration of cisplatin, 47 patients received conventional radiotherapy with 1.8-2 Gy daily doses for a further 6-7 weeks. In as much as neither chemotherapy alone nor radiotherapy alone could show significant improvements in survival, the end points of this concomitant schedule study were also inferior (32 weeks progression-free survival and 56 weeks overall survival) to those reported for the concurrent regimens (Appendix B).

2.2.3. The interplay of cisplatin and radiation

The chemical reactivity of cisplatin is determined by the chloride groups situated in the cis-position of the platinum complex. Cisplatin's radiosensitizing property is due to its affinity for the thermalised electron created by radiation induced ionisation within the DNA molecule. This affinity obstructs the recombination with the positive hole (Prestayko 1980) and may lead to irreparable damage to the DNA (Dewit 1987). This inhibition of sublethal damage repair (SLDR) by cisplatin was demonstrated by experiments on oxic mammalian cells (Coughlin

1989) and also by experiments conducted, in vivo, on human squamous cell carcinomas of the head and neck (Sharma 1999).

Cisplatin also has the ability to arrest cells in the G2 phase of the cell cycle and, eventually, induce their death. For concentrations greater than 2 μg/mL, cisplatin suppresses the DNA synthesis of L1210/0 cells (Sorenson 1988, 1990). After 4 days the cell membrane integrity is lost leading to cell death. For lower concentrations of cisplatin, the cells are just transiently blocked in the G2 phase, up to 48 hours, and after this period they regain their viability. This same DNA degradation process may be expected to occur in human tumour cells as the concentrations used in clinical chemotherapy are significantly higher than those in the above in-vitro experiments.

It is difficult to appreciate which property is predominant as some properties are more strongly manifested in bacterial systems (free radical scavenging) and others in cultured mammalian cells (SLDR inhibition) (Coughlin 1989). Whether the same characteristics are evident for humans remains one of the open questions in combined modality treatment.

2.3. Schedules for concurrent cisplatin-radiotherapy

Appendix B is a compendium of the limited number trials and studies on combined cisplatin-radiation that satisfy the previously described selection criteria. The table includes the general regimen for each trial, showing separately the schedules for radiotherapy and the cisplatin. Treatment end-points, including complete response, partial and/or overall response, and normal tissue toxicity are also tabulated. The sites of cancer were mainly the oral cavity, oropharynx, larynx or hypopharynx, with some trials including nasopharyngeal cancers as well.

With the consideration that every patient had advanced disease, most of the above trials and studies had positive results, both in term of complete response and long-

term benefit. Due to the high toxicity of cisplatin, the side effects were mainly anticipated, although in some trials the complications exceeded the expectations (Clamon 1996, Huguenin 1998). In other cases, interruptions in treatment were necessary because of excessive toxicity (Al-Sarraf 1987, Choi 1997, Jeremic 1997).

The majority of studies had adopted either daily or weekly cisplatin combined with either conventional or hyperfractionated radiotherapy, keeping a constant chemo and radiation dose administration regimen throughout the treatment. However, one regimen was developed (Harrison 1991) whereby the schedule was adjusted to take into consideration the tumour proliferation that occurs after approximately 4 weeks of therapy. The treatment was started with conventional radiotherapy with concomitant cisplatin and continued for 4 weeks, followed by another 2 weeks, with radiation twice per day, almost doubling the radiation dose (1.8 Gy/fraction for 4 weeks and 1.8 Gy/fraction-morning and 1.6 Gy/fraction-night for the last 2 weeks). With this schedule, the complete response of 64% was as high as in other trials with less advanced disease [RTOG group (Crissman 1987)].

Examination of the end points from the table of Appendix B indicates there are many trials with very similar responses (complete response between 70%-78%) even though the treatment protocols were different. Both conventional and hyperfractionated radiotherapy were used with similar results and also weekly and daily cisplatin administration were comparable. However, as illustrated by some studies, the response rates may not be the best predictors of treatment efficacy. For example, with weekly delivery of high-dose cisplatin and conventional radiotherapy Fountzilas (1994) achieved a complete response of 72%, identical to Jeremic's (1997) response rate with daily low-dose cisplatin. Similarly, Gasparini (1991) and Glaser (1993) both have the same 75% complete response in their studies, using conventional radiotherapy and a single weekly dose of cisplatin, with the same patient selection. In Gasparini's (1991) schedule cisplatin was administered 2 hours after radiotherapy and in Glaser's protocol, 3-4 hours before irradiation. In two different studies, using the same administration for the drug but different schedules for the radiation, Jeremic (1997, 2000) completed the

treatments with similar results: 72% complete response when conventional radiotherapy was used and 75% complete response with hyperfractionation. Furthermore, Robbins (1997) undertook a phase II study in which 85% of the patients completed a targeted supradose cisplatin and concurrent radiotherapy protocol (called the RADPLAT protocol), using intra-arterial delivery. The complete response for this study was 75%, as in many other intravenous trials. However, the 3 year overall survival of 60% was significantly higher than the 47% figure reported by Choi (1997) although he had an initial complete response of 94% (with mainly nasopharyngeal patients). This indicates that the tumour response is not necessarily the most relevant end point. Robbins (1997) went on to explain that rapidly responding tumours might undergo rapid repopulation while slower regressing ones may be more sensitive to therapy regarding their future proliferation.

Locoregional control has been shown to be a more accurate indicator of the long-term tumour control than the complete response (Huguenin 1998, Jeremic 2000, Serin 1999). Huguenin, using a hyperfractionated radiation regimen with simultaneous cisplatin, achieved a local control at 5 years of 74%. A similarly good result was obtained by Serin (1999), with 90% of patients having a complete locoregional response, the locoregional failure-free survival at three years being 79%. However, patient selection can be the reason for the high response in Serin's phase II study, as all patients presented with nasopharyngeal cancer, though in locally advanced stages. With a hyperfractionated radiation given concurrently with daily low-dose cisplatin Jeremic (2000) achieved 5-year locoregional progression-free survival in 50% of the patients.

2.3.1. Toxicity associated with combined treatment schedules

It is essential in correctly defining the end points that the toxicities of the different schedules are also taken into account. Most of the studies in table 2 have used the Common Toxicity Criteria adopted by the National Cancer Institute. However, in a recent article, Trotti (2000) underlined the fact that the differentiation between

the various grades of toxicity is difficult even for experienced examiners in some cases. The goal therefore is still to assure greater data accuracy through standardisation of the collected data.

One of the most affected organs by cisplatin administration is the kidney. For every schedule using high dose cisplatin, either combined with conventional fractionated or hyperfractionated radiotherapy, the nephrotoxicity was substantial (grade III or IV), even though, overall, the treatments were well tolerated. All of the patients that suffered renal failure or nephrotoxicity-related death were participating in trials that used high doses of cisplatin (100mg/m^2) every second or third week (Al-Sarraf 1987, Fontanesi 1991, Harrison 1991, Marcial 1990). Other studies with lower renal toxicity exhibited other significant side effects. Gasparini (1991) could not deliver a whole course of chemotherapy for 34% of the patients because of the high-grade stomatitis. Fountzilas (1994) similarly had to deal with considerable weight loss in half of his patients.

Robbins (1997) conducted a trial in which the selected drug route was intra-arterial rather than intravenous with the aim of delivering a higher concentration of drug (150mg/m^2) directly into the tumour and sparing of the normal tissues. However, overall, 42% of patients still had grade III or IV toxicities.

Daily low-dose cisplatin has been better tolerated in several studies (Bachaud 1997, Jeremic 1997, 2000, Leipzig 1983). Choi et al. (1997) have also used the daily low-dose cisplatin schedule, and planned interruptions during the treatment to prevent excessive toxicity. As a result, there were no renal failures or nephrotoxicity related deaths.

Variable late toxicity (post treatment) effects have been reported by a few trials. Marcial et al. (1990) have evaluated the late toxicities in the 72% of treated patients that achieved a complete response, reporting 3% with necrosis, 4% with fibrosis and 8% with other toxicities (otitis, paresthesia, dental caries). Choi et al. (1997) have reported minimal late toxicity consisting of mild fibrosis, xerostomia, otitis and dental caries with no severe toxicities being reported at follow-up. Late high-grade toxicity was observed in Jeremic's (2000) trial where xerostomia was

manifested in 22% of the patients and subcutaneous toxicities in 12% of the patients after receiving combined treatment.

2.4. Chemoresistance and radioresistance

Many tumours have a high initial response to chemotherapy, which diminishes or disappears during the course of therapy (Jakobsen 1997) (chemoresistance) that represents an obstruction in achieving long-term remission or cure (Coldman 1985). The causes of chemoresistance are various and are still under investigation. The drug type, the administered dose and the timing of the drug delivery are elements that can influence the tumour response during the treatment period (Birkhead 1986). Tumour chemoresistance is indicated by decreased drug uptake and increased DNA repair (de Graeff 1988, Perez 1998) that can be linked to the low-doses of cisplatin delivered.

Whether a drug-resistant tumour remains resistant even for high doses of cisplatin was clinically studied by Robbins et al (1996) through a tenfold increase in the administered dose. The doses used in this trial ranged from 32.5 mg/m^2 to 200 mg/m^2 per week, and to overcome toxicity, cisplatin was delivered through intra-arterial infusion with simultaneous intravenous administration of sodium thiosulfate as neutralising agent. The tenfold increase of drug dose ("decadose") showed a significant improvement in overcoming drug resistance, the results being positive even for recurrent cancers.

Experimental studies with substances like LipoAmph B (a liposomal preparation of Amphotericin B) (Ferguson 1999) were able to increase the platinum intake by human cell lines, when administered concurrently with cisplatin, thus increasing cisplatin toxicity. The study was completed on a head and neck squamous cell carcinoma line and synergism between the two drugs was indicated by an enhancement in cytotoxicity from 35% to 60%.

In clinical radiotherapy, it has been demonstrated that various tumours have the ability to regrow within the irradiated region independently of their regression rate (Peters 1982). This phenomenon leads to tumour radioresistance and it is multifactor dependent. Peters et al. (1982) examined 4 main causes of clinical radioresistance: tumour related factors (hypoxia, the number of clonogenic cells, tumour kinetics), host related factors (defence, the volume effect, dose-limiting normal tissue), technical factors (geographic miss, errors in dose delivery) and probabilistic radioresistance. The tumour-related factors are common for both drug resistance and radioresistance. The so-called cross-resistance is one of the most debated problems in combined treatment, as many tumours resistant to one agent easily become resistant to the other. Unfortunately, cisplatin-resistant head and neck tumours are generally radioresistant too (Wallner 1987). Hypoxia plays an important role in tumour resistance, to both cisplatin and radiation. Novel hypoxic cell sensitizers, like tirapazamine, have improved the cytotoxic effect of cisplatin and radiation when administered concurrently (Lartigau 2000). Dorie et al (1999) have measured the DNA damage mediated by tirapazamine in hypoxic head and neck tumours, concluding that the drug is activated by the poorly oxygenated environment, leading to radioresistant-cell kill. An extensive head and neck cancer trial is currently undergoing among the Australian hospitals (Rischin 2001) where the efficacy of tirapazamine, when combined with cisplatin and radiotherapy, is assessed.

Also to overcome the radioresistance due to hypoxia, Peters et al (1997) developed a specific drug administration that differed from the other schedules by the drug timing. They sustained the idea that drug delivery should be deferred until the final weeks of the treatment “as late intensification”.

2.5. Theory versus practice

Table 2.1 indicates that, in the past, treatment schedules have not been in full accordance with the clinical, biochemical and physical indicators. Nevertheless, when there is greater correlation between the treatment regimen and these

indicators, the tendency is towards an improved outcome, as can be seen from Jeremic et al's recent trial (2000).

Table 2.1. Theory versus practice.

Theory *(based on in vitro studies)*	*Clinical practice*
The treatment time for HNC should be kept as short as possible because of the rapid repopulation after RT (Begg 1999). The recommended treatment period is 5 weeks (Bartelink 1999).	All treatments discussed in the present review last for more than 6 weeks and up to 8 weeks.
Because of the HN tumour proliferation after beginning radiotherapy, it is not recommended to interrupt the treatment (Withers 1988).	Many treatments were interrupted for 1-2 weeks (for one or more cycles) because of different toxicities, some interruptions being programmed (Choi 1997, Fountzilas 1994) but some not (Gasparini 1991).
The formation of DNA adducts is a fast process (approximately 3.5 hours) and lasts up to 24 hours after 1 hour exposure to cisplatin. After this period most of the DNA adducts have disappeared, which can explain the total absence of an additive effect when cisplatin is given 24h before irradiation (results from *in vitro* experiments on a tumour spheroid, cultured from a HNC patient's tumour) (Schwachöfer 1991).	More than half of the schedules contain high-dose weekly cisplatin, in 2-3 cycles, which is toxic to the normal tissue rather than effective on tumour cells.
Many tumours have the capacity to increase their rate of clonogenic cell replication significantly above pre-treatment levels during the course of radiotherapy (Peters 1997).	Except Harrison's trial (1991) which takes into account that after approximately 30 days HN tumours are proliferating more rapidly than before (adjusted schedule for this case), none of the other studies or trials use such adjustments, or different doses for that certain part of the treatment.

2.6. Discussion

Since Rosenberg's initial discovery, the utilisation of cisplatin has progressed from its early use in isolation in the 70's to a variety of initial forms of combined chemo-radiotherapy in the subsequent decades. While in the 80's and early 90's most of the schedules used high-dose weekly cisplatin administration, in the mid to late 90's daily low-dose infusions were introduced and outcomes have continuously improved.

The cytotoxic effects of cisplatin are attributed to the ability of the drug to form interstrand adducts with cell DNA, to inhibit DNA synthesis resulting in cell cycle arrest, and more recently, to its inhibition of neovascularization.

While these effects are independent of other mediators, cisplatin can also work in cooperation with ionising radiation through its affinity for free electrons resulting in the inhibition of SLDR and increased oxygenation of hypoxic cells resulting in increased radiosensitivity. For this cooperation to be achieved, cisplatin needs to be delivered prior to the application of radiation. Furthermore, the clearance time of cisplatin (24 hrs) requires ongoing administration of cisplatin to sustain the cooperation. Through daily drug administration, all of cisplatin's properties are exploited and this is supported by the superior results obtained by trials using daily administration of cisplatin compared to weekly drug delivery.

The dose limiting toxicities for cisplatin must also be taken into consideration. Renal and hematologic toxicities, and also stomatitis were the most frequently reported dose limiting factors. In a number of trials, a daily cisplatin dose of 6 mg/m^2 was considered to be the upper limit in order to avoid the higher-grade toxicities (Bachaud, 1997, Jeremic 1997, 2000). Even though cisplatin is more toxic than many other anticancer drugs, it has the advantage that its toxicity does not overlap with the radiation-produced side effects. Also, cisplatin induced renal and hematologic toxicities can be overcome by daily low-dose infusion of the drug and the use of antiemetics and hydration to reduce nephrotoxicity. Inevitable

side effects, like stomatitis and xerostomia, disappear after the completion of treatment (unless very high doses of cisplatin are used).

Similarly to drug-dose fractionation (daily administration), the use of accelerated and/or hyper-fractionated radiotherapy has led to better outcomes than conventional radiation treatment. Tumour resistance to chemo/radiotherapy is one of the reasons for treatment failure. Radioresistance is reduced by hyperfractionation and accelerated radiotherapy. While this is still an area for further investigation, this response may reflect the accelerated cell growth ('kick-off') post initiation of treatment with head and neck cancers. Similarly, chemoresistance can be overcome by increasing the drug dose. The disadvantage of increased drug dose is the increase in toxicity. Therefore other alternatives are to use drug combinations or to administer substances like LipoAmph B that are able to increase the platinum intake by the tumour. However, normal tissue toxicity must be considered when discussing long-term disease-free survival or locoregional control.

At present, there is no optimal schedule for treating head and neck cancer and the most efficient and least toxic cisplatin dose has still not been established (Glynne-Jones 2002). However, Jeremic's phase III trial (2000) conducted on patients with advanced head and neck cancers using hyperfractionated radiotherapy and concurrent low-dose daily cisplatin, achieved substantial tumour responses with acceptable normal tissue toxicities and available data are good starting points for further trials.

The optimal timing between drug delivery and radiotherapy remains to be solved by larger and more conclusive trials. Also, the results of clinical trials will be improved by a better understanding of the underlying mechanisms by which chemotherapy enhances the effectiveness of radiation.

The present review has provided foundation for a computerised simulation of treatment schedules of a virtual head and neck tumour (Marcu 2002) (Chapter 3) which, eventually, has served as a basis for a temporal study of the combined chemo-radiotherapy (Chapter 6).

2.7. Conclusions

The aim of the combined chemo-radiotherapy treatment is to achieve a higher therapeutic ratio compared to the single-agent therapy through either a better tumour response or reduced normal tissue damage. The present work has reviewed a selected number of trials for unresectable squamous cell carcinoma of head and neck with cisplatin used as a single chemotherapeutic agent with and without irradiation. Treatment regimens that correlate better with the pharmacokinetics and the radiobiological properties of the therapeutic agents resulted in the achievement of better outcomes although large, conclusive controlled and randomised trials are lacking.

Optimisation of the treatment can be improved through further study and modelling of the pharmacokinetic and radiobiological interactions between cisplatin and radiotherapy.

Chapter 3

Modelling tumour growth

3.1. Elements of cell biology

3.1.1. The cell cycle

Cell division is a basic biological process that results in an increase in somatic cell numbers over time. Mitosis (cell division) is common in both normal cells and tumour cells, however cancer cells grow uncontrollably. In normal tissues there is a balance between cell proliferation, differentiation and cell loss. Conversely, tumours grow because the homeostatic control mechanisms that maintain the appropriate number of cells in normal tissue are defective, leading to an imbalance between cell proliferation and death, which will create an expansion of the cell population.

Cells propagate through an orderly sequence of four phases (Figure 3.1) constituting the cell cycle: mitosis (M) when the cell divides in two daughter cells, the postmitotic phase or the first "gap" (G_1) during which the cell prepares for DNA synthesis, the synthetic phase (S) when the DNA is duplicated and the postsynthetic phase or the second gap (G_2) when the cell prepares for division. Some cellular types, after mitosis, enter a resting phase called G_0. This phase is out of the cell cycle, and the resting (quiescent) cells may remain in G_0 indefinitely or re-enter the cell cycle in response to an external stimulus.

The lengths of the various phases of the cycle have been determined by cytometric measurements (Hall 2000). The only consistent phase-length for different cell lines is the S phase, and commonly represents one third of the whole

cell cycle time while mitosis is the shortest (1-2 hours) and G_1 is the most variable, but usually the longest.

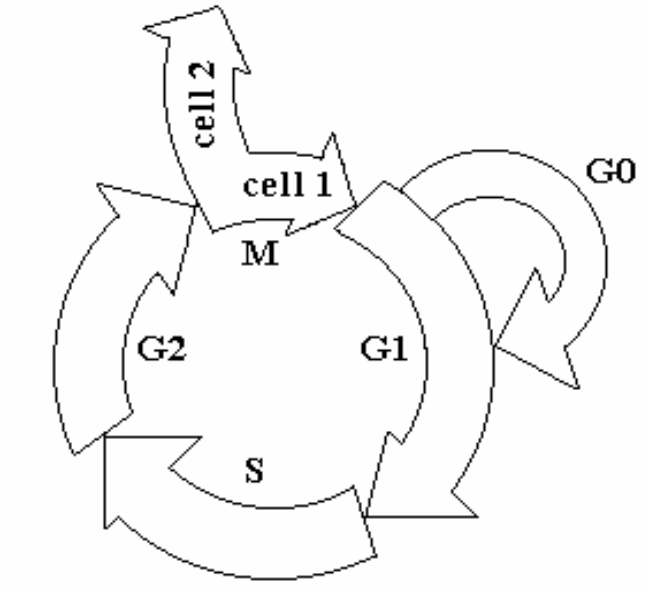

Figure 3.1. Schematic representation of the cell cycle.

Mammalian cell populations usually proliferate in asynchronous growth. Therefore cells will be distributed through the cell cycle phases, however unevenly. The most probable distribution is supposed to be the exponential one, with the largest population in G1 and smallest in mitosis (Hall, 2000).

Depending on their position in the mitotic cycle, cells respond differently to radiation. It was found that, cells are most radiosensitive during and close to M phase, and most resistant in late S phase (Sinclair 1969). Also, cells with longer G1 phases have a resistant peak early in G1. The quiescent cells situated in G0 are also known to be relatively radioresistant (Nias, 2000).

3.1.2. Tumour kinetic parameters

Tumours are complex entities, diverse and heterogeneous, yet all share the ability to proliferate beyond the constraints limiting the growth in normal tissue. The growth of the tumours is best represented by an exponential increase of cell number in time. The exponential growth is the simplest mode of growth assuming

no cell loss or infertility. By growing exponentially, the tumour volume increases by a constant fraction in equal time intervals. Volume doubling time is a kinetic parameter representing the time for the tumour volume to double. The volume doubling time is generally larger than the cell cycle time due to cell loss and cells moving into non-proliferating phase (G0).

Many human tumours during their growth show exponential behaviour, however there are tumours going through irregular or decelerating growth (Steel 1977). A more accurate description for the irregular tumour growth is given by the Gompertzian growth curves (Figure 3.2). In a Gompertzian growth the doubling time increases steadily as the tumour grows larger. The progressive slowing of Gompertzian growth may be more the result of decreased cell production rather than of increased cell loss (Steel 1977).

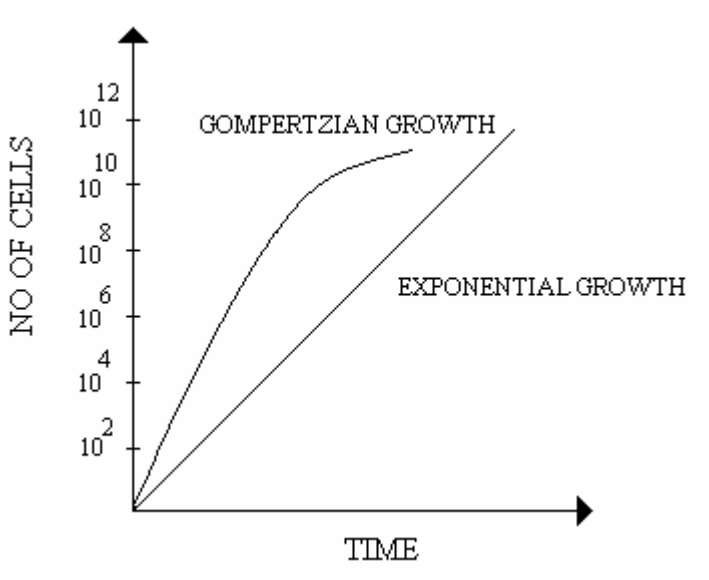

Figure 3.2. Tumour growth curves

Potential doubling time, T_{pot}, is a cell kinetic parameter representing the time for the tumour to double its size when there is no cell loss. T_{pot} can be expressed as a function of the length of the S phase, T_S, and the thymidine labelling index, LI, which is the percentage of cells in the S phase:

$$T_{pot} = \lambda \frac{T_S}{LI}$$

where λ is a correction factor for the irregular age distribution of growing cell population and usually is within the range of (0.7 – 1).

Tumour cell loss is estimated from the cell loss factor (Steel 1977), which is defined as a function of T_{pot} and the volume doubling time, T_d:

$$Cell\ loss\ \ factor = 1 - \frac{T_{pot}}{T_d}$$

Tumour cells can go through apoptotic death ('programmed', potentially controllable death), similarly to normal cells from the tissue of origin. The other mechanisms of cell loss are necrosis (cell death produced by the progressive degradative action of enzymes) and differentiation (cells attaining adult structure and functional capacity).

3.1.3. Tumour composition and characteristics of tumour cells

Tumour cells can be classified into two main categories: proliferating cells and nonproliferating cells. Non-proliferating cells can be either quiescent (resting) that are capable to re-enter the cycle, or sterile cells that are no longer able to divide. There are also stromal cells that would not contribute towards tumour growth and, finally, dying cells which in time are eliminated from the tumour through the circulatory and lymphatic systems. Figure 3.3 shows a classification of tumour cells as a function of their proliferative ability (Begg 1997).

Cells with indefinite proliferative potential are mentioned in the literature as either clonogenic or stem cells. Stem cells are defined as the cells that have the ability to perpetuate themselves through self-renewal. Clonogenic cells are described as the cells that can divide indefinitely. The terminology is still debated since the existence of stem cells within the tumour is still a hotly disputed topic (Kummermehr 2001).

However, there are some aspects to support the ‘cancer stem cell’ concept (Reya 2001):

- The mechanisms that regulate self-renewal of normal cells and cancer cells are similar
- There is a possibility that tumour cells arise from normal stem cells
- There are cancer cells within the tumour with indefinite proliferative ability that drive the formation and growth of tumours.

In the present work, the property of indefinite proliferation is attributed to the stem cells, therefore assuming the existence of cancer stem cells.

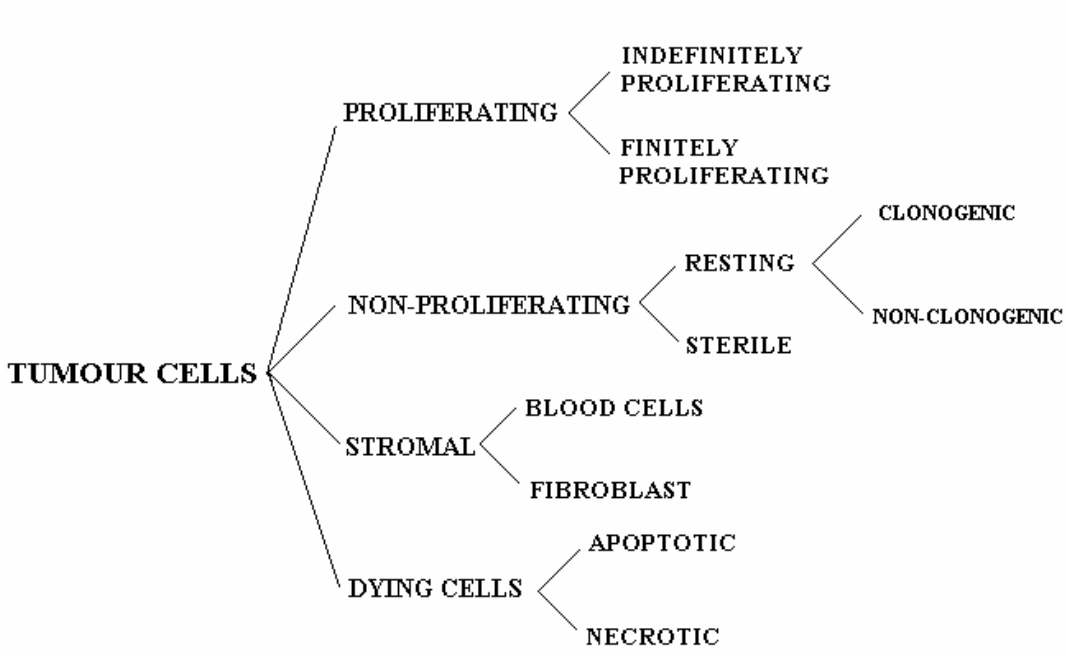

Figure 3.3. Classification of tumour cells

3.2. Literature review on temporal models of tumour growth

Tumour growth models have been previously developed based on either analytical methods (Aroesty 1973, Swan 1990, Wheldon 1988) or probabilistic functions (Donaghey 1980). In the analytical approach, the model is specified as a set of equations (mainly differential), and the equations are solved for an exact solution.

However, analytical techniques in general do not have the flexibility to enable the variation of different parameters (e.g. cell movement, tumour proliferation) which can be incorporated in probabilistic modelling. One of the earliest models for tumour growth and cell cycle simulation using the Monte Carlo approach is CELLSIM (Donaghey 1980). CELLSIM operates with a large initial number of cells, placed in different phases of the cell cycle. Cells are not followed individually because of the significant number of parameters, but are modelled in groups. Therefore each group enters and exits a state together. When the number of groups reaches a certain limit, a reassignment algorithm will combine them making larger groups, where the new parameters are calculated using the weighted average of the previous ones. CELLSIM simulates cell cycle and distribution of cells along the cycle with and without cytotoxic treatment and it does not focus on tumour growth curves. However, the description of the model implies exponential growth behaviour.

Several early tumour growth models have also considered the Gompertz distribution to describe the shape of the tumour growth curve. Gyllenberg and Webb (1989) explained the Gompertzian growth curve by expressing the rates of cells transitioning reversibly between the proliferative and resting states as a function of tumour size, therefore incorporating variable growth fractions. Their mathematical model employs quiescence as a mechanism to explain characteristic Gompertz-type growth curves. The model distinguishes between two types of cells within the tumour, proliferating and quiescent. The theory behind the tumour growth model is based on empirical data suggesting that the larger the tumour, the more likely it is that a proliferating cell becomes quiescent and the more unlikely it is that a quiescent cell re-enters the proliferating cycle, therefore diminishing the growth fraction. The same group (Gyllenberg 1990) has later incorporated into the model a new parameter defining the size of individual cells and modelled the dependence of tumour growth on this parameter, in addition to cell transition between compartments.

It is generally accepted that human cancers grow in an exponential or Gompertzian manner. This assumption is based on analysis of the growth of

transplantable animal tumours and on averages of tumour growth in human populations. Furthermore, there are data which are not consistent with exponential or Gompertzian kinetics but are explainable by irregular growth kinetics. Although not valid for all individual tumours, exponential growth may accurately describe averages of human tumour growth (Retsky 1990).

3.3. Growth of a virtual tumour using probabilistic methods of cell generation.

3.3.1. Introduction

A computer generated virtual population of characteristic head/neck tumour cells has been developed using a stochastic method of cellular generation starting from an initial single stem cell. The model is an extension of the previously published works as it follows each individual cell from birth to death. Tumour composition and development as well as cell age distribution can be assessed in time. Through the use of Monte Carlo techniques and probability functions, the continued division of a cell and its daughters can be followed up to the point of detectability (10^9 cells) or lethality to the host (10^{12} cells). The probability functions were based on established cellular behaviour, as described in the following sections, and then refined for conformity with macroscopic tumour patterns.

The present work does not consider cell size as a critical parameter determining tumour growth pattern in time, therefore all cells have similar geometrical characteristics.

The establishment of a model will provide a virtual but realistically characteristic population of tumour cells with which the interaction and cooperation of radiation and chemotherapy can be examined (Chapter 6).

3.3.2. Biological foundation for model development

As described in §3.1.1, cells propagate through a sequence of four phases (Figure 3.1) constituting the cell cycle: mitosis (M), the postmitotic phase or the first "gap" (G_1), the synthetic phase (S) and the postsynthetic phase or the second gap (G_2). Also, non-proliferating cells enter a resting phase called G_0.

The duration of a cell cycle varies from one cell generation to the next, leading to a cell population that is distributed exponentially around the cell cycle (Hall 2000) at any one point in time. The variation of the cycle time between individual cells (Tannock 1992) is a truncated Gaussian distribution with a mean value for head and neck cancer of 33 hours and a standard deviation of 13.7 hours. Truncation of the function limits the range to biologically functional values between 20 and 60 hours, range adopted from the reviewed literature.

There are three basic cellular types modelled: stem (S cell), proliferative differentiating (P cell) and non-proliferative (N). In head and neck tumours, there are less than 2% S cells and up to 85% N cells (Tannock 1998) i.e. the S:P:N ratio is 2:13:85. Stem cells are considered to be able to indefinitely proliferate (Begg 1997) while a proliferative differentiating cell (or simply referred to as 'proliferative' in this work) is restricted to a finite number of cell divisions. A finitely proliferating cell undergoing mitosis creates another proliferative cell and, as a second daughter, either a proliferative or a nonproliferative cell (P:N ratio) (Figure 3.4). A non-proliferative cell (N cell) cannot divide; after leaving the mitotic phase (M phase) of the cell cycle, the N cell enters the resting (quiescent) phase (G_0).

Tumour growth may be classified as having two distinct periods: the latency period and the clinical-growth period. The latency period starts with the initial mutation of the normal cell and lasts until the tumour grows into a clinically detectable size (10^8-10^9 cells representing ~1g of tumour mass) (Tannock 1998). The clinical-growth period is of the order of one third of the latency period; the tumour requires about 30 doublings in volume to grow from a single cell to a

detectable mass but just a further 10 doublings are required to achieve a lethal size (1kg, 10^{11}-10^{12} cells). For head and neck cancers, the mean tumour doubling time during the clinically-detectable life span of the tumour is 45 days (Tannock 1998) therefore, if growth rate in subclinical phase is the same as in large clinically-detectable tumours, after 40 doublings, a single mutated cell develops into a detectable tumour in approximately 5 years. The overall latency period for a head and neck tumour might be longer, but in the present work the very initial stage of the various mutations of a normal cell into a mutated one is not considered. Because of computational-memory limitation the tumour developed by the computer grows to a microscopic size so extrapolation, through the growth rate factor, is used to obtain the clinically detectable-sized tumour.

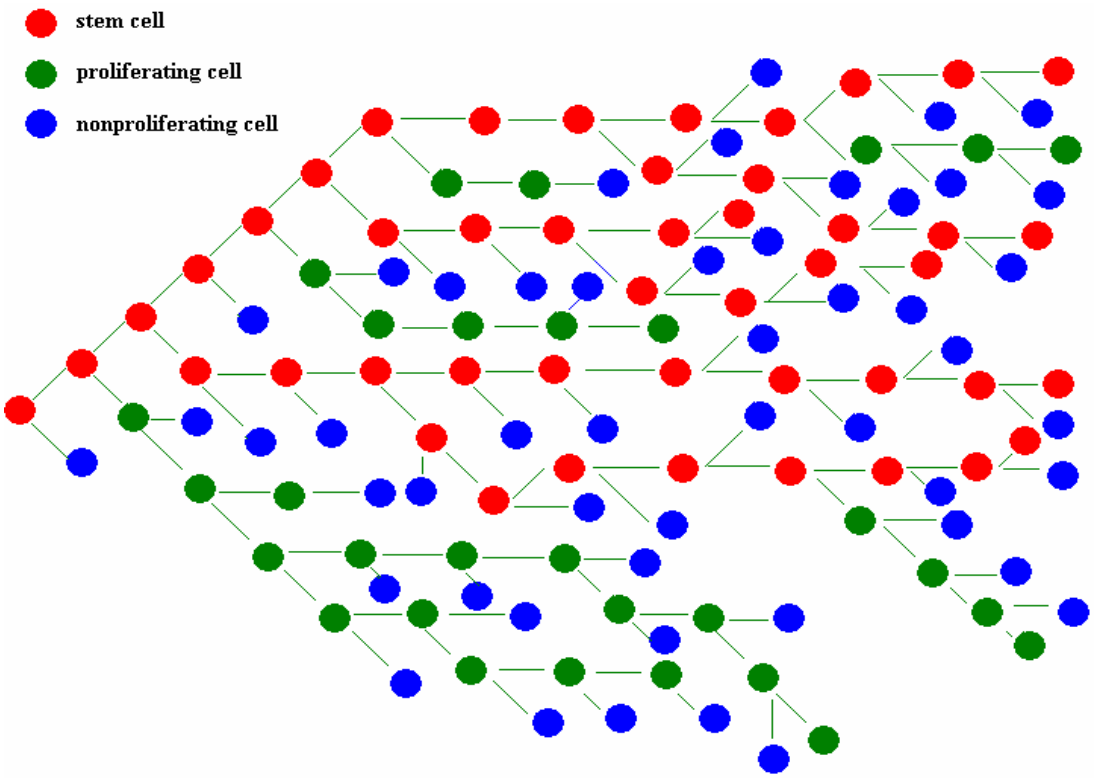

Figure 3.4. The tumour growth model

In contrast to tumour growth, limitations in physical space, delivery of nutrients and oxygen, apoptosis and necrosis all lead to a substantial cell loss within the tumour. For head and neck cancer, this cell loss is as high as 85% of the total tumour population (Begg 1997).

Table 3.1 presents the literature data available for the main tumour kinetic parameters for squamous cell carcinomas of the head and neck (H&N SCC). The data adopted for computer simulation are also presented.

Table 3.1. Published and adopted cell kinetic parameters for H&N SCC.

Cell kinetic parameter or tumour property	***Mean value (model)***	***Mean value & range (literature)***	***Publication***
Volume doubling time	52 days	45 days (33-150)	Begg & Steel, 2002
Labelling index	5% (theoretical)	7% (5-17)	Steel, 1989
Cell loss factor	85%	85%	Steel, 1989
T_S *(length of the synthetic phase)*	11 hours	10.7 hours (4.4-45.7) 11 hours 11.9 hours (8.8-16.1)	Begg et al, 1999 Tannock & Hill, 1998 Begg & Steel, 2002
T_C *(cell cycle time)*	33 hours (20-60)	$3xT_S$	Hall, 2000
Tumour composition	- Stem cells - Finitely proliferating cells - Nonproliferating cells	- Stem cells - Cells capable of a limited number of cell divisions - Nonproliferating cells	Tubiana, 1986
Percentage of stem cells in the tumour	2%	< 0.1% 1-2%	Tubiana, 1986 Wigg, 2000

3.3.3. Methods

3.3.3.1. Model description

The growth of a tumour has been modelled using probabilistic functions sampled by computer generated random number sequences i.e. the Monte Carlo method. The model maintained the biological constitution of a tumour through the generation of stem, finitely proliferating and non-proliferating cells. Non-cancerous cells and necrotic (dead) cells within the tumour were not taken into consideration by this model as they did not contribute to the targeted goal of a virtually grown tumour having all the characteristics described above.

The modelling process comprised of four main stages: input set up, cell generation and characterisation, timing control, and calculation and display of results (see flow chart of Figure 3.5).

The input module defined and initialised program variables: the overall number of cells to be tracked, the S:P:N ratio, the stage of the cycle (the relative lengths of the phases of the cell cycle), the average cell cycle time, the cell loss factor, the number of generations of proliferative cells and the P:N ratio.

Starting from a single stem cell, the cell generation module initiated the creation of new cells, being the software equivalent of the biological stage of mitosis. Three pathways could be followed within the module depending on the input cell being either a stem, a finitely proliferating or a nonproliferating cell. A stem cell divides in two daughter cells, one of them being another stem in accordance with the self-renewal property of stem cells. The cellular type of the second daughter cell was sampled from a uniform distribution provided by the random number generator, in proportion with the biological S:P:N ratio. A proliferative (P) cell that underwent mitosis resulted in a proliferative cell with a decremented number of proliferations and a second cell with the type randomly selected from a uniform distribution in proportion with the required P:N ratio. A 50:50 ratio for P:N was considered initially but a final value of 30:70 was determined on iterative

refinement of all the cell parameters to achieve agreement with accepted biological tumour characteristics.

Each newly formed cell was assigned a cell cycle time by randomly sampling from a truncated Gaussian distribution with a mean value and standard deviation that reflected known biological characteristics. Similarly, the duration of the four phases for each cell were attributed in accordance with the following proportions of the cell cycle: M-7%, G_1-40%, S-30% and G_2-23%. An 85% cell loss of non-proliferative cells was incorporated through sampling from a uniform distribution immediately upon cell generation as well as on every third generation of finitely proliferating cells.

The control of the flow of cell creation and promulgation was temporally based. The first stem cell was defined as entering mitosis at time zero. Each cell formed thereafter was attributed a start time and an end time. The start time was the sum of the duration of all its preceding generation's cell cycle times since time zero. The end time was the start time plus the cell cycle time of the current cell. At each interval of a master clock, each cell was scanned to see if its end time fell with the clock interval and was processed accordingly.

The results and display module kept track of the overall number of cells, the number of particular cell types and also cell distribution along the four phases of the cycle. These parameters were listed every 100 hours of biological growth time.

A growth rate factor (GRF) (the ratio of cell counts between two consecutive 100 hour intervals) was also determined.

3.3.3.2. Model sensitivity study

The constitution and behaviour of the cell population at any one time has, at the current level of knowledge, an unspecified relationship with the cell characterizing parameters and probability distribution functions. Simple redefinition of one of the parameters (e.g. the proportionality of S:P:N) at the start

of the growth simulation will not necessarily generate the required biological tumour constitution and growth factors, because the other parameters (cell cycle time, cell loss factor, P:N ratio) may influence the outcome. To evaluate these interactive processes, each parameter was individually iterated to establish its impact on the tumour's development and response.

The parameters and their ranges (within realistic values as per published data - see Table 3.1) used in this sensitivity study were as follows:

1. probability of S cell creation (1.5% – 12%),
2. probability of P cell creation (1% - 25%),
3. the P:N ratio (10:90 – 50:50),
4. the mean cell cycle time (20h – 60h),
5. N cell loss (10% - 99%) and
6. number of generations of P cells (1 generation – 5 generations).

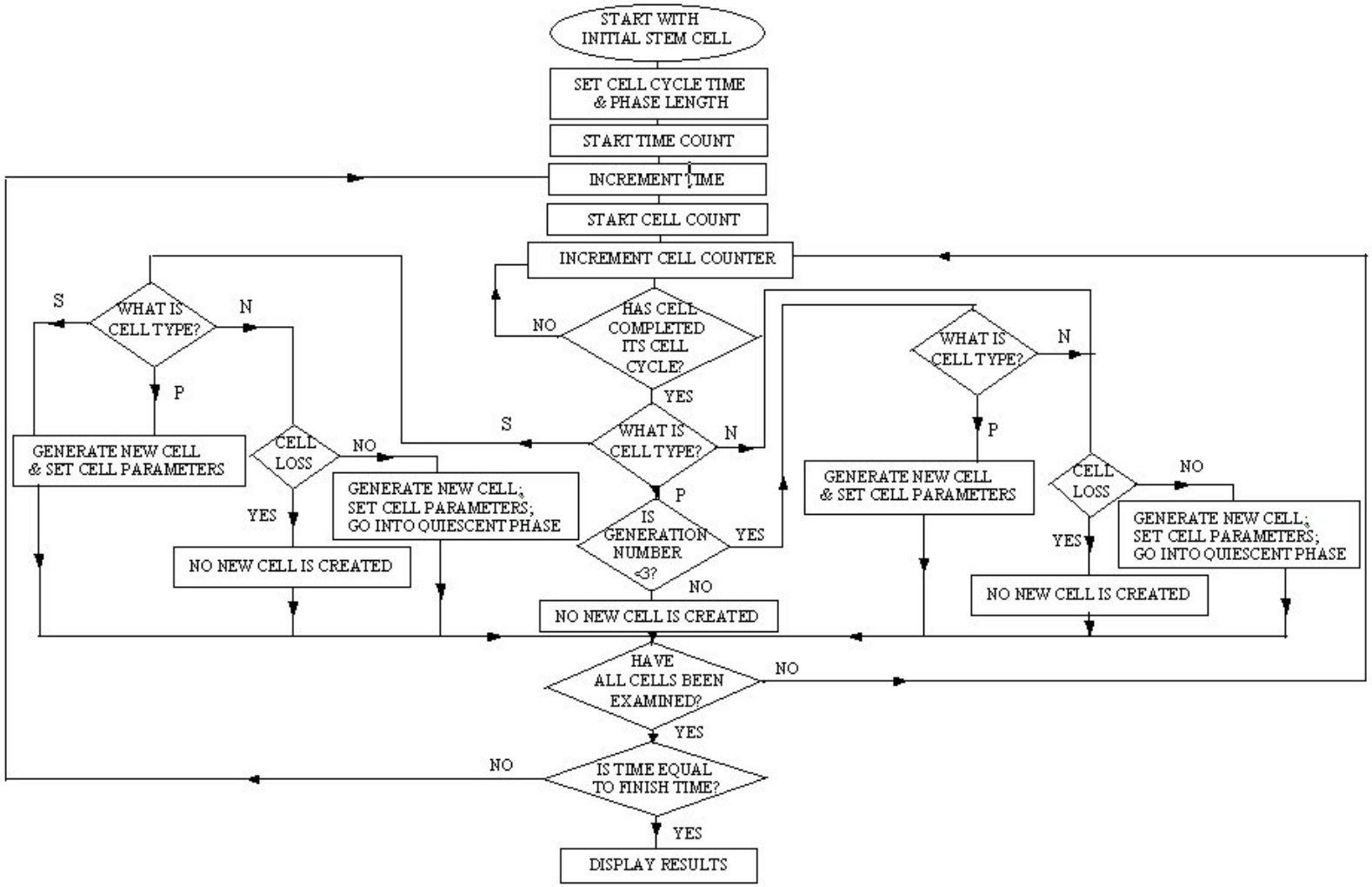

Figure 3.5. Tumour growth model : flow chart.

3.3.4. Results and discussion

3.3.4.1. Cell population development and characteristics

The initial set of parameters leading to the required macroscopic tumour behaviour was established through manual iteration of the above described cell parameters. As a result, the following ratios for the cell parameters were obtained: a stem cell creation probability of 1.9%, a P cell creation probability of 6.1%, a P:N ratio of 30:70, a mean cell cycle time of 33 hours, a N cell loss factor of 85% and a P cell lifetime of three generations. The growth in the number of cells of the virtual tumour under unperturbed conditions (cell loss only from natural causes) was exponential as required (Steel 1997) (Figure 3.6). The mean volume doubling time was 50 days, which is comparable with the biological median of 45 days (and within the range of 33-150 days).

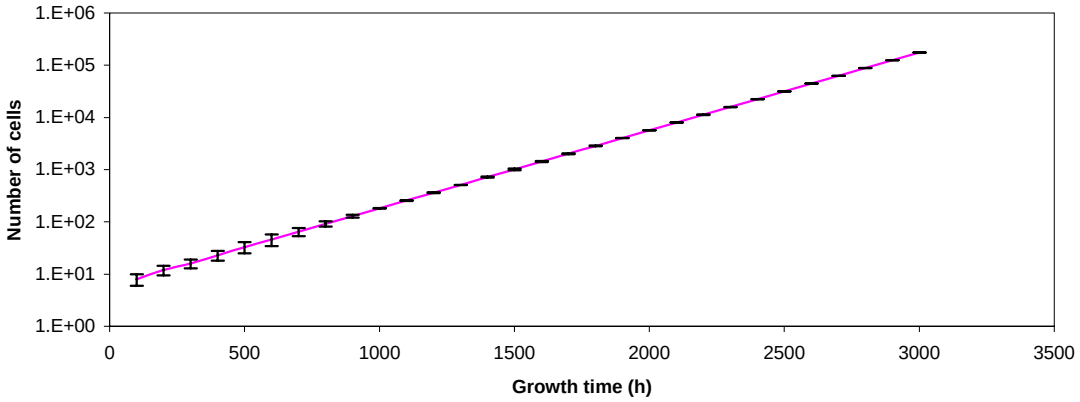

Figure 3.6. The exponential growth of an untreated tumour (semi-logarithmic scale)

The tumour growth rate starting with different seeds for the random number generator is presented as a function of time in Figure 3.7. The initial variances at the microscopic level of tumour growth were due to statistical fluctuations (small number of cells). Tumour progression, even among tumours of the same histopathological type, can vary widely as a function of their intra- and extratumoral environment (Steel 1997). Therefore the initial fluctuations in tumour growth illustrated by the model are analogous with the

growth pattern of biological tumours. The growth of the tumour model converges towards a stable growth rate factor, which is consistent with the behaviour of a biological tumour, confirming the validity of the model.

The ratio between the latency period and the clinical-growth period has been calculated for the modelled tumour at 3:1, which also was in accordance with the literature (Tannock 1998). This ratio is independent of initial cell probabilities (S, P or N), overall number of cells and growth rate factor and does not depend on the initial state (seed) of the random number generator.

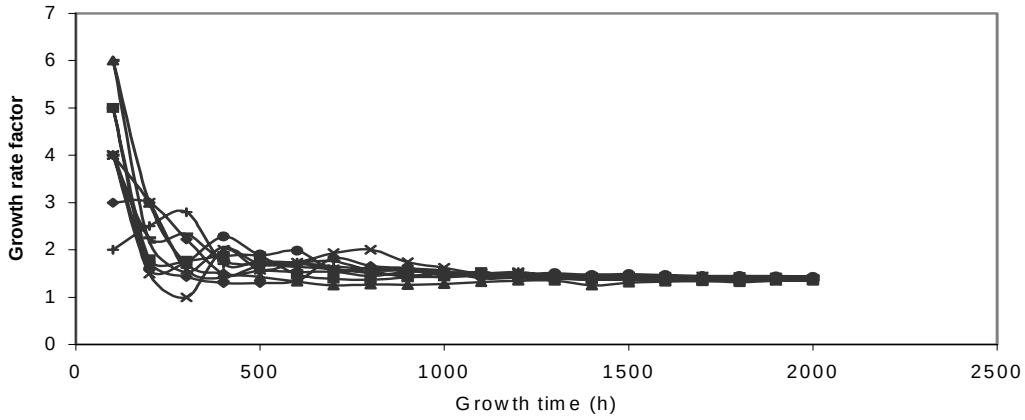

Figure 3.7. Growth rate factor as a function of tumour growth time (for various seeds of the random number generator).

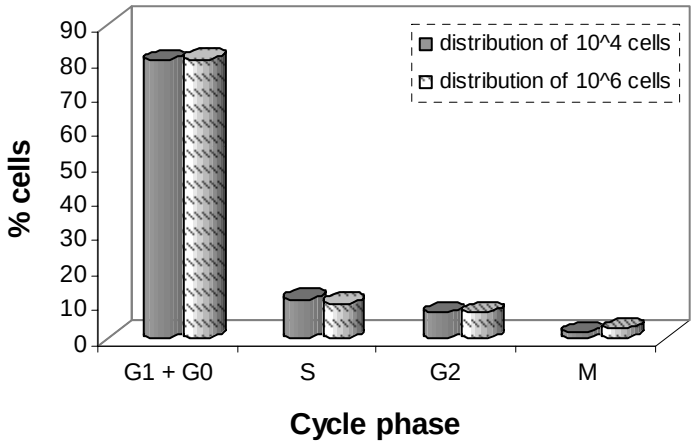

Figure 3.8. Cell distribution along the cell cycle for 10^4 cells and 10^6 cells respectively.

The initial set of manually derived best-fit probability parameters to the macroscopic tumour behaviour also provided a tumour cell population of the required biological composition. An exponential distribution of cells along the cell cycle (Figure 3.8) and the proportionality between the populations of the four phases was maintained as the tumour grew.

3.3.4.2. Sensitivity of model to cell parameter variation

The growth rate factor as a function of stem cell creation percentage, plotted on a linear scale, and also the tumour growth for different stem cell percentages are shown in Figure 3.9a on a semi logarithmic scale. The error bars on the "growth rate factor" curves represent the standard deviations from a median growth rate factor for different starting seeds of the random number generator.

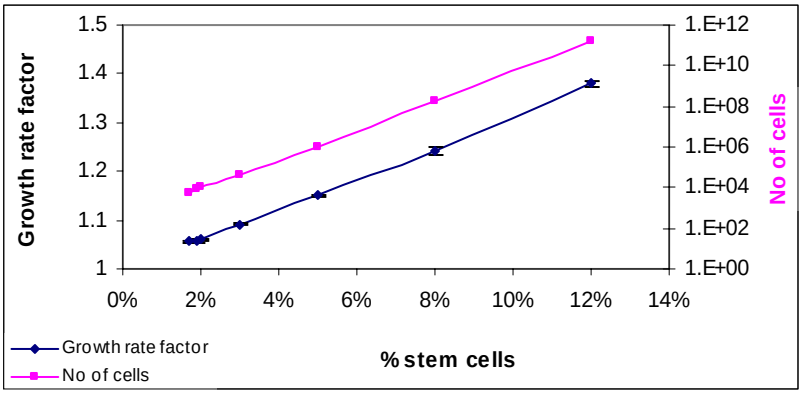

Figure 3.9a. Growth rate factor and number of cells as a function of the probability of stem cell generation.

For low values of stem cell creation probability (1.5%-2%), the slope of the growth rate factor curve is close to zero (Figure 3.9b), however the number of tumour cells increases exponentially. With greater probability values (2%-12%) the growth rate factor increases significantly and similar increase in slope is observed for the cell-number curve. This change in growth rate factor (that also led to a steeper tumour-growth curve) is due to the properties of stem cells. By increasing the initial percentage of stem cells more viable cells are created and less cells are lost (no cell loss from S cells).

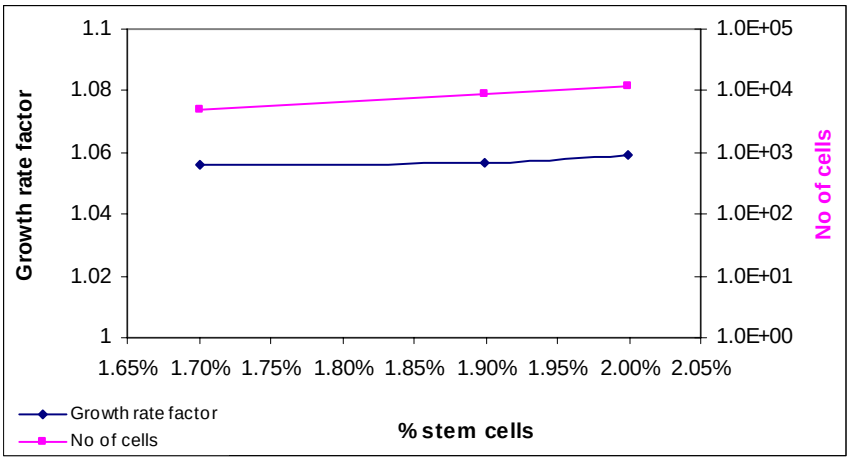

Figure 3.9b. Enlargement of the initial slope of the growth rate factor and number of cells as a function of the probability of stem cell generation.

The growth rate factor curve (Figure 3.10) was not influenced when different probabilities were set for the creation of P cells. This outcome reflects that the P cell creation is being matched by the P cell loss after the prescribed number of generation cycles. Likewise, only a slight increase in tumour growth was achieved with an increased P cell creation probability.

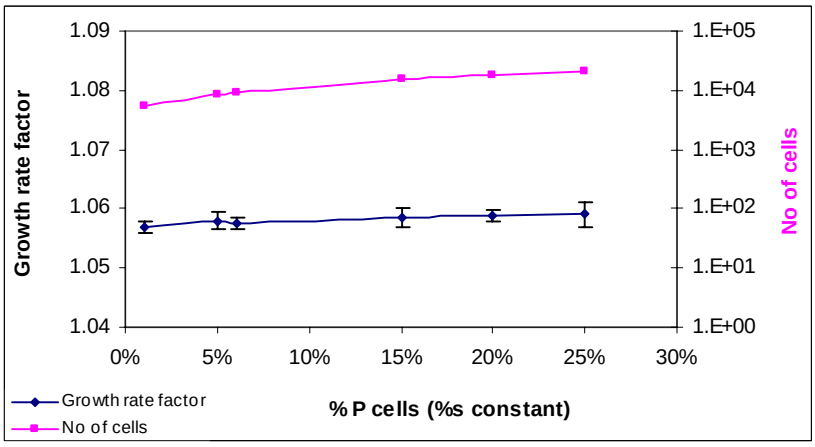

Figure 3.10. Growth rate factor and number of cells as a function of the proliferative cell generation probability.

By comparing Figures 3.9 and 3.10, the major difference between stem and finitely proliferating cells can be deduced. Their different capacities for proliferation greatly influence the growth rate factor of a tumour and hence explain why the main targets in cancer treatment are the stem cells, as they are able to regenerate the whole tumour. The

value of 6.1% as an initial set up for proliferative cells was chosen to achieve the biological S:P:N ratio, and to control the growth of the tumour in achieving the 50 days volume doubling time.

Figure 3.11 illustrates the influence of P:N ratios on growth rate factor and also on tumour growth. The optimal P:N ratio for the model was determined by iterative processes, while keeping the biological balance of the S:P:N ratio.

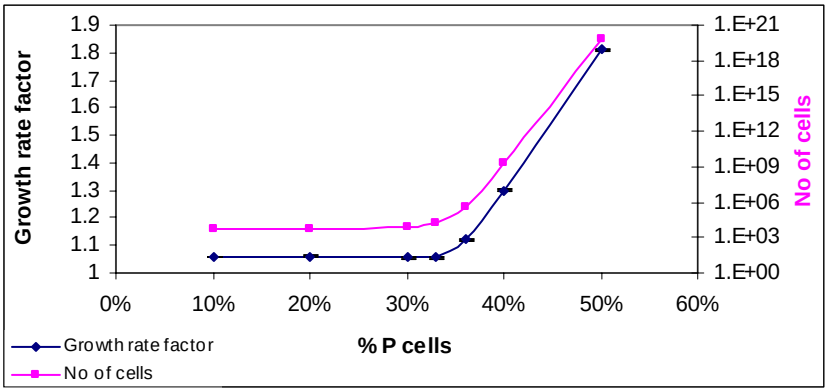

Figure 3.11. Growth rate factor and number of cells as a function of the P:N ratio (the abscissa is in terms of the numerator of the P:N ratio).

While a P cell proliferates for a finite number of generations, an N cell rests in the quiescent state, G_0, out of the cycle, not capable of division. Furthermore, the cell loss due to N cells is more significant (85%) than the cell loss caused by the P cells (every 3rd generation). Therefore, the greater the P:N ratio, the steeper the tumour growth curve and more pronounced the growth rate factor. Up to the 30:70 ratio the growth rate factor is nearly constant and the tumour growth slow. There is an increased growth rate factor and number of cells at the 35:65 ratio and these keep increasing with higher P:N ratios.

The growth rate factor and the tumour growth for different mean cell cycle times is shown in Figure 3.12. For longer cell cycles tumour proliferation is slow as less cells enter mitosis, while for short cycle-times the tumour grows more rapidly.

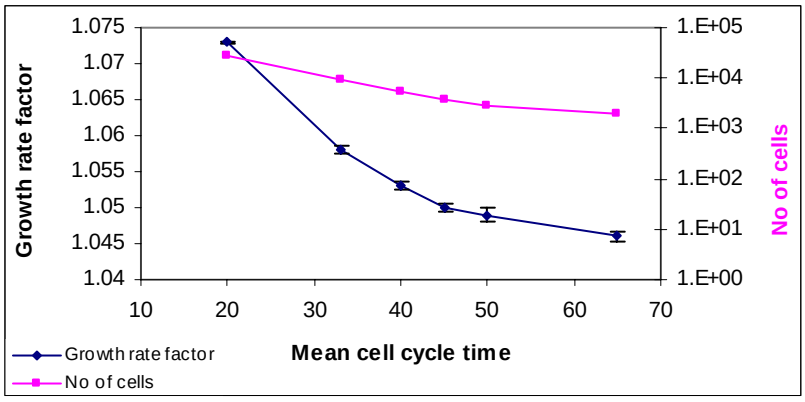

Figure 3.12. Growth rate factor and number of cells as a function of the mean cell cycle time.

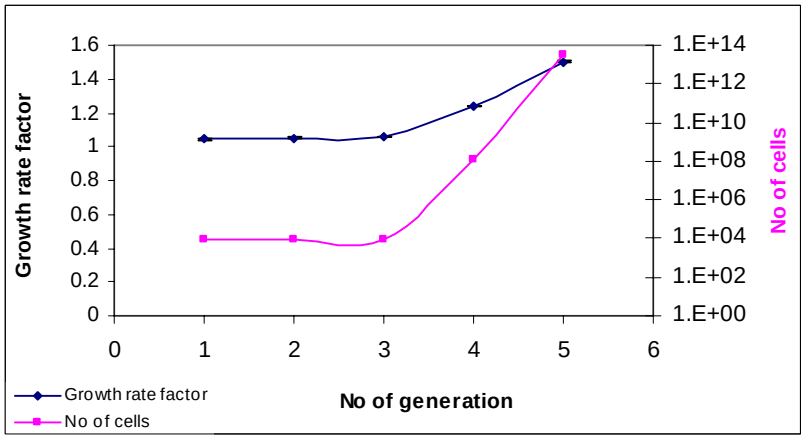

Figure 3.13. Growth rate factor and number of cells as a function of the number of generations attributed to P cells.

The impact of the number of generations (allowed mitosis) of P cells is presented in Figure 3.13.

With small numbers of generations (1-3), there is a slight increase in tumour growth. Furthermore, for cell loss in more advanced generations (greater than 3) the growth curve becomes steeper and the growth rate factor curve as well. The longer the generation chain, the greater the P cell population with less cell loss, thus the larger the slope of the growth curve.

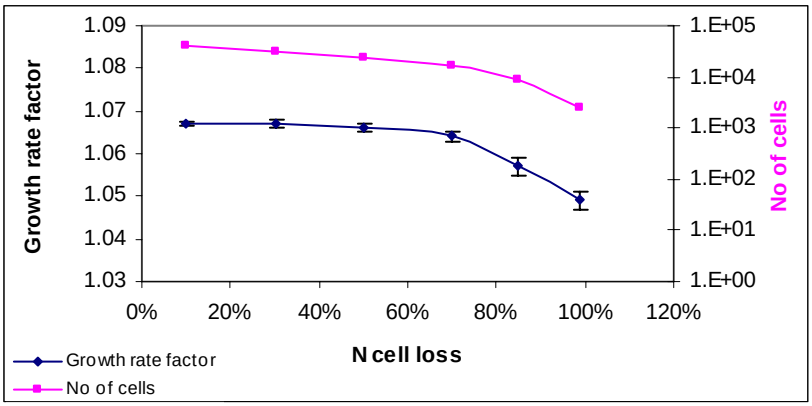

Figure 3.14. Growth rate factor and number of cells as a function of cell loss from N cells.

An increase in the percentage of N cell loss does not influence the growth of the tumour to the same extent as that of P cell loss. The growth rate factor decreases slightly with the cell loss, the same change being observable for the tumour growth curve (Figure 3.14).

In summary, the probability of stem cell creation needs to be adequately small (1.9%) in order to control tumour growth, the probability of proliferative cell creation has to be small enough to keep the biological proportion between stem and nonproliferative cells but sufficiently large to contribute to the tumour growth (6.9%). The P:N ratio needs to equilibrate the production of proliferative : nonproliferative cells in order to control tumour growth (30:70). Cell loss due to both proliferative and nonproliferative cells further contributes to maintain tumour characteristics within biological parameters.

3.3.4.3. Model optimization: is there an optimum value for the cell kinetic parameters?

It was mentioned in §3.2 that although not valid for all individual tumours, exponential growth may accurately describe averages of human tumour growth (Retsky 1990). The inter- and intra-patient variation of cell kinetic parameters within the same histopathological type of tumour, and the disparities in the patterns of cancer growth is well documented in the literature. Consequently, in order to describe the behaviour of a class of tumours (like squamous cell carcinomas of the head and neck), it is more

accurate to relate to value ranges for various parameters rather than to a single number (Table 3.1). The mean value represents, however, the most plausible number within the specified range.

Table 3.2 shows the ranges used for iteration of each parameter of the current tumour growth simulation, as well as the mean values given by the model.

Table 3.2. Mean values and variation ranges for the main tumour kinetic parameters

Tumour kinetic parameter	**Variation range used for the sensitivity study**	**Mean value used in the model**
Probability of S cell creation	1.5% – 12%	1.9%
Probability of P cell creation	1% - 25%	6.1%
P:N ratio	10:90 – 50:50	30:70
Mean cell cycle time (T_c)	20h – 60h	33h
N cell loss	10% - 99%	85%
Number of generations of P cells	1 generation – 5 generations	3 generations

The graphs given by the above value ranges have been plotted as a function of the growth rate factor (Figures 3.9-3.14). Figure 3.15 shows the correlation between the tumour kinetic parameters and the optimal set of values given by the intersection point of the curves.

It is seen from Figure 3.15 that there is a set of values that is more favorable for the head and neck cancer growth model in order to provide realistic tumour growth characteristics (volume doubling time of 52 days, labelling index of 5% and biologically sensible tumour composition). However, a slight variation in the growth rate factor (within 2%) would still lead to a valid tumour growth curve.

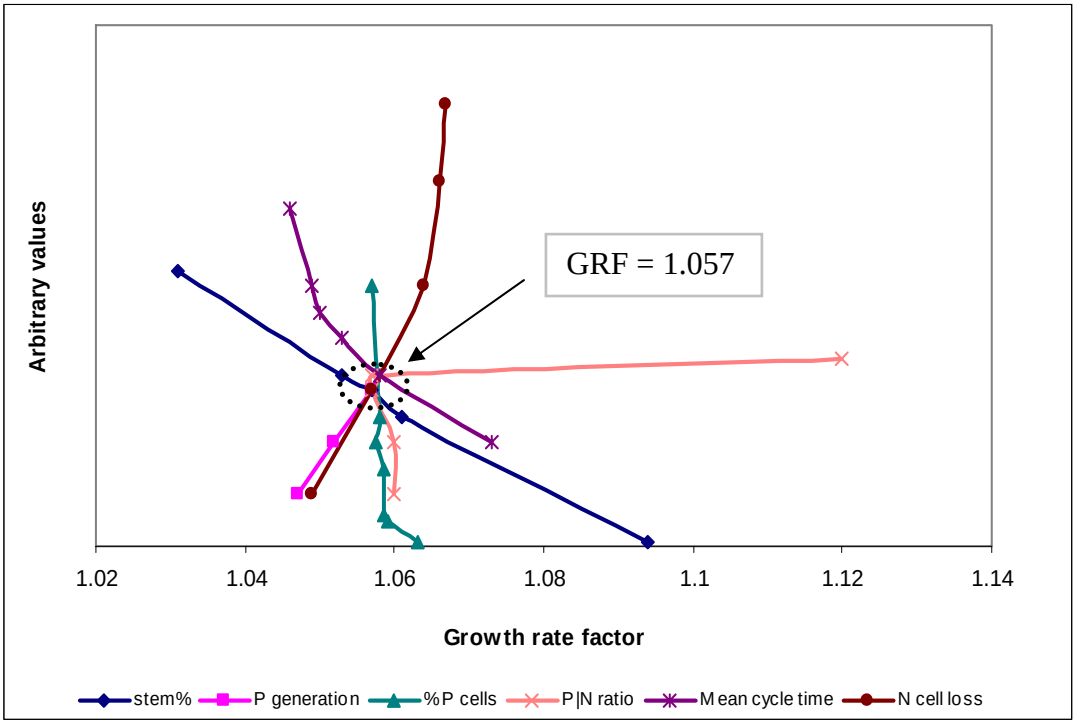

Figure 3.15. Correlation among tumour kinetic parameters

3.3.5. Conclusion

The biological growth of a tumour has been modelled through the application of probabilistic functions and cellular characteristics to a Monte Carlo methodology. The resultant cell population was compared with accepted biological tumour constitution and growth characteristics and agreement was achieved in terms of the exponential tumour growth, the volume doubling time and an exponential distribution of cells along the cell cycle.

The development of a virtual population of tumour cells offers a mechanism for further study and understanding of the impact of different factors on the tumour growth, potentially highlighting the situations where treatment is most effective.

Chapter 4

Modelling the effect of radiotherapy on tumour growth

4.1. Cellular response to radiation

4.1.1. Introduction

When interacting with the living tissue, ionizing radiation is known to produce ions that are not in stable equilibrium. Many molecules in aqueous solutions exist in an ionized state due to dissociation into positively and negatively charged ions that coexist in a stable equilibrium (Nias 2000). However, the ions created by ionizing radiation are highly reactive abnormal pairs, called free radicals. Free radical ions disrupt normal molecular structures and damage the biological target, the deoxyribonucleic acid (DNA). Radiation deposition results in DNA damage manifested by single- and double-strand breaks in the sugar phosphate backbone of the molecule.

Radiation damage is largely manifested by the loss of cellular reproductive integrity. Some cells undergo apoptosis (triggered death), others would not show morphologic evidence of radiation damage until they attempt to divide.

4.1.2. Cell survival curves

The graph in Figure 4.1 is a survival curve of a cell population hit by sparsely ionizing radiation. The fraction of cell survival is plotted on a logarithmic scale against dose on a linear scale. Dose D_1 characterizes the initial slope of the curve (due to single event killing) and D_0 characterizes the final slope (due to multiple event killing). Both D_1 and D_0 are doses required to reduce the fraction of surviving cells to 37% of its previous value [if the initial number of cells is N_0 (for zero dose) and the number of cells for a given dose D is N, the single hit survival curve is $N = N_0e^{-D/D_0}$; for $D = D_0$, $N = N_0e^{-1}$, thus $N = 0.37N_0$]. The presence of the shoulder in the survival curve for sparsely ionizing radiation is possibly due to repair processes. The shoulder region is quantified by extrapolation of the exponential portion of the curve to the y-axis intercept. This point is referred to as the extrapolation number (n), while the dose in between the 100% survival point and the extrapolation line is called quasi-threshold dose (D_q).

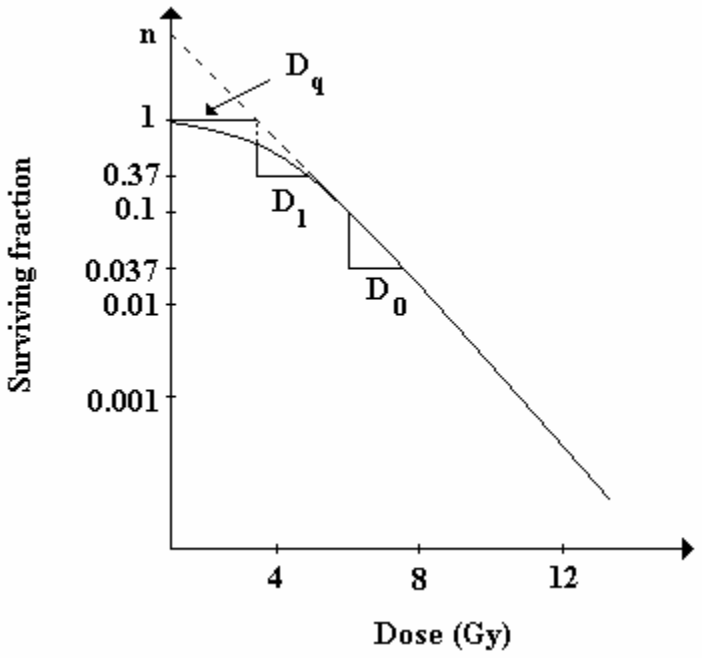

Figure 4.1. Survival curve parameters

4.1.3. The LQ model

The linear quadratic (LQ) model was originally formulated by Lea and Catcheside (1938) and re-introduced by Douglas and Fowler in the seventies. The LQ model is currently used to fit radiation survival data to a continuously bending curve. Although it does not have a firm biological basis, the linear quadratic formalism is a convenient model for describing a survival curve mathematically.

The equation that represents the model shows the dependence between cell survival and the radiation dose. To measure the effect, E, of radiation on a tissue, one can use the equation:

$$E = -\ln S$$

where S is the surviving fraction of target cells.

The linear quadratic equation shows that:

$$S = \exp(-\alpha D - \beta D^2)$$

where D is the total dose delivered and α, β are the parameters of the cell survival curve. The linear component (α) is proportional to the dose while the quadratic component (β) is proportional to the square of the dose. The dose at which the α and β components are equal is referred to as the α/β ratio, which characterizes the curvature of the curve (Figure 4.2).

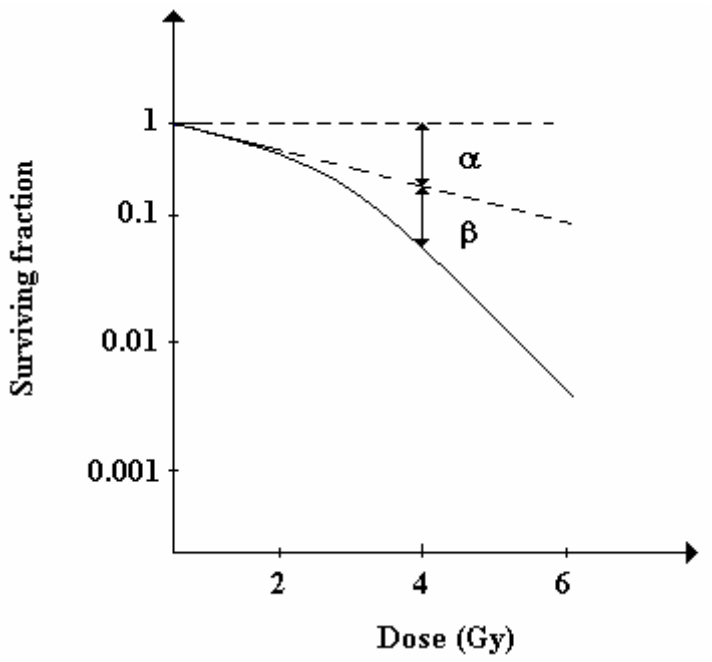

Figure 4.2. The α and β components of the Linear Quadratic model

When radiotherapy is fractionated in 'n' number of fractions each delivering a dose 'd', then the linear quadratic equation becomes:

$$S = \exp[-n(\alpha d + \beta d^2)] = \exp[-n d(\alpha + \beta d)]$$

The initial slope of the survival curve in Figure 4.2 is determined by the linear component (α) and the shoulder is given by the quadratic component (β). The linear component represents single-hit killing kinetics and dominates the radiation response at low doses. The quadratic component represents multiple-hit killing and causes the curve to bend at higher doses.

4.2. Determination of cell cycle phase-specific α parameters for squamous cell carcinomas of the head and neck

4.2.1. Introduction

Radiosensitivity, repair, redistribution, repopulation, and reoxygenation are key elements in the efficacy of fractionated radiotherapy and improved tumour control (through redistribution and reoxygenation) and less normal tissue toxicity (through repair and repopulation). Radiosensitivity is a complex parameter that presents both intra- and inter-tumoral variability. Intra-tumoral characteristics are due to the activation of natural radio-protectors and the existence of molecular checkpoint genes that result in cells exhibiting different radiosensitivities along the mitotic cycle. Mammalian cells are most sensitive in mitosis, similarly sensitive in G_2 and most resistant in the late-S phase (Sinclair 1969). Cell types with a long G_1 phase have a resistant peak early in G_1. Also quiescent cells demonstrate resistance to radiation, comparable to cells in the DNA synthetic phase (Brown 2000).

Recruitment is the process by which cells situated in the quiescent phase re-enter the cycle with proliferative capacities. Radiation acts as a stimulus on quiescent cells which are re-cycling, therefore contributing to the redistribution along the cycle. Full synchronisation (cells positioned in one phase) never happens i*n vivo*. *In vitro* experiments are performed to achieve cell synchronisation and to measure diverse kinetic parameters that are used as predictive tools for treatment. None of the synchronising techniques (i.e. mitotic harvest or agent-induced synchrony) is simulated in the present work as the aim was to describe the *in vivo* processes.

Previous works (Biade 1997, Zaider 1996) combining experimental data with theoretical models have performed cell distribution studies using the linear quadratic formalism. Their emphases were mainly on illustrating the differences in radiosensitivity among various cell lines (Biade 1997). Also, radiation-induced cellular inactivation has been investigated in the presence of sublethal damage repair, repopulation and redistribution by the same research group. Models to simulate cell progression through the mitotic cycle under continuous low-dose-rate irradiation have been described as well (Dillehay 1990). The modelling process has been done both analytically (Zaider 1996) and using probabilistic methods (Dillehay 1990).

Tumour characteristics vary to some extent between previous models and the work presented here. Based upon biological studies presented in Chapter 3, the daughter cells have a different age distribution than the mother cells (different cell cycle time), the tumour is composed of both proliferating and nonproliferating cells and the process of cell recruitment is considered in the present model. The difference between stem cells and finitely proliferating cells is made and cell loss is considered, to reproduce the properties of a biologically growing tumour. These considerations altogether have lead to a virtual head and neck tumour, grown under appropriate kinetic parameters (volume doubling time, cell loss, proportion of various cell types) and real-time radiotherapy simulation.

Although the average value of the α/β ratio for squamous cell carcinomas is well documented in the literature (Malaise 1986, Wigg 2000), there are no published values of the phase-specific parameters. The emphasis of the present study is on the influence of the intrinsic radiosensitivity on cell distribution across the mitotic cycle and also upon the proportions between cell categories (stem, finitely proliferating and nonproliferating). Two models are presented in parallel: the ‘average’ model, which considers the literature-given average surviving fraction, SF_{av} and the ‘specific’ model with the consideration of phase-specific surviving fractions, SF_{ph}, derived from cycle-phase radiosensitivity data given by the literature. With the obtained SF_{ph}, and with an average $\alpha/\beta = 8$ for head and

neck cancers (Bentzen 2002), cell cycle specific α parameters are determined via the linear quadratic formalism.

Cell recruitment is also simulated for both models, and the contribution of recruited cells to cell distribution and proportion of various cell types is discussed. Tumour regrowth between fractions due to recruitment is assessed for the two models and comparative study in regard with the variation in cell type percentage is performed. At this stage, the other possible mechanisms responsible for tumour regrowth (i.e. loss of asymmetrical division, accelerated stem cell division) are not considered as they would not affect the comparative study of cell distribution for the two models. However, because of partial simulation of tumour regrowth mechanisms, the virtual tumour is killed before the end of the 7 weeks of treatment.

4.2.2. Methods

The present study builds upon previous work (Chapter 3) (Marcu 2002) which generated a simulated tumour characterised by kinetic parameters specific for squamous cell carcinomas (volume doubling time of 50 days, thymidine labelling index of 5%, 85% cell loss). The simulated tumour is composed of three cell types: stem, finitely proliferating and nonproliferating. The main cell cycle time is 33 hours, with the S phase of 11 hours. Cells are distributed exponentially along the cycle. A conventional fractionated radiotherapy treatment has been simulated for the tumour: daily dose of 2Gy, 5 days a week, over 7 weeks.

The Linear Quadratic model has been used to determine values for α and β (see Appendix C) along the five phases (four cycle phases plus the quiescent phase). Phase-sensitivity ratios, indicated by the literature (Sinclair 1969, Hall 2000) have been used in the derivation process, in which $SF_S = 3SF_M = 3SF_{G2} = 1.1SF_{G0}$ ($SF_{M,G1,S,G2,G0}$ represent the surviving fractions in the five phases considered). The allocated value for surviving fraction in G1 was the average surviving fraction: $SF_{G1} = SF_{av}$ (54%) (Malaise 1986). The total cell population before and after radiotherapy has been expressed as a function

of the individual population in the five phases and specific surviving fractions have been deduced. Applying the linear quadratic formulation, the individual values for the surviving fractions served to express the specific α parameters (see Appendix C). For the G1 phase, the quadratic parameter was derived in proportion with the linear parameter, so the α/β ratio has an average value of 8 Gy. Based on the phase-specific radiosensitivity studies undertaken by Sinclair on Chinese hamster cells (Sinclair 1969), the survival curves for cells in mitosis and G2 are steep and have no shoulder. This result is indicative of very small quadratic parameter (as there is poor repair), and also high linear parameter (as for the high cell kill). On the other hand, the radioresistant phase (S) has shown a curved survival curve, with a shoulder indicative of a large quadratic parameter. The large alpha and small beta for a radiosensitive phase (large α/β ratio) changes into a small alpha and large beta (small α/β ratio) for the resistant phase. Taking into account these observations, the present work has suggested that the α/β ratio is not constant along the cell cycle. The variation within the phase-specific α/β ratios can be three folds when comparing a radiosensitive with a radioresistant phase. Furthermore, it is shown that the surviving population changes in time for the phase-specific model, therefore the α/β ratio changes accordingly during treatment.

The effect of parameter variability on the modelling process has been illustrated by cell distribution and cell surviving curves.

The tumour growth model has been built to simulate the *in vivo* processes taking place before and after radiotherapy. Therefore, the population of cells irradiated through simulation is asynchronous, gaining a certain level of synchrony after radiotherapy as a result of cell recruitment and also due to the selectively increased cell killing in more sensitive phases of the cycle. However, cells remain distributed throughout all phases of the cell cycle, thus no total synchrony is achieved.

Cell recruitment has been simulated by reintroducing, with every radiotherapy fraction, an equal percentage of randomly selected quiescent cells (G0 phase) back into the G1 phase of the mitotic cycle. These cells re-gain their original (before they entered the G0

phase) proliferative capacities upon re-entering the cycle and contributing to tumour repopulation.

A cell recruitment sensitivity study has been performed to determine the influence of the size of the portion of re-cycled cells on the phase distribution. Since the literature has no mention of the percentage of cells recruited after radiotherapy, cells have been recruited instantaneously after each 2 Gy fraction in groups representing 5%, 20%, 50% and 90% of the total number of quiescent cells respectively. The outcomes have been compared for the ‘average’ and ‘phase-specific’ models for each recruitment case.

Figure 4.3 is a schematic representation of the treatment routine. When irradiation starts, surviving fraction values are defined for all the phases of the cell cycle. The treatment routine is the same whether ‘specific’ or ‘average’ values are defined. The properties of the individual cells within the tumour population are checked at the moment of irradiation, and depending on their cycle phase, the appropriate percentage of cells is killed based on the surviving fraction values. Cell kill is governed by probabilistic techniques. When recruitment is not considered, tumour kill will continue in the same way when radiation is applied again. Once ‘recruitment’ is activated, the respective percentages of the G0 population are recruited based on the recruitment factor. The mechanism of recruitment occurs with every radiation dose, with equal percentages of quiescent cells being re-cycled each time.

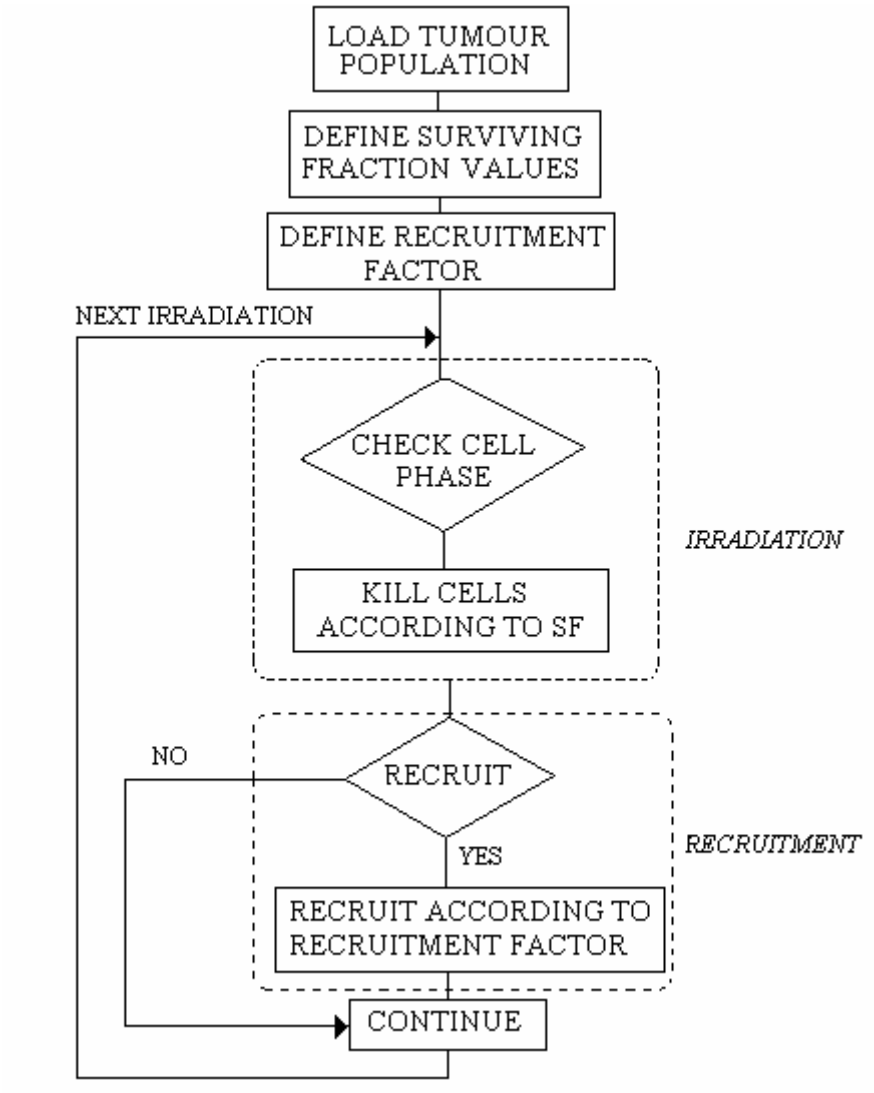

Figure 4.3. Flow chart of the treatment routine

4.2.3. Results and discussion

4.3.3.1. Radiotherapy without recruitment

The phase-specific radiosensitivity parameters deduced for the four phases of the cell cycle plus the quiescent phase are specified in Table 4.1.

Table 4.1. Determined values for phase-specific alpha parameters.

α_{G0}	α_{G1}	α_S	α_{G2}	α_M
0.23	0.25	0.185	0.597	0.597

The α value for G_1 coincides with the average value for α, as the G_1 phase of the mitotic cycle is considered to have an average radiosensitivity. The other α's are derived in conformity with the phase-sensitivity ratios, indicated by the literature (Sinclair 1969) in which $SF_S = 3SF_M = 3SF_{G2} = 1.1SF_{G0}$. The α/β ratio is not constant along the cycle as β varies as a function of phase-resistance. For more resistant phases (S, G0), the ratio of the quadratic parameter to the linear parameter increases, as the dose-response curve presents a shoulder responsible for damage repair. On the other hand, the most sensitive phases (M and G2) present with a steep and almost straight curve, which is indicative of the poor repair occurring in those phases. Figure 4.4 is a representation of dose-response survival curves for the five phases of the cycle, determined with the above-presented parameters.

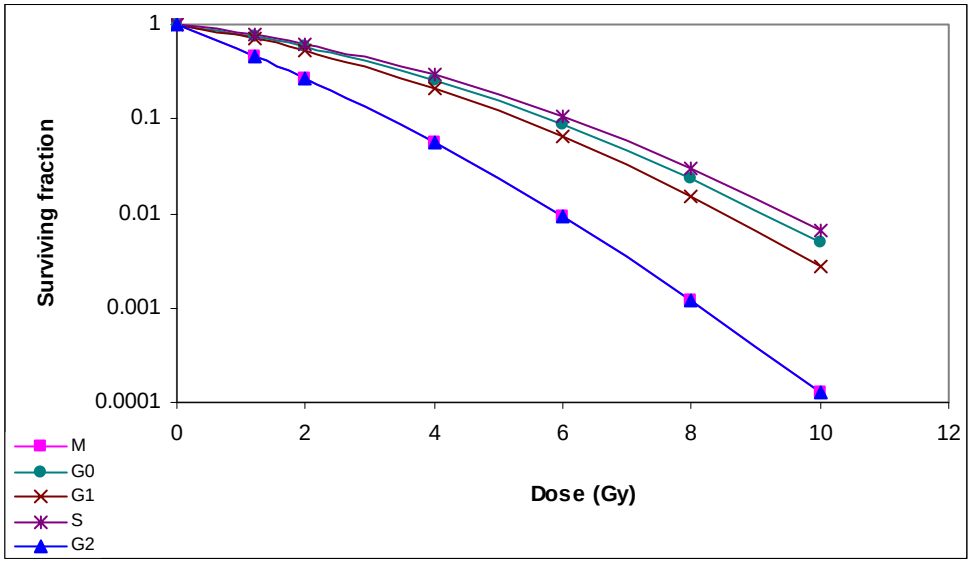

Figure 4.4. Dose-response survival curves for various phases of the cell cycle.

Survival curves (without considering cell recruitment) for the whole cell population are presented comparatively for the phase-specific SF and average SF respectively in Figure 4.5, during a 5 week treatment, with 5 days/week, 2 Gy/day dose. The two curves show only statistical variations between surviving fractions, which are more detectable at very small cell numbers.

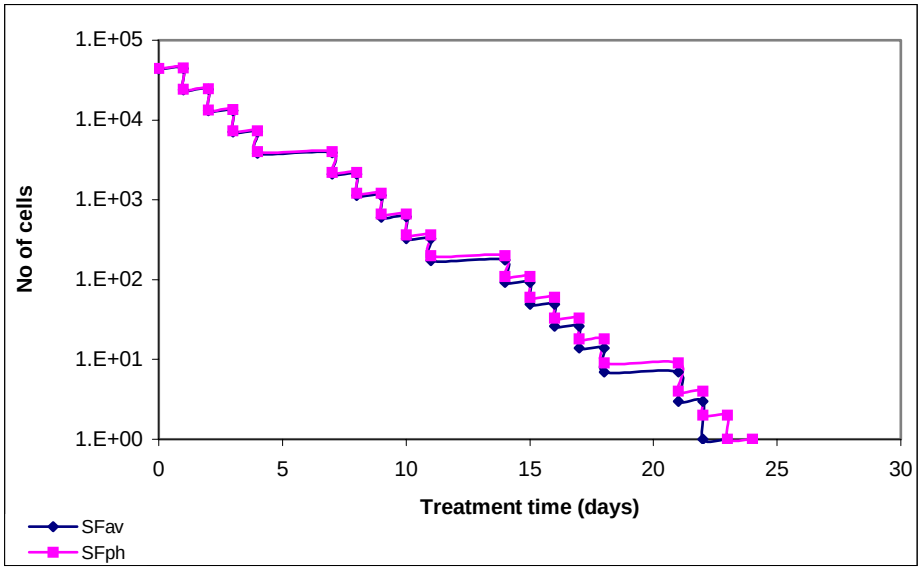

Figure 4.5. Survival curves for cell populations modelled with α_{av} and α_{ph} respectively (no recruitment).

Figure 4.6 illustrates that redistribution occurs after a single fraction if specific α's are used, whereas the average α leads to equally proportional cell kill in all phases.

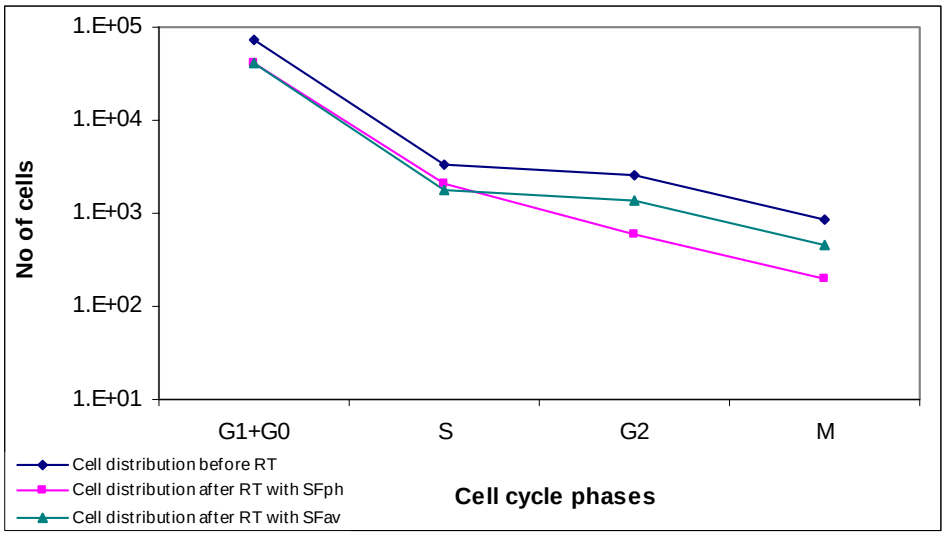

Figure 4.6. Comparative chart of cell distribution before and after a single 2 Gy fraction of RT for average and phase-related radiosensitivity parameters respectively.

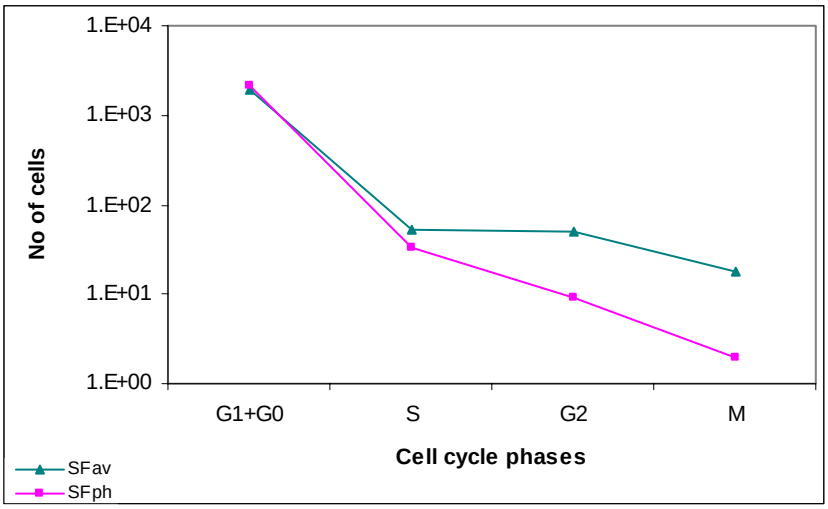

Figure 4.7. Comparative chart of cell distribution after the fifth RT fraction for average and phase-related radiosensitivity parameters respectively.

The cell distribution along the mitotic cycle after the first week of treatment (5 fractions) is shown in Figure 4.7. As the treatment continues, the differences in the proportions of cells in various phases increases. After a single fraction, the ratio of cells in the M phase for α_{av} against α_{sp} is 2.4 and this increases to 9 after five fractions. The change in population is a result of five 2 Gy fractions offset by continued growth of tumour and movement of cells into and out of the M phase. A less pronounced change is seen for the S phase: from 0.85 to 1.6. It is to be noted that the change is less for the S phase than for the M phase. The justification for this behaviour lies in the α values for the S and M phases, respectively, in the two models. The ratio between α_S (0.185) and α_{av} (0.25) is 1.35, while α_M (0.597) related to α_{av} is 2.4 times greater. Therefore, the discrepancies between surviving fractions in the two models (average and specific) for the M and S phases, respectively, will depend upon their radiosensitivities as compared to the average value. The model predicts increasing synchrony due to selective cell killing and a spread in cycle times among surviving cells.

The behaviour of the whole cell population during the simulated radiotherapy has been followed for both models (figures 4.8a, 4.8b, 4.9a & 4.9b). In Figures 4.8a and 4.9a, the percentage of the total population in each phase of the cell cycle is shown over the full course of treatment for the 'average' and 'phase-specific' models respectively. As the

majority of cells are quiescent before treatment, the most populated phase is G0. The distribution of the cycling cells is represented, on a magnified scale, in figures 4.8b (for the 'average' model) and 4.9b (for the 'specific' model). With the magnified scales, a more sudden decrease in cell population for the 'specific' model is seen. However, it was shown in Figure 4.5 that a tumour modelled with phase-related radiosensitivity parameters has comparable survival curve with the tumour modelled using the average parameter.

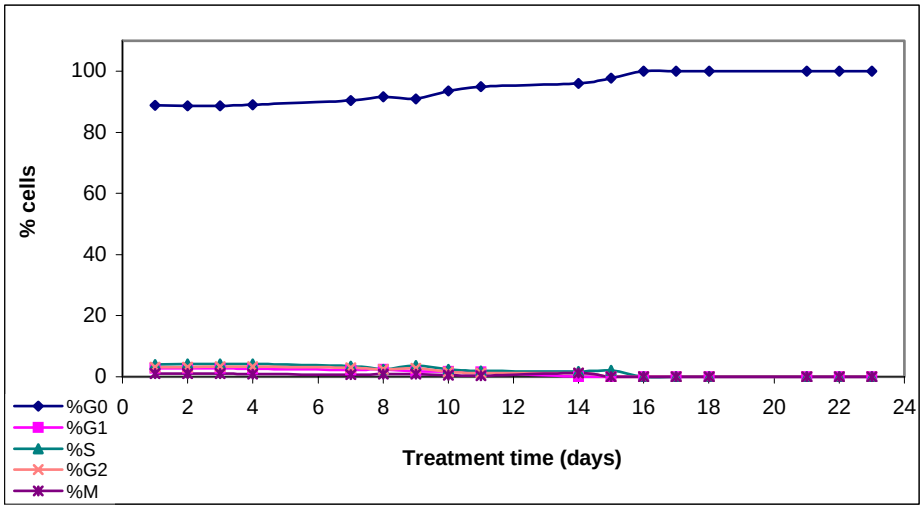

Fiure 4.8a. Cell distribution within the phases of the cell cycle for an average radiosensitivity parameter.

It may be concluded, from the above observations, that the G0 phase equilibrates the balance of the surviving cells. Cells in the quiescent phase are radioresistant, and with the allocation of the applicable α_{G0} parameter, the survival fraction is increased compared to the 'average' model. This will have an impact on cell reassortment when recruitment from the quiescent phase is considered.

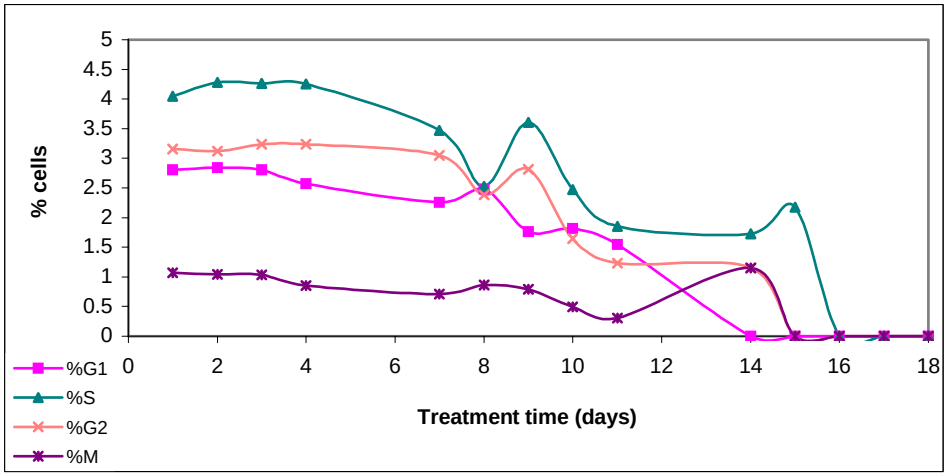

Figure 4.8b. Cell distribution within the phases of the cell cycle for an average radiosensitivity parameter (magnified scale).

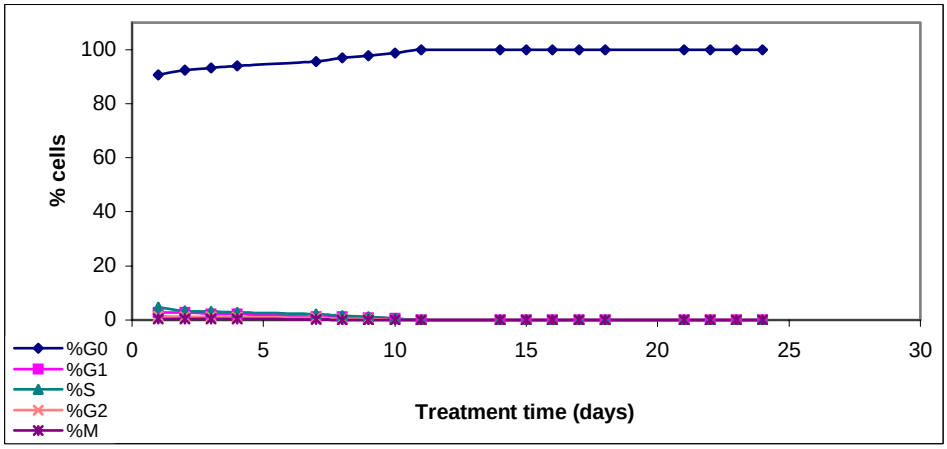

Figure 4.9a. Cell distribution within the phases of the cell cycle for specific radiosensitivity parameters.

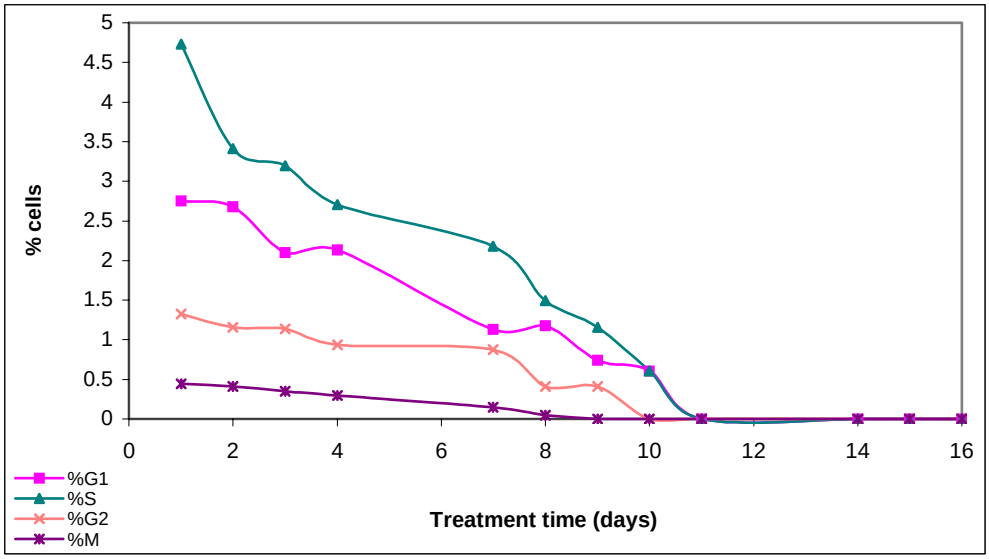

Figure 4.9b. Cell distribution within the phases of the cell cycle for specific radiosensitivity parameters (magnified scale).

4.2.3.2. Cell recruitment into the cell cycle

Compared to the 'no recruitment' case where the survival curves for the two models were very similar, when recruitment is modelled (Figure 4.10a), considerable difference in the two survival curves can be seen. This is mainly due to cell cycle phase reassortment after radiotherapy for the two models, leading to variations in the surviving fractions. The surviving fraction (SF_2) of 54% has been constant in the 'average' model.

On the other hand, the simulation resulted in a smaller surviving fraction of 49.1% (as an average) during treatment with phase-specific parameters. This result is in accordance with the recent literature data (Hopewell 2003) showing an enhanced radiosensitivity of tumour population following fractionated irradiation. Furthermore, the extent of cell recruitment has demonstrated a strong influence on the average surviving fraction, as illustrated in figure 4.10b. The larger the percentage of cells recruited, the larger the variation of survival fraction.

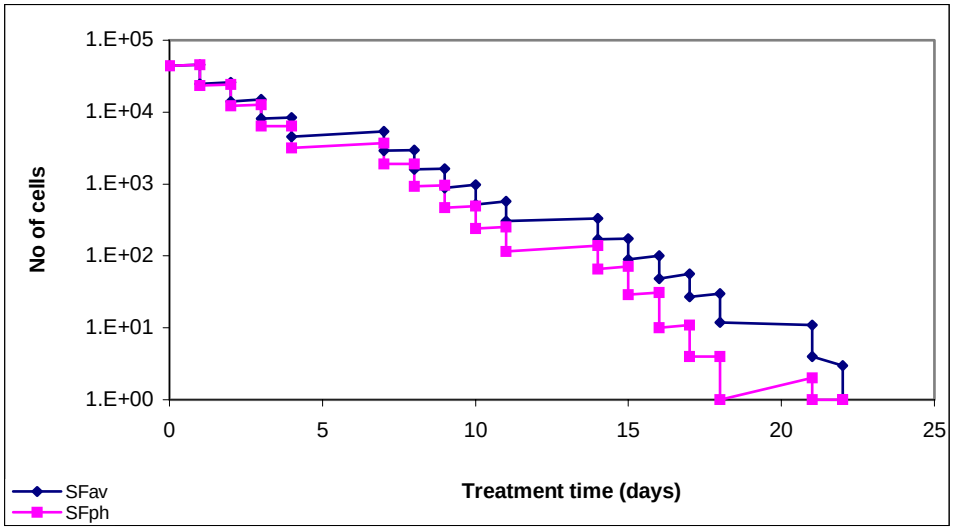

Figure 4.10a. Survival curves after 20% recruitment for cell populations modelled with α_{av} and α_{ph} respectively.

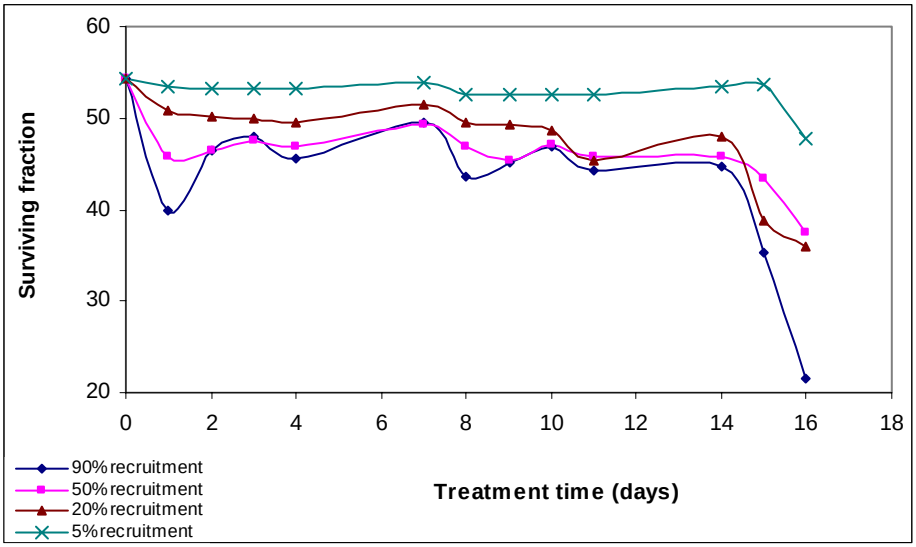

Figure 4.10b. Variation of survival fraction in time as a function of cell recruitment.

Figure 4.11 shows that with cells recruited from the quiescent phase, the *post-first-fraction* distribution along the cycle does not show any differences from the situation when no recruitment was considered (Figure 4.6). The explanation lies in the fact that, when re-entering the cell cycle, recruited cells acquire the resistance of the G1 phase, which is the same for both models, so there is evenly proportional cell kill within that phase with or without recruitment.

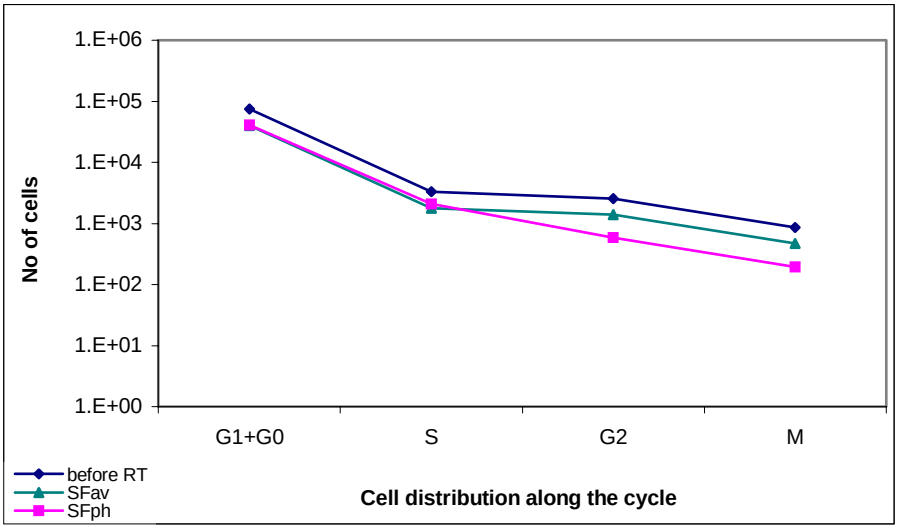

Figure 4.11. Comparative chart of cell distribution with 20% recruitment, before and after RT for average and phase-related radiosensitivity parameters respectively.

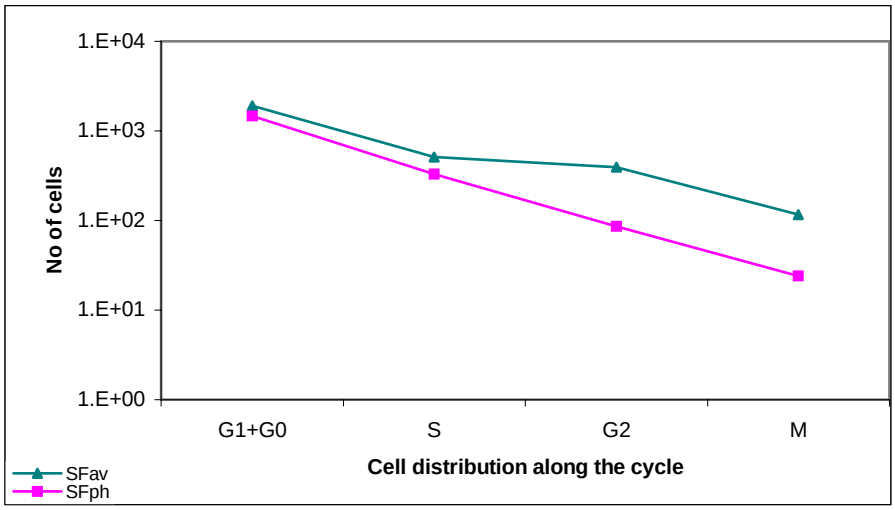

Figure 4.12. Comparative chart of cell distribution with 20% recruitment, after the fifth RT fraction for average and phase-related radiosensitivity parameters respectively.

A slight shift in the curves (SF_{av} related to SF_{ph}) is observed after the *fifth fraction* (Figure 4.12), demonstrating again the variation in cell reassortment along the cycle for the two models and also explaining the variation in the surviving fractions described above.

For both the ‘average’ and ‘specific’ models, the intra-phase distributions (Figures 4.13 & 4.14) show some degree of synchrony in response to re-cycling 20% of cells at a time from the quiescent phase. Fluctuations in the curves for the ‘average’ model are more pronounced particularly for the quiescent cells where the population decreases from 72% to 33%, while for the ‘specific’ model, there is no decrease in G0 population below 52%. The differential between the two cell populations is created by the distinction in the radiosensitivity parameter of the G0 phase in the two models.

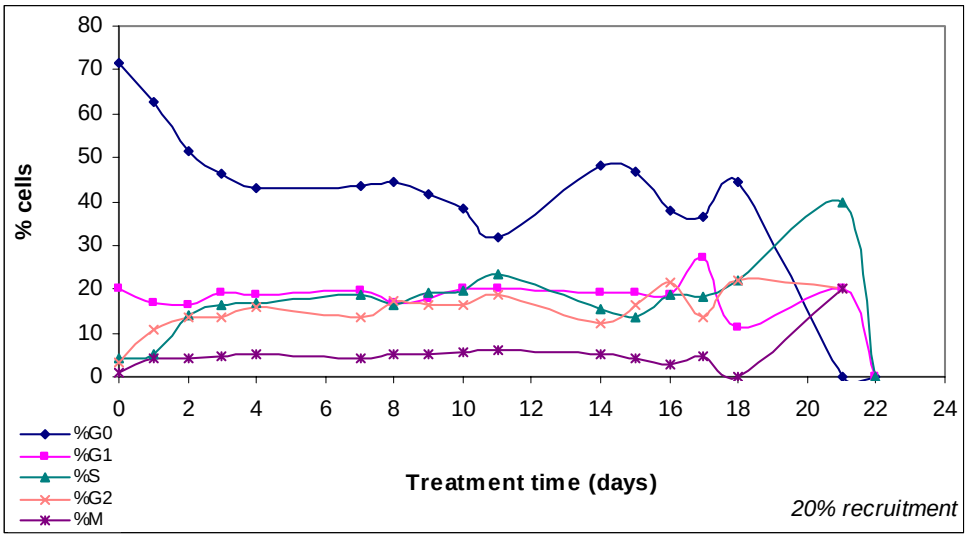

Figure 4.13. Cell distribution with recruitment within the phases of the cell cycle for average radiosensitivity parameter.

In the ‘specific’ model, the M and G2 phases are clearly illustrated as being the most sensitive to radiation by having the lowest cell population , while in the ‘average’ model, the G2 phase appears within the mid-radioresistant phases (like G1) since it is treated like having the same radioresistance as G1. Of main interest is the S phase, the DNA synthesis phase, which is the most radioresistant. Given that resistant cells respond poorly to radiotherapy, tumour control is strongly dependent on the management of these cells, especially the stem cells among them, which are able to repopulate the tumour if they are not totally eradicated. The following cell recruitment sensitivity study discusses, comparatively, the distribution of cells along the S phase for the two models.

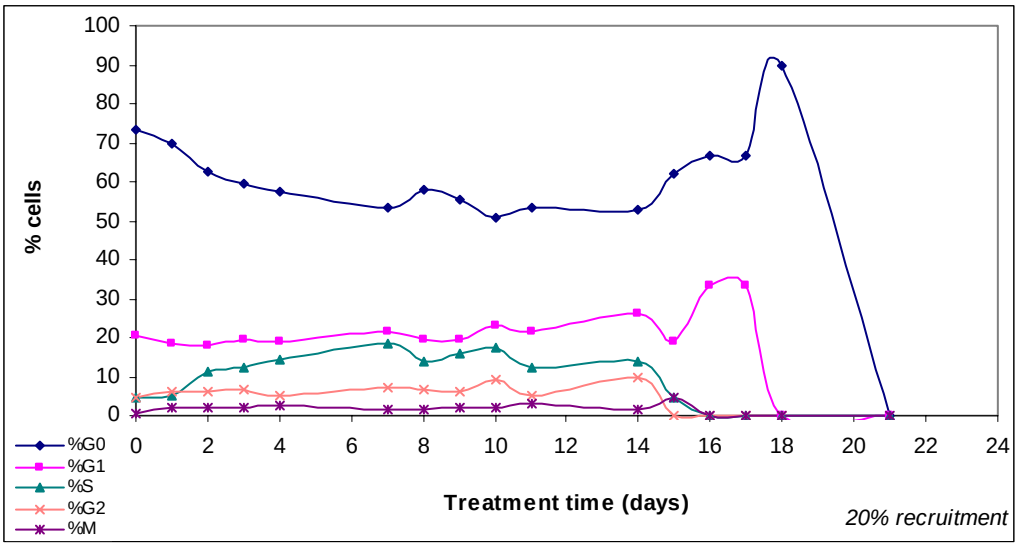

Figure 4.14. Cell distribution with recruitment within the phases of the cell cycle for specific radiosensitivity parameters.

4.2.3.3. Cell recruitment sensitivity study

The mechanism of cell recruitment has been modelled as a cyclic process, where a well-defined percentage of previously quiescent cells start re-cycling as a response to the cell death caused by the external stimulus – radiation. Figures 4.15 (a-d) show, for the 'average' and 'specific' models, the percentage of cells in the S phase during treatment for 5%, 20%, 50% and 90% recruitment fractions, respectively. Depending on the percentage of recruited cells, the two curves related to the 'average' and to the 'specific' models respectively show various discrepancies.

By comparing the two 'S' curves within each graph (Figure 4.15), there is a clear variation in the temporal distribution of cells. At the beginning of the treatment the disparity is not pronounced as redistribution just starts to affect the cycle. However, whereas the percentage of S cells after the 17th day of treatment with 20% recruitment (figure 4.15b) in the 'average' model is 16%, after the same number of fractions the S phase in the 'specific' model is populated by 24% of cells. Towards the end of the treatment (before tumour kill) the difference is even more prominent for all recruitment cases considered. The main reason for the differences is the high number of quiescent

cells which once recruited, will contribute differently to cell redistribution along the cycle due to variations in radiosensitivities between the two models.

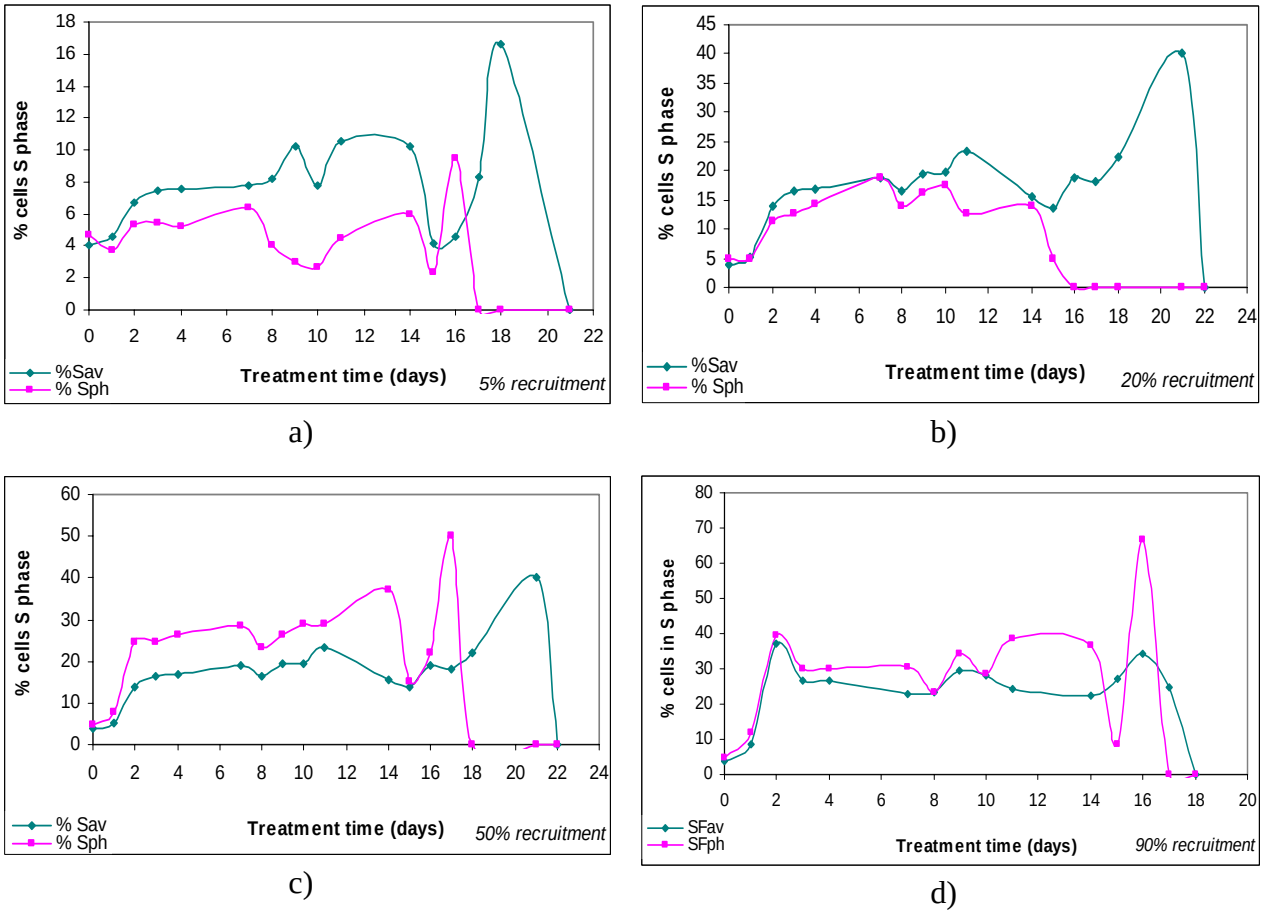

Figure 4.15. Cell distribution with various recruited fractions along the S phase for the 'average' and 'phase-specific' models.

The literature data on recruitment processes is not well documented. Nevertheless, independently on the percentage of cells recruited, the differences in cell distribution between the 'average' and the 'specific' model are existent.

Although one of the main differences between normal cells and cancer cells consist of their cell kinetics and proliferative capacity, still a large population of cells within the tumour is quiescent. Similarly to their tissue of origin, many tumours respond to injury (cell loss) by recruiting cells from the G0 phase. Data in the literature (Sinclair 1969, Brown 2000) shows that cells in G0 have a high radioresistance (comparable to cells in

the S phase). Therefore, when considering a highly resistant G0 phase ('specific' model) and a G0 with an average resistance ('average' model), the process of recruitment will create the above shown discrepancies between the two models. Having more knowledge about the offset of recruitment and the percentages of cells involved in the process, that would allow a more accurate study of intra-variability of the radiosensitivity parameter on cell redistribution along the mitotic cycle.

4.2.3.4. Study on the variability of α

Because of the differences in the α parameter between tumours, the intra-tumoral sensitivity of alpha has been assessed (Figure 4.16). The graph presents cell distribution along the S phase, with 5% recruitment, when considering a specific α and the two extreme values of the variation range. A 27% upper and lower variation for the α parameter has been considered (Wigg 2000) and modelled for the distribution study along the mitotic cycle. The three curves follow the same pattern which indicates the independency of the model on the variation range of the α when all the phases are affected equally.

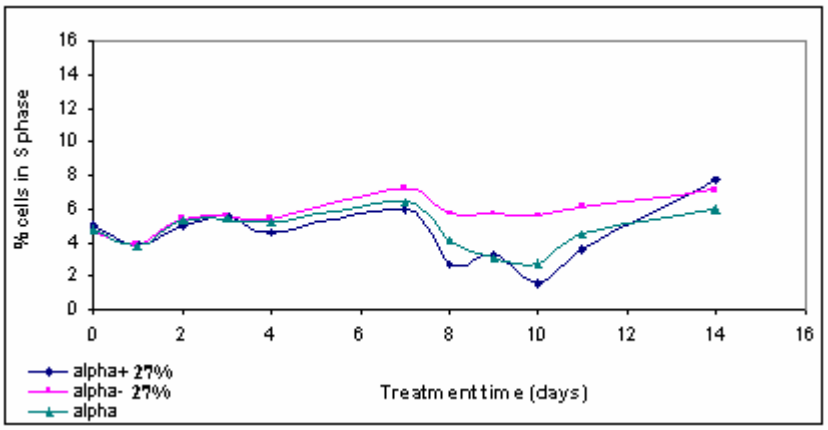

Figure 4.16. Sensitivity study on the variability of the specific α parameter within the S phase.

By comparing Figure 4.16 and Figure 4.15a, it is observed that the differences *within* the specific α parameter when varied by ±27%, are much less that *between* the specific and the average αs.

4.2.4. Conclusions

The values of phase-specific linear parameters (α) for head and neck squamous cell carcinomas, and also the corresponding surviving fractions have been determined according to the variation in intrinsic radiosensitivity along the cell cycle. A comprehensive comparative study including an ‘average’ model (considering the literature-given average parameters) and a ‘phase-specific’ model (with phase-specific radiosensitivity parameters and surviving fractions) has been completed. Cell survival curves for the tumour population as a whole for the two models were shown to be similar; however, there was a more sudden decrease in the cycling population for the ‘specific’ model. This was explained by the different contribution of the non-cycling cells to tumour regression for the two models due to the differences in the radiosensitivity parameters allocated: high for the ’specific’ model and average for the ‘average’ model.
It was shown that redistribution occurs after a single fraction if specific α's are used, whereas the average α leads to equal proportional cell kill in all phases. After the first week of treatment the differences in the proportions of cells in various phases increased.

Cell recruitment has been simulated for the ’average’ and the ‘specific’ models, respectively, and cell distribution along the cycle studied. Compared to the ‘no recruitment’ case where the survival curves for the two models were very similar, when recruitment is modelled considerable difference in the two survival curves can be seen. This is mainly due to cell reassortment after radiotherapy for the two models, leading to variations in the surviving fractions. For both the ‘average’ and ‘specific’ models, the intra-phase distributions show some degree of synchrony in response to re-cycling 20% of cells at a time from the quiescent phase. Fluctuations in the curves for the ‘average’ model are more pronounced particularly for the quiescent cells where the population decreases from 72% to 33%, while for the ‘specific’ model, there is no decrease in G0 population below 52%. Again, the discrepancies are created by the distinction in the radiosensitivity parameter of the G0 phase in the two models.

A cell recruitment sensitivity study has been undertaken by re-cycling various cell percentages from G0 (5%, 20%, 50% and 90%). The results show variations up to 25% between the ‘average’ and the ‘specific’ model, where the differences are more pronounced for higher recruitment. These differences in the radioresistant phases create a decision-making problem when modelling fractionated/hyperfractionated radiotherapy and phase-specific chemotherapeutical agents.

Having more knowledge about the offset of recruitment and the percentages of cells recruited would allow a more accurate study of the effect of intra-variability of the radiosensitivity parameter on tumour behaviour during treatment.

4.3. Tumour repopulation during radiotherapy

4.3.1. Introduction

Loco-regional failure in the treatment of the rapidly proliferating tumours (mainly squamous cell carcinomas) has been attributed to accelerated repopulation (Withers 1993). Accelerated repopulation is a marked increase in the growth rate (15 to 20 times faster) after the commencement of radiotherapy. Accelerated repopulation is not *clinically* evident at the beginning of the treatment because the vast majority of tumour cells are sterilized and the tumour is regressing before the small number of surviving stem cells begin to repopulate. Repopulation is a cumulative process in response to the progressive radiation damage during fractionated radiotherapy (Trott 1999). However, there is no indication that repopulation cannot be triggered from the beginning of the treatment, and rapid, inherent growth is a characteristic of a small proportion of tumours.

Repopulation becomes measurable usually 3-4 weeks after the start of the treatment. Nevertheless, compensatory proliferation in tumours may also be due to a decrease in the

level of hypoxia and malnutrition, which have previously been the growth-depriving factors (Turesson 2003).

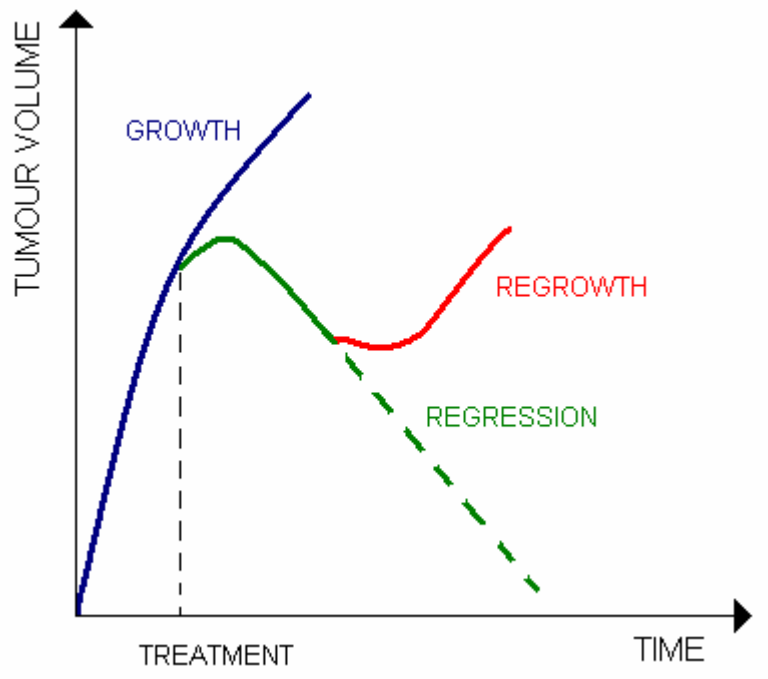

Figure 4.17 . Theoretical curve illustrating tumour growth, regression and regrowth.

Figure 4.17 represents a theoretical curve of tumour growth, regression and regrowth during treatment.

Experimental data on squamous epithelia (Dörr 1997) have shown that the accelerated repopulation response is analogous to the acute response of normal tissue after injury. It is suggested (Trott 1991) that squamous cell carcinomas retain some of the homeostatic control mechanisms attributed to their tissue of origin. Similarly, several other papers support the evidence that normal and cancerous squamous epithelia share the same behaviour in response to injury (Trott 1991, Trott 1999, Denham 1996). Therefore, the mechanisms responsible for normal tissue repopulation may be considered pertinent to tumour repopulation. Dörr (1997) states the main regrowth mechanisms as the three A's of repopulation: asymmetry loss, acceleration of stem cell division and abortive division (limited number of sterilized-cell divisions, not discussed in the present work). Hansen (Hansen 1996) considers recruitment and accelerated stem cell division as the responsible

mechanisms for repopulation. The results obtained by Withers and Elkind (1969) from crypt cell experiments have indicated that division cycle synchrony is a source for repopulation. Trott's work (Trott 1999) also underlines that the most plausible explanation for accelerated regrowth is the loss of asymmetric stem cell division (Table 4.2).

Table 4.2. Possible mechanisms responsible for the accelerated tumour growth.

Mechanism	**Source**
Cell recruitment	Hansen et al, 1996
Accelerated stem cell division	Withers, Elkind, 1969 Dorr, 1997 Hansen et al, 1996
Asymmetry loss in stem cell division	Withers, Elkind, 1969 Trott, Kummermehr, 1991 Dorr, 1997
Abortive division	Dorr, 1997

The paragraphs below are short descriptions of the repopulation mechanisms listed in Table 4.2.

Cell recruitment is the re-entry of the quiescent cells (cells in the G_0 phase) into the mitotic cycle. Accelerated stem cell division refers to the shortening of the cell cycle after the start of radiotherapy, and the loss in asymmetrical division expresses the change in division pattern of the stem cell, from an asymmetrical division (one stem and another finitely proliferating/nonproliferating cell) to a symmetrical division (two stem cells).

The difficulty in assessing accelerated regrowth is that the process starts when the tumour population has decreased to a number of a few thousand of cells, which is not clinically

detectable (Withers 1993). Therefore, theories on the qualitative appraisal of repopulation need more substantiation.

The following part of this chapter presents the results of the onset of repopulation obtained from experimental studies on monolayer cell cultures as well as from computer simulation. Also the mechanisms responsible for tumour repopulation are implemented into the model and their individual, as well as combined contribution towards repopulation studied.

4.3.2. The onset of tumour repopulation

4.3.2.1. Experimental methods

Experiments on cell cultures were undertaken to examine the start of repopulation. It is acknowledged that cell line experiments have their limitations since *in vitro* systems are not controlled homeostatically to be compared to the *in vivo* processes. However, cell cultures can offer qualitative analyses of the effect of radiation on cells.

A cell line derived from a squamous cell carcinoma of the tongue (SCC-25) was grown under laboratory conditions and irradiated with a 4 MV X-ray beam using Varian 4/100 linear accelerator. Single irradiation, as well as fractionated radiotherapy was applied to the cell line, and cell count after each treatment session was performed.

In the first experiment, the cells were irradiated with 2 Gy and 8 Gy single fractions, respectively, and survival curves were compared with the control cell cultures. Two flasks for each dose were exposed and multiple samples from each flask were counted to minimise statistical errors. Average values for the cell populations were considered when processing the experimental data.

To study the effect of fractionation on tumour repopulation, a second experiment was undertaken, where cells were irradiated on two consecutive days, two days after seeding. The dose applied was 8 Gy to obtain approximately a 50% survival after the first dose, for a clinically comparable outcome. Cell count was performed before and after each irradiation.

The colony forming ability of the irradiated cells has been studied as well. Cells irradiated with 2 Gy have been multiply diluted and reseeded in wells, to allow individual follow up of the cells. The following day, a qualitative observation of the colonies has been done. Cells have been followed up over the weekend as well.

4.3.2.1.a Cell culture

The human oral carcinoma of the tongue (SCC-25, originally an ATCC line) was obtained from Peter MacCallum Cancer Institute, Melbourne, Australia.

Cells were grown in 90% DMEM (Dulbecco's modified Eagle's medium) - Ham's F12 (45%:45%) and 10% fetal bovine serum (FBS) in small flasks of 5ml surface. Hydrocortisone was added to the medium in a concentration of 0.4 μg/ml. For precautionary reasons 100 U/ml of penicillin/streptomycin was also added to prevent bacterial contamination.

The cultures were kept at 37°C in a humidified atmosphere of 95% air and 5% CO_2 in an incubator. The medium was replaced every three days and subcultures seeded.

For cell harvest and subculture, the spent medium was removed by aspiration and the cells were rinsed with Hanks buffered salt solution and 1 ml of a trypsin-EDTA solution was added in order to release them from the flask surface. The cell culture was kept in the incubator for 5 minutes, until cells became detached. The flask was gently tapped to aid cell release, and progress was followed using an inverted microscope. Detached cells in trypsin/EDTA were diluted with cell culture medium to inactivate trypsin, and pelleted

by centrifugation at 200 g. Cells were washed twice more by centrifugation and counted using a standard haemocytometer. For further culture, cells were resuspended in culture medium at 2 x 10^5 cells/ml before dispensing into tissue culture flasks (Picture 4.1).

4.3.2.1.b Experimental setup and methodology for cell irradiation

To confirm the dose delivered to the cells, measurements using thermoluminescent dosimeters (TLD) were undertaken a priori. Lithium fluoride (LiF) TLD disks were prepared, annealed and calibrated then irradiated and checked for reproducibility. Afterwards, the TLDs were placed within the radiation field, both inside and outside the empty flask in order to evaluate the dose distribution in the flask, then irradiated with 200 Monitor Units (MUs) using a beam from a 4 MV linear accelerator. The experimental setup consisted of a 5 cm thick wax phantom that allowed the flask to be inserted in the centre, a block of 10 cm solid water, placed underneath the wax phantom, to provide the backscatter radiation, and 1 cm thick solid water on top of the flask for achieving the depth of maximum dose at the flask surface (d_{max}). The radiation field size was 20 cm x 20 cm and the measurements were done at 100 cm Source-to-Surface Distance (SSD). Reference irradiation of known 2 Gy dose was performed for three TLDs under reference conditions (10 cm x 10 cm field size, 100 SSD at d_{max}). By correlation with the reference dose, the dose delivered to the TLDs positioned in the flask could be determined. Consequently, 190 MUs were delivered to achieve the desired 2 Gy. Similarly for higher doses, taking into account dose linearity within ±5% until 12 Gy (E. Bezak, personal communication).

The TLD reader used was a Pitman Toledo 654 with research module. The readings were corrected for background radiation and also for the individual sensitivities.

Cell irradiation was performed at the Royal Adelaide Hospital (RAH) site using the same 4 MV linear accelerator which was used for TLD irradiation. The cell flasks were transported from the Institute for Medical and Veterinary Sciences (IMVS) to the RAH using a safely sealed container. These two sites are neighbouring buildings, thus the cells were not exposed significantly to the changes in environmental conditions. Moreover, the

control flasks were transported together with the irradiated ones, therefore any change in the media would have affected all flasks equally.

4.3.2.2. Results and discussions

4.3.2.2.a Cell line experiments: the onset of repopulation

In the dose response study of the cell line, it was observed that the conventional 2 Gy dose used in clinical treatments of the head and neck cancers, applied *in vitro* in the current study, led to a 73% surviving fraction, instead of the 50% for *in vivo* irradiation given by the literature. The discrepancy is created by the different environmental conditions between the *in vivo* and the *in vitro* tumours. The dose to give a 50% survival of SCC-25 cells was identified to be 8 Gy. Therefore this dose was used in the cell line experiments in order to give outcomes similar to the clinical settings.

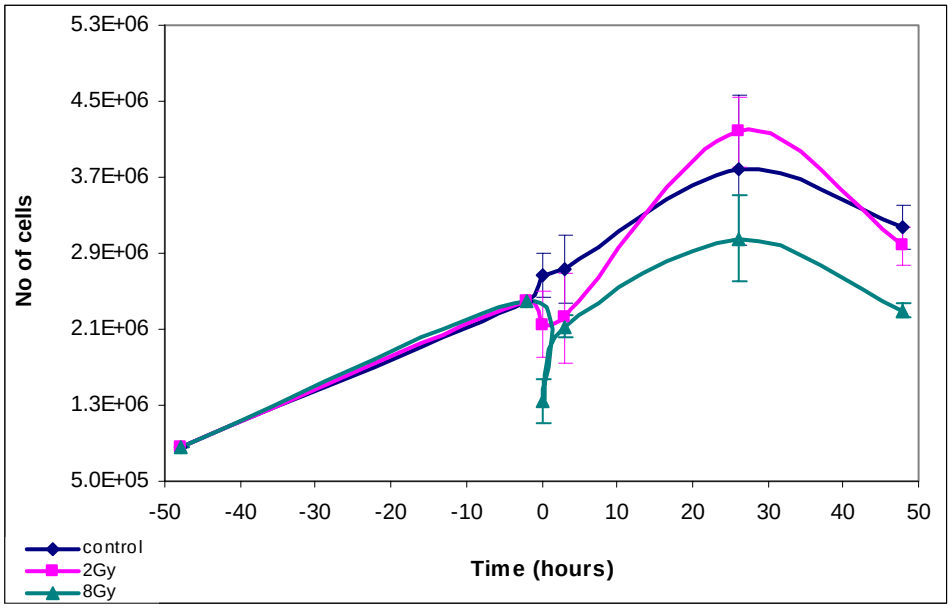

Figure 4.18. Cell survival curves after one dose of radiation.

Figure 4.18 shows the survival curves for the SCC-25 cell line irradiated with a dose of 2 Gy and 8 Gy, respectively. The results are compared with the curve given by the control cell line which was not irradiated, but was exposed to the same growing conditions as

well as environmental conditions during transportation from the laboratory to the linear accelerator site. The cells were irradiated at time 0, and counted within 30 minutes after irradiation. The time before irradiation shows the unperturbed growth while the positive time scale illustrates cell behaviour after irradiation. After one dose of radiation, the drop in cell number for the two irradiated lines varies proportionally to the dose. The 2 Gy dose produces less significant damage (drop in cell number 11%) whereas the 8 Gy dose reduces the cell population by 47%. The cell populations from the three flasks were followed up and counted 3, 26 and 48 hours after irradiation. The graph shows an increase in cell number for the 2 Gy cell line above the control population. This behaviour might be explained by a stimulated response of the cell population to radiation injury. Although the 8 Gy has produced much more damage than 2 Gy, considerable cell recovery is seen for the 8 Gy-curve as well. However, the extent of cell damage could not be compensated by regrowth as it was for the 2 Gy flask.

The decline in viable cell number after 24 hours presented in Figure 4.18 is due to cell confluence (Picture 4.2). If the growing medium of the cell culture is not renewed, cells will overgrow, therefore cell follow-up would not give reliable results for this region. By re-seeding the cells, the fresh medium creates suitable growing conditions that will change the profile of the growing curve, illustrating a high cell growth. However, the cell growth may be due to the renewed nutrient supply, rather than just a stimulus from radiotherapy. Therefore cells have been studied without a medium change, accepting that cell confluence will be a limiting factor.

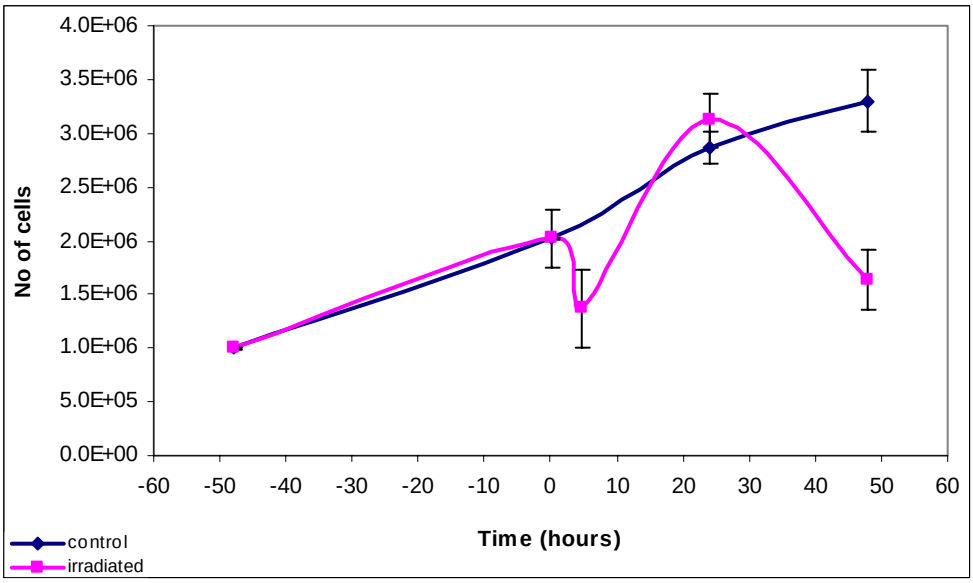

Figure 4.19. Cell survival curves after daily irradiation with 8Gy over 3 days.

Figure 4.19 shows the survival curves for the irradiated and the control SCC-25 cell line, respectively. In this case, cells were irradiated on two consecutive days, two days after seeding. The dose applied was 8 Gy to obtain approximately 50% survival after the first dose, for clinically comparable outcome. Cell count (total cells per flasks) was done before and after the first irradiation, before the second irradiation and after the third irradiation (see experimental points in Figure 4.19).

The graph shows a 9% increase in the irradiated cell population compared to the control flask between two consecutive irradiations. The experimental curves therefore indicate the possibility of an immediate onset of repopulation with the start of the treatment. Though the error bars imply considerable uncertainties when samples for cell counting are taken, the two experiments show an indication towards early repopulation.

4.3.2.2.b Cell line experiments: study of the colony forming ability of irradiated cells

To study the colony forming ability of the SCC-25 cells, irradiated cells have been multiply diluted and reseeded in wells (Picture 4.3). Picture 4.4 represents the individual cells, while the results of the cell follow up for the subsequent days have been illustrated in Pictures 4.5 and 4.6.

The study of the colony forming ability of irradiated cells has given indications in regard with the individual response of cell to radiation. It was noticed the cells have not been affected evenly by radiation: some cells have developed colonies, others remained as single cells. Although there was no quantitative measurement of the colonies only qualitative observation, the experiment has illustrated the variability in the cell response to radiation.

4.3.2.3. Conclusions

The experimental curves derived from data obtained from squamous cell line irradiation indicate the possibility of the immediate onset of repopulation with the start of the treatment. Though the error bars imply considerable uncertainties when samples for cell counting are taken, the two experiments show an indication towards early repopulation.

Since there are no ‘recruitable’ cells in a monolayer cell line, it is concluded that recruitment is not the key mechanism in tumour repopulation in the presented study. Therefore, accelerated repopulation should be attributed to the other two mechanisms: accelerated stem cell division and loss of asymmetrical division of stem cells.

Picture 4.1. Flasks with SCC-25 in the growing medium

Picture 4.2. Confluent SCC-25 cells

Picture 4.3. SCC-25 cells reseeded in wells

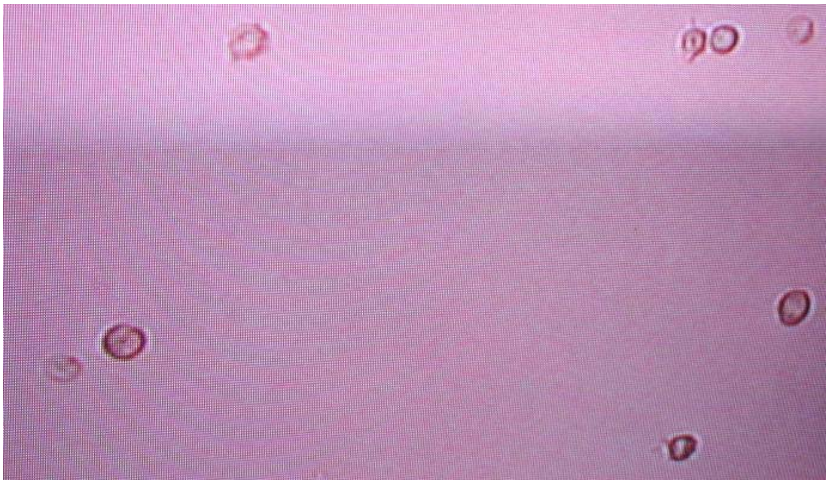

Picture 4.4. Single cells reseeded in wells

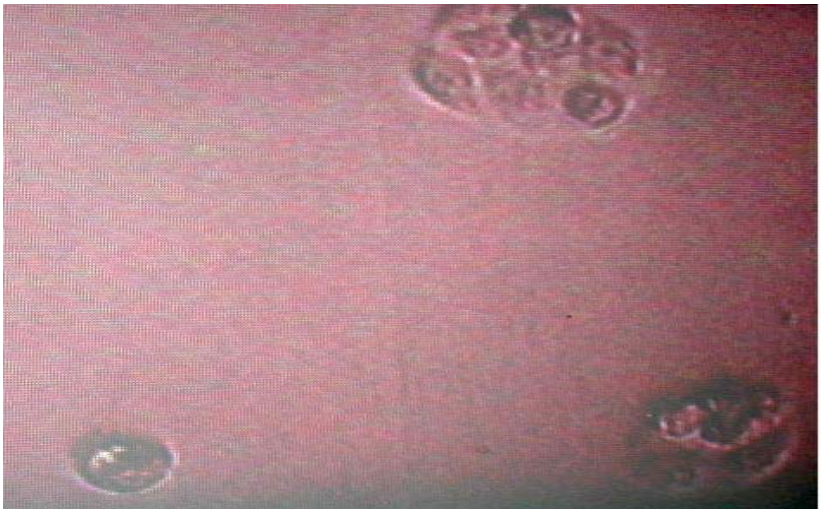

Picture 4.5. Colonies one day after reseeding

Picture 4.6. Colonies and single cells after the weekend

4.3.3. Tumour repopulation mechanisms: modelling of post irradiation accelerated repopulation in squamous cell carcinomas

4.3.3.1. Methods used in the theoretical modelling

In order to evaluate the plausibility of cell recruitment, accelerated stem cell division and loss of asymmetry in stem cell division being the mechanisms responsible for accelerated tumour repopulation during radiotherapy, the three mechanisms have been implemented into the developed tumour model.

Conventional radiotherapy for squamous cell carcinomas of the head and neck with a standard fractionation schedule (2 Gy/fraction, 1 fraction/day, 5 days/week over 7 weeks) has been simulated on the virtual tumour consisting of 10^5 cells and with repopulation mechanisms implemented. The surviving fraction after a dose of 2 Gy (SF_2) for squamous cell carcinomas of the head and neck indicated by the literature is in the order of 54% (Malaise 1986). This SF_2 value has been implemented in the model and all the repopulation mechanisms simulated are applied to the surviving cells.

4.3.3.1.a Cell recruitment

Cell recruitment has been simulated as a cyclic process by which every radiotherapy fraction stimulates a certain percentage of resting cells into proliferation. With every recruitment sequence, a percentage (t_q) of the quiescent cells re-enters the mitotic cycle, regaining their ability to proliferate. These cells are, in part, finitely proliferating cells (P) that have limited capabilities for mitotic division and also stem cells (S), with infinite proliferative ability. The percentage of the recruited stem cells has been set to s_q. Thus s_q out of t_q recruited cells are re-cycling stem cells (Appendix D). The exact proportion of stimulated cells is not well documented in the literature. For simplicity, a value of 50% has been chosen for the total recruitment and 4% for the stems recruited. As the

percentage of quiescent cells is approximately 85% N (where N is the total number of cells), the amount of re-cycling stems is 1.7% N.

4.3.3.1.b Accelerated stem cell division

Accelerated stem cell division implies a decrease in cell cycle time. The mean value for the cell cycle time of the virtual squamous cell carcinoma is 33 hours. This has been reduced to a fixed value of 3 hours for stem cells, as a response to radiation injury. Although such short cell cycle time might be improbable in mammalian cells, the reason for modelling with extreme values is to quantify the effect of accelerated stem cell division on tumour repopulation for a wide range of cell cycle times (rather than extrapolating from higher values) and to obtain a comprehensive cell survival curve. Consequently, at the start of radiotherapy, all the stem cells undergoing mitosis will have their daughter cell cycle times shortened. Shorter cell cycle times (< 3h) have also been employed in order to indicate possible tumour regrowth due to accelerated division as a sole mechanism. The cell cycle time of the finitely proliferating cells has not been affected.

Also, the influence of the onset of repopulation by accelerated stem cell division, on tumour control was studied. A sensitivity study on the onset of repopulation was undertaken, with accelerated stem cell division being triggered by various tumour sizes, therefore at different times after the start of treatment. The time for the onset of repopulation varied in the range of 1-7 days after the start of the treatment.

4.3.3.1.c Combined accelerated stem cell division <u>and</u> cell recruitment

The sensitivity of the recruitment related parameters to variations in t_q and s_q has been analysed. Firstly, various $t_q : s_q$ ratios have been considered that provide the same amount of stem cells recruited. Surviving curves have been plotted and compared, and also the variation of cell population with stem cell cycle time for various $t_q : s_q$ ratios analysed. The pre-irradiation cell cycle time of the stem cells (33h as a main value) has been decreased after the start of radiotherapy with values ranging between 1h and 10h (because of the lack of clinical data, allocating a distribution function to these values

would give the same level of uncertainty as working with fixed values). Secondly, the percentage of recruited cells t_q was kept at a constant rate (50%) while the fraction of recruited stem cells s_q was varied (between 2% and 90%). Furthermore, the effect of the length of stem cycle time on tumour repopulation, both with and without recruitment, was analysed.

4.3.3.1.d Loss of asymmetrical division

Finally, the loss of asymmetrical division of stem cells has been built upon the above mentioned mechanisms. The loss in asymmetry creates symmetrical cells at mitosis, which means that the number of stem cells should double with each division. As the percentage of stems affected by this mechanism is not well documented, a sensitivity study has been performed to obtain clinically realistic values. Consequently, percentages of stem cells ranging from 3% to 10% have been subject to symmetrical division and the outcomes analysed.

4.3.3.2. Results and discussion

4.3.3.2.a Cell recruitment

The two cell survival curves for a no-regrowth model and a cell recruitment model (total recruitment versus stems recruited (t_q/s_q ratio of 50/4) are shown in Figure 4.20. Daily cell kill is substantiated by the 'step' pattern of the survival curve where the plateau areas represent the behaviour of the tumour over the weekend, when there is no treatment. The differences in tumour kill are more evident towards the end of the treatment when the population drops to a small number of cells. There is a slight shift of the recruitment curve towards shorter treatment times, indicating a better tumour control compared to the case when no recruitment is employed. The reason for this behaviour is the redistribution of quiescent cells back into mitotic cycle. Cells in the quiescent phase have higher radioresistance than cycling cells, therefore, once in the cycle, the probability of cell kill increases.

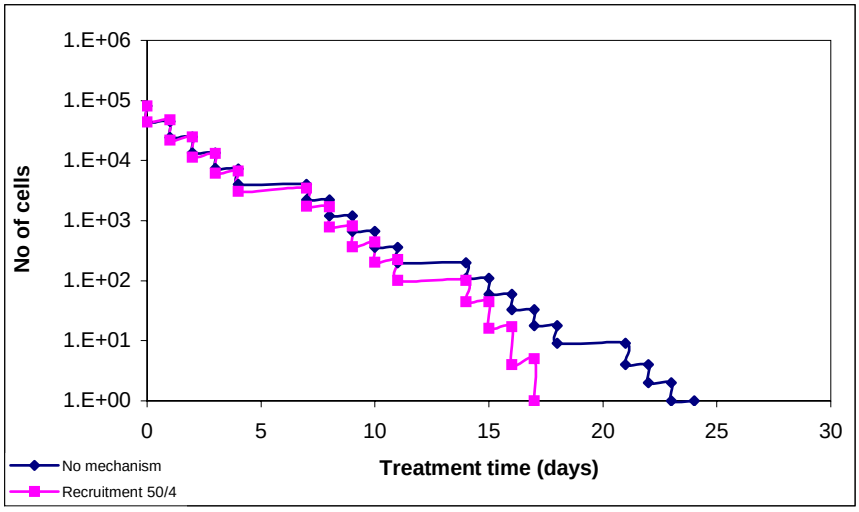

Figure 4.20. Cell survival curves: recruitment (50/4) versus no recruitment.

Four t_q/s_q ratios (5/40, 25/8, 50/4 and 67/3), leading to the same percentage of stems recruited (1.7% N), have been analysed to examine the sensitivity of regrowth on the t_q/s_q ratio. The total cell survival and the stem cell survival curves for these ratios are illustrated in Figure 4.21. Only the curve given by the average values is presented and the error bars show the variance (corresponding to the four ratios), at treatment time (t), in survival numbers with the four simulations. This curve demonstrates that cell recruitment

a) does not significantly alter the shape of the survival curve, irrespective of the t_q/s_q ratio.,
b) does not change the proportion of stem to total number of cells in the survival curves.

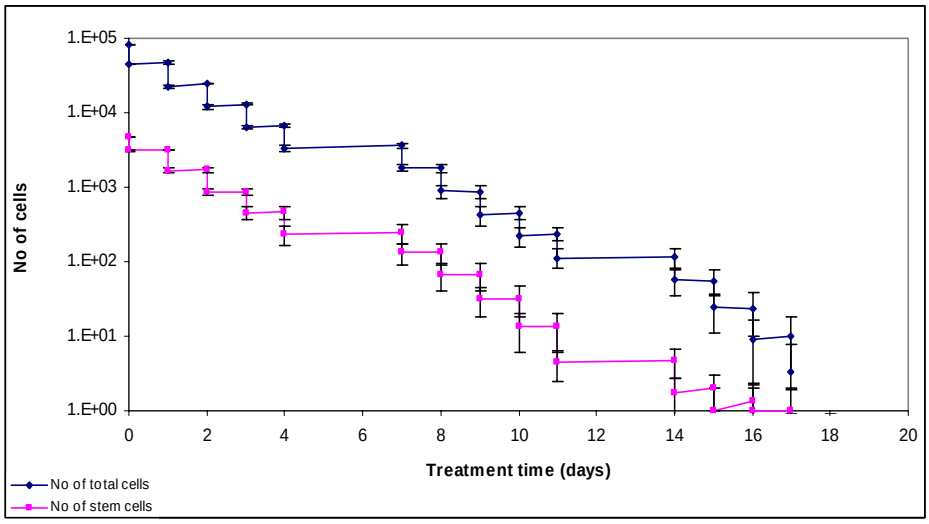

Figure 4.21. Cell survival curves for tumour population as a whole and also for the population of stem cells.

These results also support the use of only one of t_q/s_q ratio (50/4) to be representative of all ratios when cell recruitment is combined with other accelerated growth mechanisms.

The overall conclusion that may be drawn therefore is that cell recruitment does not lead to accelerated regrowth and, more specifically, increases the slope of the total cell survival curve through the radiosensitizing effect of bringing quiescent cells into cycle.

A sensitivity study on the variation of recruitment-related parameters has been completed. The percentage of total recruitment (t_q) was kept at a constant rate of 50%, while the fraction of recruited stem cells (s_q) was varied between 2% and 90%.

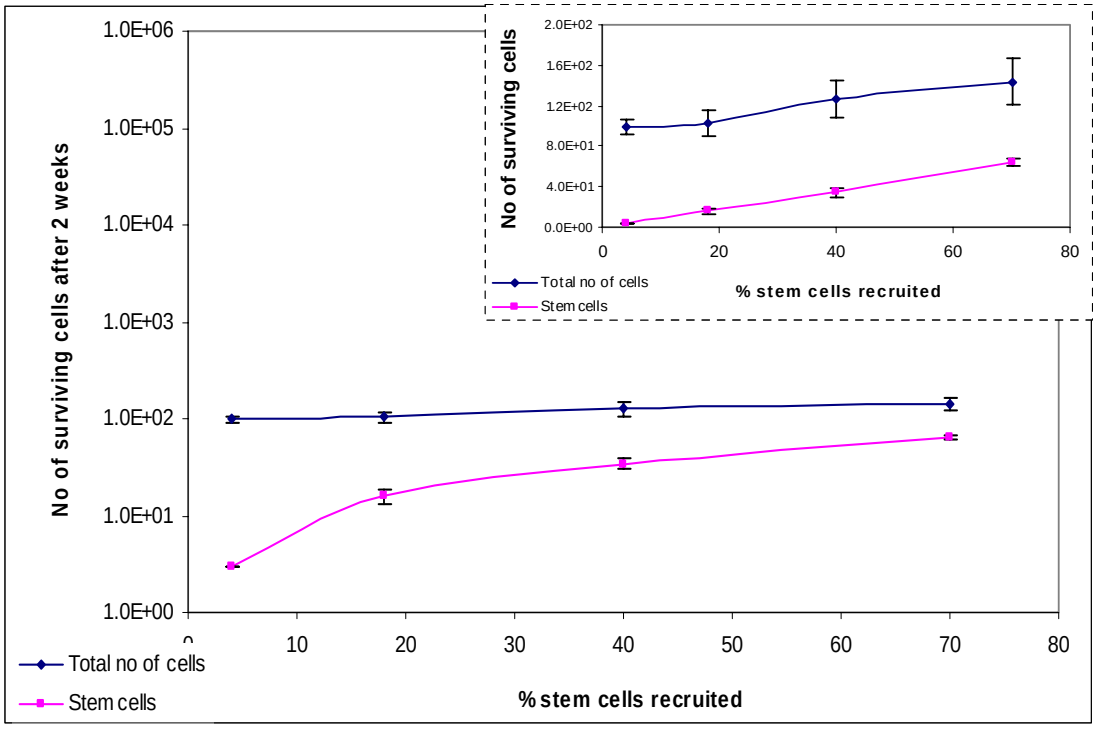

Figure 4.22. The effect of percentage of stem cells recruited from a fixed overall recruitment on cell population.

Figure 4.22 represents the number of surviving cells after two weeks of radiotherapy both for *the tumour as a whole* and for *the stem population*. There is a linear dependence (see the window of Figure 4.22 with the graphs represented on the linear scale) between the percentage of stem cells recruited and the number of surviving tumour *stem cells* (N_r). Considering the semi logarithmic scale, this relationship can be simply formulated as:

$$N_r = k_1 \ln f_{stem} - k_2,$$

where f_{stem} represents the percentage (fraction) of stem cells recruited and k_1 and k_2 are constants.

Less accentuated is the influence of stem recruitment on the *tumour as a whole*, as the increase in cell number due to recruitment is compensated by the cell loss (both natural and radiation kill). As G_0 is a more resistant phase than G_1, once in the cycle, the previous quiescent cells are more prone to radiation damage than before. Thus cell kill will balance cell production supplied by the recruitment mechanism.

4.3.3.2.b Accelerated stem cell division

A cell survival curve that includes accelerated stem cell division (cell cycle time of 3 hrs) has a lesser slope than a cell survival curve including recruitment (Figure 4.23). Accelerated stem cell division implies a shortening of the cell cycle time, thus an increase in stem cell production. The in-between fraction regrowth quantitatively illustrates the strength of the two mechanisms.

Repopulation has been expressed as the percentage increase in cell population between fractions. With cell recruitment at a t_q/s_q ratio of 50/4, the overnight repopulation increased up to 12% in the second week of treatment, with an almost zero increase over the weekend. The tumour was eradicated after the third week of treatment. Overnight repopulation with accelerated stem cell division reached 25% while repopulation over the weekend exceeded 100% after the fourth week.

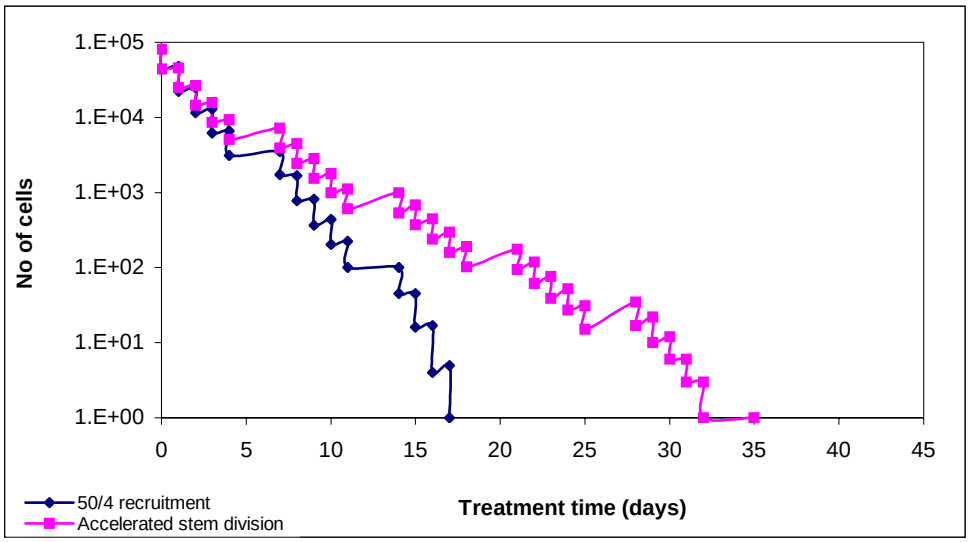

Figure 4.23. Cell survival curves: accelerated stem cell division versus recruitment.

A study on the influence of stem cell cycle time on the tumour population as a whole and also on the stem population has been executed.

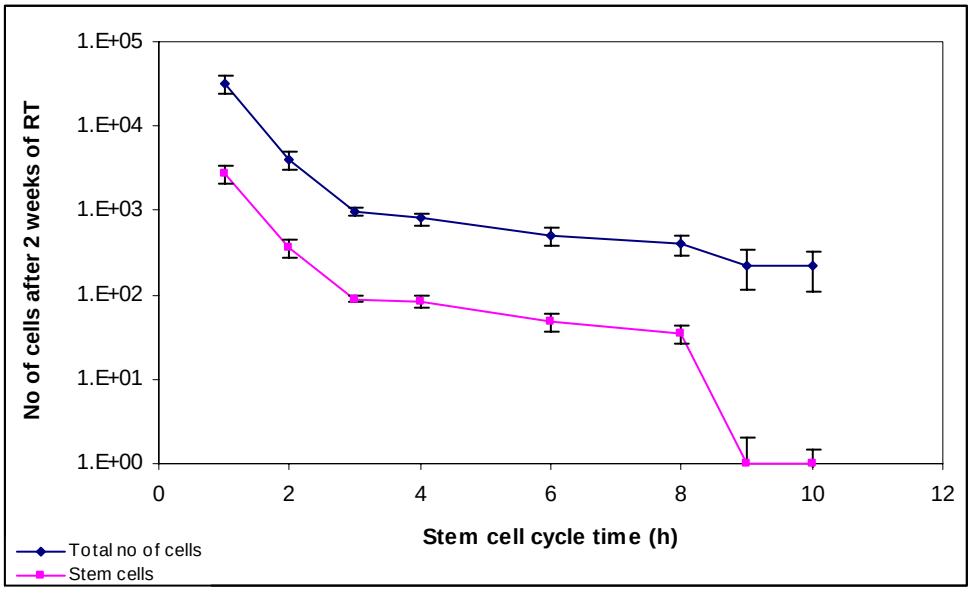

Figure 4.24. The variation in the number of surviving cells as a function of stem cell cycle time.

Figure 4.24 illustrates the increase in cell survival (N_s) with the shortening of the cell cycle time (t_{stem}), which, on a semi logarithmic scale, is described by a power function:

$$N_s = \frac{k_3}{t_{stem}^n}$$

where k_3 is constant.

When very short cell cycle times are employed (Figure 4.25), it is to be noted, that only a 1 hour-short cycle time can lead to repopulation, considering accelerated stem cell division as sole repopulation mechanism. It is shown that the 2 h cell cycle time for the stems is inferior in regard with tumour control to the 3 h one, however, the maximum cell cycle time that could lead to repopulation would be 1 h. Obviously, the question arising from these results would concern the biological validity of this value. A 1 h cell cycle time would be quite improbable to occur as a response to radiotherapy. Therefore, it would be pertinent to conclude that accelerated stem cell division, although it contributes towards accelerated repopulation, is not the key mechanism leading to this phenomenon.

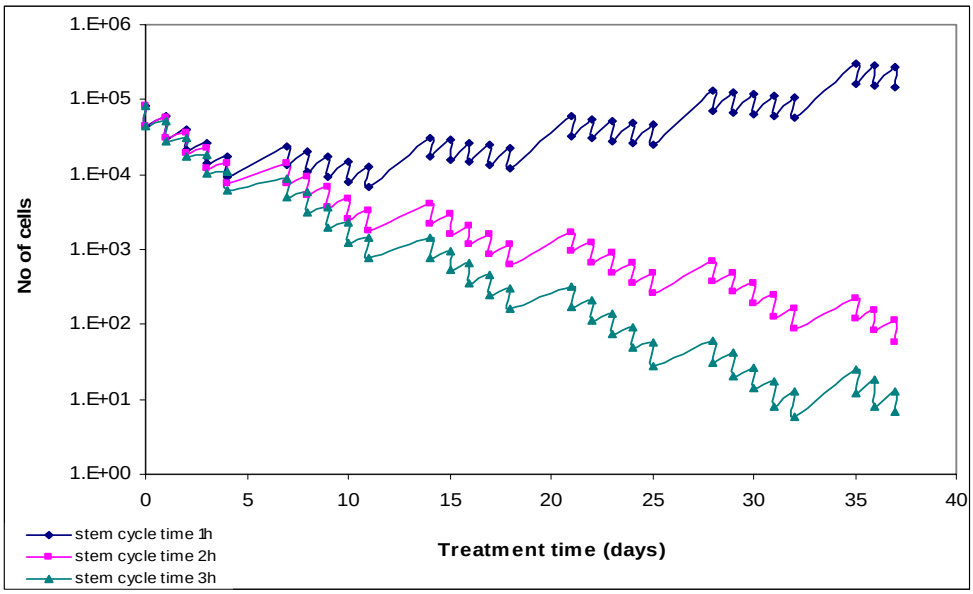

Figure 4.25. Cell survival curve with accelerated stem cell division with various cell cycle times.

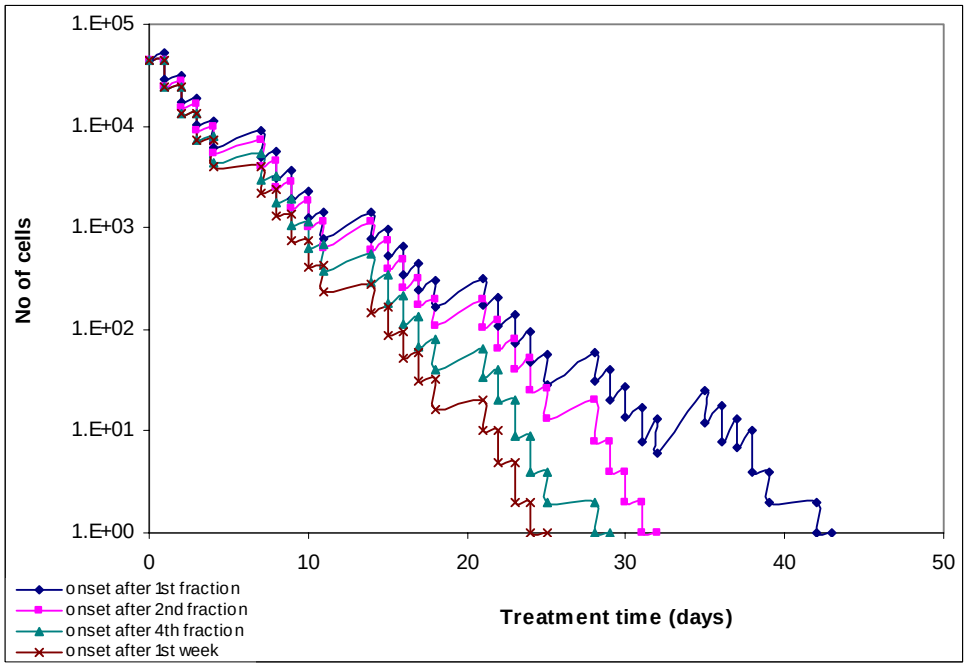

Figure 4.26. Cell survival curves for various onset times for accelerated repopulation (cell cycle time 3h).

The influence of the onset of repopulation by accelerated stem cell division, on tumour control, was studied. The curves in Figure 4.26 represent cell survival with accelerated stem cell division, for a constant value of cell cycle time of 3 hours. The onset of repopulation was varied, from the very first radiation fraction to the end of first week of treatment. The curves illustrate the increasing tumour control with later onset of repopulation. Since the number of stem cells during treatment decreases, the later the mechanisms of accelerated stem division is activated, the less number of stems are affected, so fewer cells will contribute towards repopulation.

As the experimental data from the squamous cell carcinoma line has indicated that the immediate onset of repopulation might be possible, this consideration has been adopted for subsequent studies.

4.3.3.2.c Combined accelerated stem cell division <u>and</u> cell recruitment

The combination of the two mechanisms indicates an additive response (Figure 4.27). Quantitatively, with a contribution of accelerated stem cell division (cell cycle time of 3 hrs) and t_q/s_q ratio of 50/4, the overnight repopulation reached 40% while repopulation over the weekend was over 190% (tumour population before the Monday's fraction as compared to the surviving population after the Friday's irradiation) after the fourth week., which illustrates the additive effect of recruitment and accelerated stem division.

Although recruitment leads to a greater rate of kill (section 4.3.3.1), when combined with accelerated stem cell division there is a decreased rate of cell kill (accelerated growth) beyond that of accelerated stem division alone. The accelerated growth is explained by the mutual interaction between the mechanisms of cell recruitment and accelerated stem division. Explicitly, as the recruited stems are undergoing mitosis, their stem progenies will suffer a shortening of the cell cycle, which in time is materialised by an increase in stem population, thus a more rapid growth. Therefore, in the 'combined' scenario, the process of recruitment contributes towards regrowth with re-cycled stem cells, thus a

larger number of stems are involved than in the situation when accelerated stem division is modelled alone.

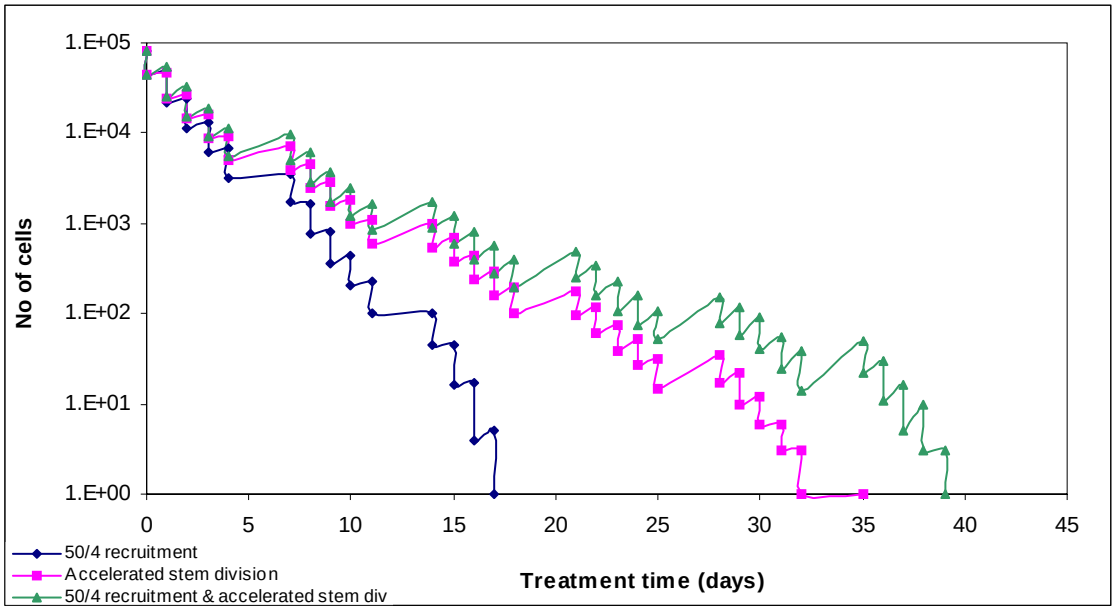

Figure 4.27. The effect of accelerated stem division combined with recruitment.

However, tumour kill still dominates regrowth which is illustrated by the continuously decreasing survival curve. Therefore volume response to treatment is represented by the regression curve, as shown by the graph (Figure 4.28).

When combining recruitment and accelerated stem cell division (Figure 4.29), the survival curves for a fixed recruitment and various stem cycle times show the same pattern as the curves for accelerated division alone.

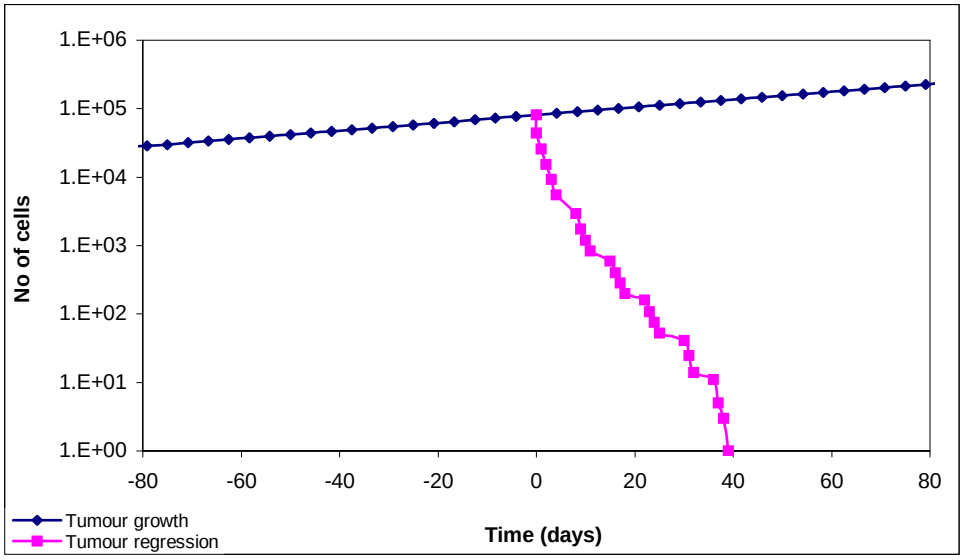

Figure 4.28. Tumour growth and regression curves with recruitment and accelerated stem cell division.

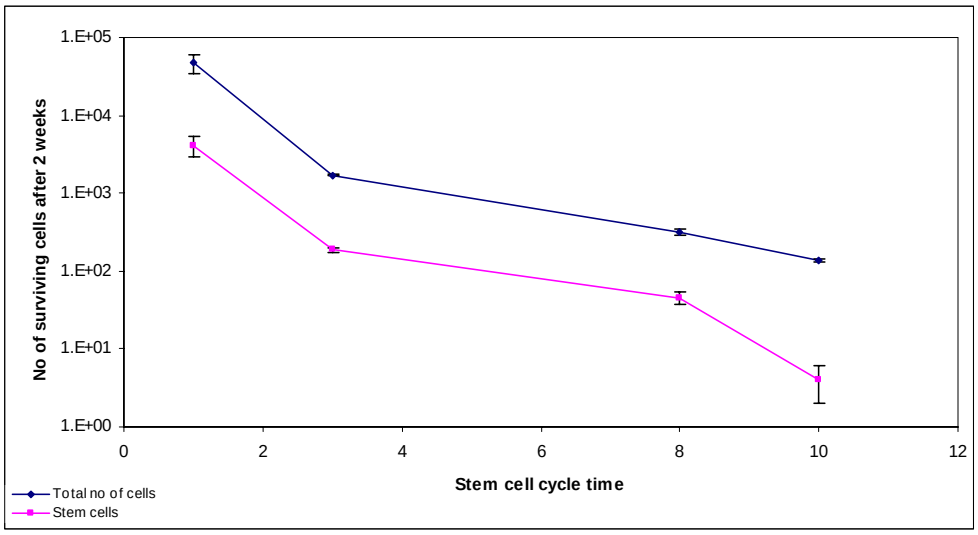

Figure 4.29. The effect of the combined recruitment – accelerated stem division on cell survival for various stem cell cycle times.

Thus:

$$N_{r,s} = \frac{k_4}{t_{stem}^n},$$

where $N_{r,s}$ is the number of surviving cells after the impact of the combined mechanisms, and k_4 is a constant dependent on the percentage of cells recruited. The effect of the

combined mechanisms on cell regrowth shows that the length of the stem cell cycle time is a more powerful parameter than the recruitment factor.

4.3.3.2.d Loss of asymmetrical division

Figure 4.30 demonstrates that only a small percentage of stem cells (<10%) must lose their asymmetry otherwise the repopulation of the tumour would reach unrealistic proportions in a very short time (within a week). Even with 5% symmetrical division during the whole treatment, tumour repopulation is so high that not even partial eradication is achieved.

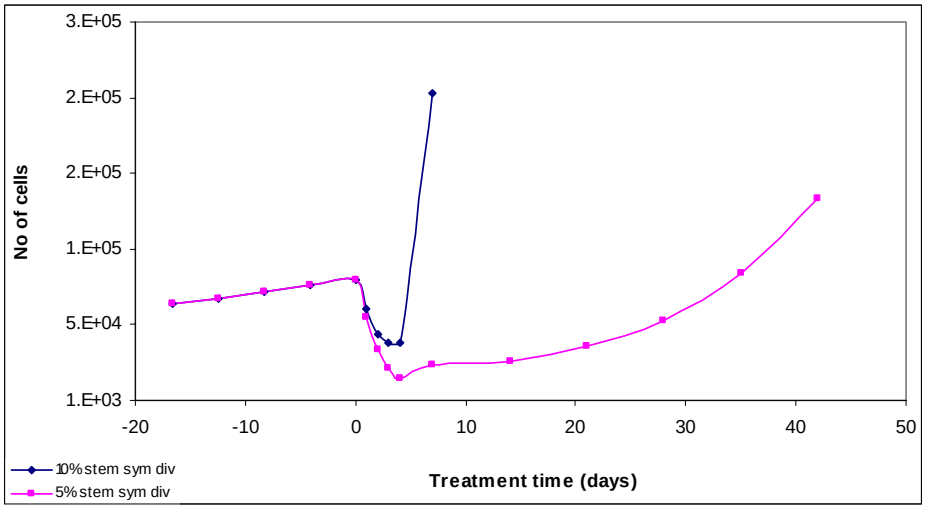

Figure 4.30. Graphs illustrating tumour repopulation during radiotherapy when loss of asymmetry for 5% and 10% of cells is employed.

Furthermore, the process of symmetrical division should reach a saturation stage (similar to the unperturbed tumour growth) unless a continuously increasing repopulation during treatment is expected. A mathematical requirement to achieve a saturation stage would be a decrease in time of the percentage of stems subject to symmetrical division. This result can be attained either by cell death or return to the previous stage of asymmetric division.

The loss of asymmetrical division has been modelled as a cumulative process that starts shortly after treatment, as a response to cell loss and injury, and involves progressively a greater proportion of cells as treatment advances. Therefore, at the beginning of

radiotherapy, there is no significant impact of symmetrical division upon the cell survival curve as the number of cells involved is small, but during the course of treatment, the contribution towards regrowth from newly created stem cells becomes evident and has a strong impact on the survival curve.

4.3.3.2.e Combined asymmetrical division, accelerated division and recruitment

With all the above considerations, Figure 4.31 incorporates the three repopulation mechanisms: with 50/4 recruitment, a stem cell cycle time of 3 hours and an initial of 3% stems dividing symmetrically then increasing to 6% and getting back to the asymmetrical division. The regrowth shoulder imposed by the variation in stem population along treatment is seen in the volume response curve, shortly after treatment started.

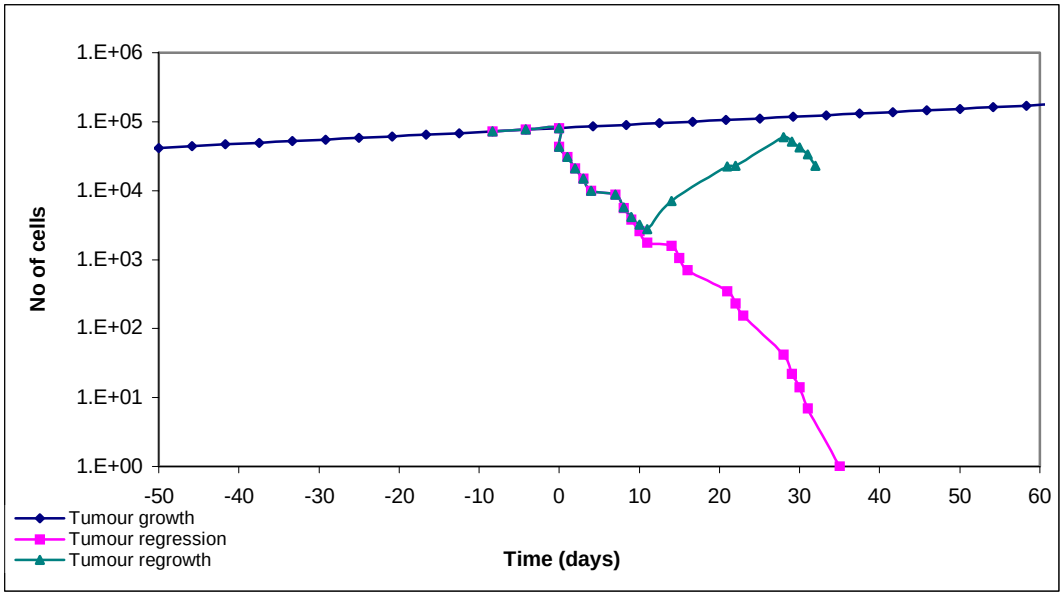

Figure 4.31. Tumour growth, regression and regrowth curves for loss of asymmetrical division.

4.3.3.2.f Distributions of cell types

The percentage of the three cell types (stem:finitely proliferating:nonproliferating) has been represented as a function of treatment time. When no mechanism is considered, the quiescent cells are predominant, while the percentage of stem and finitely proliferating cells is very small, similarly to an unperturbed tumour (as the only difference here between irradiated and unperturbed tumour is the total number of cells) (Figure 4.32).

With recruitment and accelerated stem division, the S:P:N ratio is changed after 4 weeks of treatment, from 5:8:87 for the no-mechanism case to 18:58:24 (Figure 4.33). The S:P:N ratio predominantly changes over the first 4 days of treatment due to the early onset of repopulation. The increase in S%, from 5% to 18%, is of a major importance towards accelerated repopulation since only stem cells are able to repopulate the tumour because of their 'indefinite' proliferative capacity.

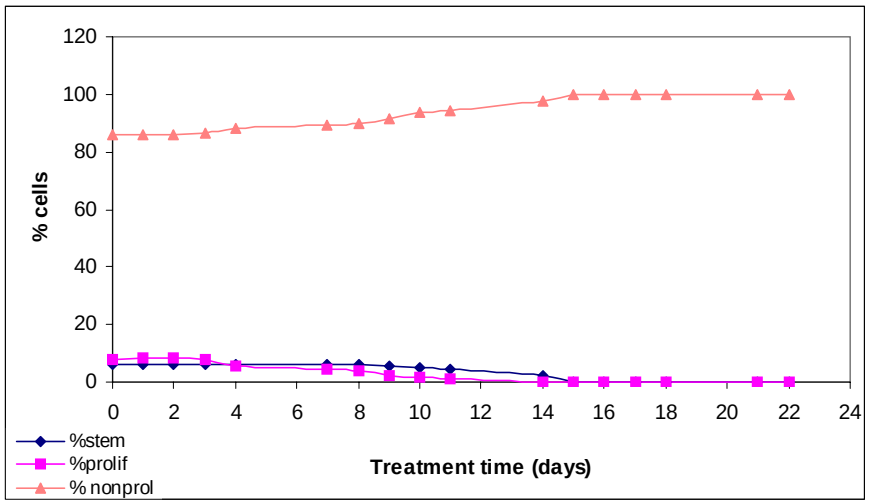

Figure 4.32. S:P:N ratio without radiation- induced mechanisms (on treatment day '0' the effect of the first dose is already simulated).

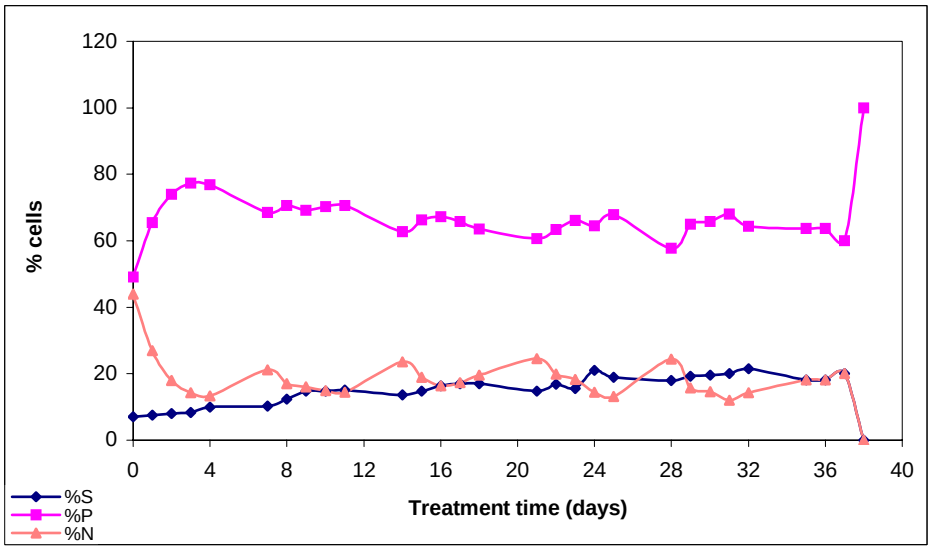

Figure 4.33. S:P:N ratio with radiation- induced cell recruitment and accelerated stem division.

The inclusion of loss of asymmetrical division with the other two mechanisms dictates a new S:P:N ratio of 25:49:26 after 4 weeks of treatment. Because of the non-linear distribution for asymmetry loss (§4.3.3.2.d), the S:P:N ratio continually changes along treatment, reaching a peak of 31% for the stem cells of in the second treatment week (Figure 4.34).

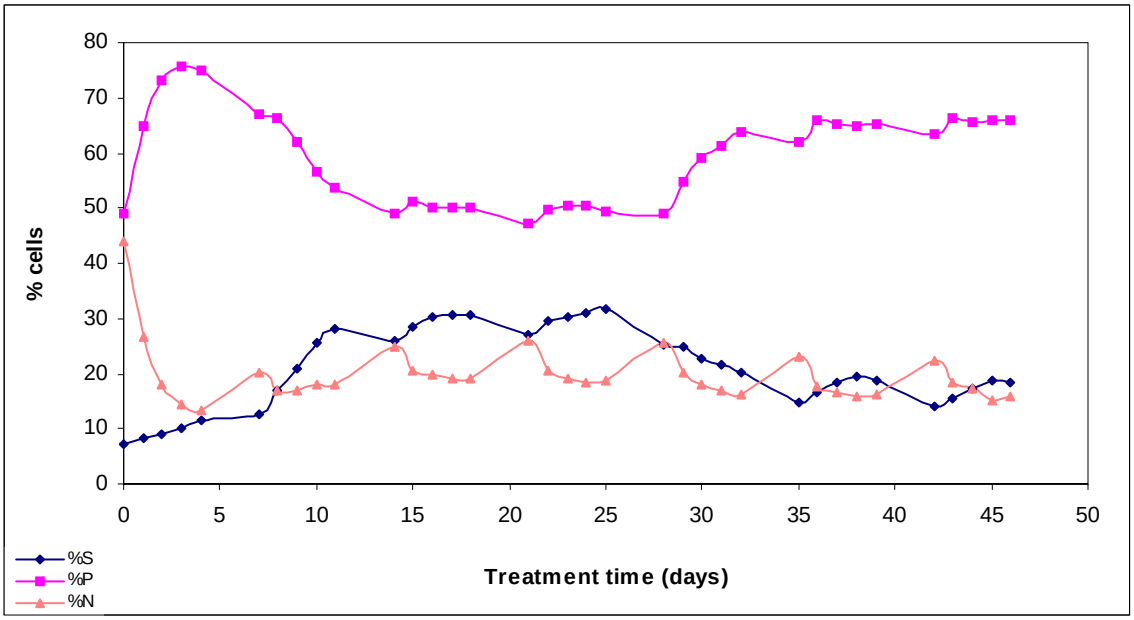

Figure 4.34. Change in S:P:N ratio for asymmetry loss.

It is appropriate to note that the aim of the present model was to study the temporal distribution of the tumour: tumour regrowth and regression on a time scale. The regrowth mechanisms implemented in the model are discussed in the literature (Dorr 1977, Trott 1999, Trott 1999). In none of the above mentioned papers is the effect of spatial change on the regrowth mechanisms indicated as dominating over the temporal effects. The major trigger that the current model has considered was the cell loss due to treatment, which is described in a temporal manner, and so are the regrowth mechanisms that are activated once the treatment started.

4.3.3.3. Conclusion

Cell recruitment does not constitute a key mechanism in tumour repopulation after radiotherapy. However, when combined with accelerated stem cell division, cell

recruitment shows a contribution towards regrowth through the additive effect of the two mechanisms. The mechanism of accelerated stem cell division shows a twofold decrease in tumour control (Figure 4.23) (which indicates the presence of tumour regrowth) compared to cell recruitment. Nevertheless, tumour regrowth was shown to be more pronounced with recruitment *and* accelerated division than with accelerated stem division alone.

Loss of asymmetry in stem cell division could be the key process in tumour regrowth.
It has been concluded by the present work that stem cells must be affected by the loss of asymmetry only in small percentage (less than 10%), otherwise the repopulation of the tumour would reach unrealistic proportions in a very short time (within a week). The work shows, that even for small percentage of stems (5%) affected by symmetrical division during the whole treatment, tumour repopulation is so high that not even partial eradication is achieved. Furthermore, the process of symmetrical division should reach a saturation stage (similar to the unperturbed tumour growth) unless a linear repopulation during treatment is expected. Moreover, the stems affected by this mechanism should follow a non-linear distribution function. With a linear implementation of asymmetry loss the tumour grows continuously, despite the cell kill produced by radiation. A more appropriate description is given by a non-linear distribution, which reaches ‘saturation’ and afterwards decreases as the rate of cell kill overcomes the rate of repopulation.

The percentages of the three cell types: stem, finitely proliferating and nonproliferating varies during radiotherapy, thus altering the initial composition of the tumour. Tumour repopulation involves a drastic change in the S:P:N ratio along the treatment.

Cell recruitment, accelerated stem cell division and the loss of asymmetrical division of stem cells, are all mechanisms determining, to a certain extent, tumour repopulation after radiotherapy.

4.3.4. Conclusions derived from experimental data supporting the theoretical model

The onset and the mechanisms of repopulation for a squamous cell carcinoma have been studied both experimentally and theoretically (§4.3.2 and §4.3.3). This section is a summary of the conclusions derived from the two studies:

- The onset of tumour repopulation due to radiotherapy could be activated from the commencement of the treatment. The survival curve resulting from the experimental data has indicated a possibility for the immediate start of repopulation with treatment. Also, the theoretical model has illustrated that the later the onset of repopulation, fewer proliferating cells are available to rebuild the tumour, therefore the rate of tumour repopulation during radiotherapy is reduced.

- Cell recruitment is not the key mechanism in repopulation. From the cell line experiment it was shown that repopulation occurs, even without having quiescent cells available for recruitment, therefore other mechanisms should be found responsible. Even when large percentages of quiescent cells have been recruited, the survival curve gave no indication that the tumour would repopulate during treatment.

- Stem cells are not affected equally by irradiation. The qualitative examination of the cell population reseeded in wells has indicated that some cells have formed colonies, others remained undivided. Also, some of the colonies were smaller, others larger in size. The theoretical model has resulted in limited amounts of stems dividing symmetrically, as large number of stem cells loosing their asymmetrical division would have overgrown the tumour in unrealistically short period of time.

Chapter 5

Modelling the effect of chemotherapy (cisplatin) on tumour growth

5.1. Introduction

Although chemotherapy has revolutionized the treatment of haematological tumours, in many common solid tumours the success has been limited. Some of the reasons for the limitations are: the timing of drug delivery, resistance to the drug, repopulation between cycles of chemotherapy and the lack of complete understanding of the pharmacokinetics and pharmacodynamics of a specific agent.

Chemotherapy is a rather general term used to describe the treatment of tumours with drugs, as each chemotherapy agent acts via many different pathways. Drugs often differ in biochemical structure, molecular mode of action, pharmacology, clearance and side-effects. Moreover, in chemotherapy there is no formalism corresponding to the linear quadratic model used in radiotherapy which would describe, in a simple manner, cell survival. Therefore, modelling chemotherapy can be a difficult task. However, there is abundant literature on models of drug pharmacokinetics and pharmacodynamics, using either analytical or probabilistic methods (Weldon 1988).

Quantitative modelling has a great potential, but requires knowledge of the numerical values of large number of parameters in order to characterize chemotherapy regimens. This information is rarely available, therefore the modelling of combination-

chemotherapy regimens, or of large classes of chemotherapy agents can induce errors and inaccuracies in the simulation process.

While radiotherapy is the primary treatment method for unresectable head and neck carcinomas, chemotherapy comes as a supplementary treatment with added or even synergistic effects. Cisplatin is among the most effective cytotoxic agents in head and neck cancer, with single agent response rates ranging from 25% to 30% (Schwachöfer 1991). When modelling cisplatin as a single agent, only particular properties of cisplatin need to be taken into account, reducing the number of assumptions that are considered in the generalized chemotherapy models: the cisplatin specific molecular action on tumour cells is applied and the implementation of relevant parameters into the theoretical modelling is simplified.

This chapter presents the modelling process of the biological properties of cisplatin, and the implementation into the model of various treatment schedules with cisplatin as a sole chemotherapeutic agent. Furthermore, the simulation of the mechanisms leading to drug resistance and the effect of cisplatin resistance on tumour control are presented. Also, repopulation during chemotherapy, a so far neglected factor, is simulated and the effect of repopulation on tumour control versus drug resistance analyzed.

5.2. Cisplatin

The platinum complex cis-diammine-dichloro-platinum was first synthesized in 1845 (Trimmer 1999), however, the useful biological effects of the compound were not discovered until 1965, when biophysicist Barnett Rosenberg was examining the effects of electrical fields on *Escherichia Coli*. He observed that cells held between charged platinum electrodes grew in size but did not divide (Rosenberg 1965). The inhibitory effect on cell division suggested that cisplatin might have potential as an anticancer agent.

5.2.1. Structure

Cisplatin (cis-diammine-dichloro-platinum) is a heavy metal complex, with a central platinum atom surrounded by 2 chlorine atoms and 2 ammonia molecules (Figure 5.1.a). With cisplatin, the chlorine atoms are situated on the same side of the platinum complex (*cis* position).

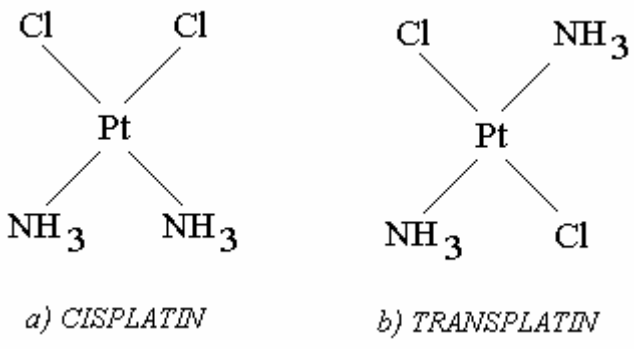

Figure 5.1. The structures of cisplatin and transplatin.

5.2.2. Properties

There are 5 major characteristics that are considered to be responsible for the cytotoxic effects of cisplatin:

- radiosensitiser - through the inhibition of the repair of potentially lethal damage and sublethal damage caused by radiation,
- hypoxic cell sensitiser,
- cell-cycle perturbator,
- angiogenic inhibitor,
- ability to form DNA adducts.

The paragraphs below describe briefly cisplatin's properties.

Randomized trials on head and neck cancers have shown that combination treatment (cisplatin – radiotherapy) improves survival compared to radiation treatment alone. This result is due to the cooperation between cisplatin and radiotherapy at the cellular level.

Radiosensitization of tumour cells by cisplatin is believed to be mediated through a variety of mechanisms, including inhibition of DNA repair, a radiation-induced increase in cellular platinum uptake and cell-cycle arrest (Lawrence 2003). Fortunately, the uptake of cisplatin in normal cells is not amplified by the combined modality treatment. To date, the selectivity of cisplatin radiosensitization still remains unsolved.

Radiosensitization of hypoxic cells by cisplatin was demonstrated in laboratory by Douple and Richmond (1979). The process of sensitization was due to the scavenging of hydrated electrons by the platinum complex and creation of local concentrations of OH radicals which, eventually, damage the DNA.

Although considered a cell cycle phase non-specific drug, cisplatin is more toxic to dividing cells than to quiescent cells. Besides its cytotoxicity, cisplatin is also cytostatic, by arresting the cells in the G2 phase of the mitotic cycle. At low concentrations, cells accumulate in the G2 phase for 1-3 days in order to repair critical damage before continuing to proliferate. At higher concentrations, the cells still progress to G2, and eventually undergo apoptosis (Sorenson 1990, Lippert 1999). Cell cycle arrest at G2 is very relevant to the in vivo action of cisplatin, and subsequent lethal mitosis may be the most significant mechanism of cell death induced by cisplatin (Lippert 1999).

The suppression of tumour neovascularization by cisplatin is a property that has been identified recently and is under further investigation (Yoshikawa 1997). In this study, the effect of cisplatin on endothelial cell proliferation in vitro was examined. Significant inhibition of endothelial cell growth was observed at concentration which is attainable in the serum of treated patients.

Probably the most important property of cisplatin is the ability to form DNA adducts. Cisplatin is proficient in forming both intrastrand and interstrand adducts with DNA (Prestayko 1980). Although the number of interstrand cross-links (Figure 5.2.) is less

than 1% of the total adducts, Reed and Kohn (1990) consider this type of adduction responsible for the cytotoxic effect of cisplatin. The *trans* isomer (with the chlorine atoms located across the platinum complex), transplatin (Figure 5.1.b), has proved to be inactive on tumour cells (Reed 1990) as it cannot be linked interstrand to the DNA, but can form intrastrand adducts. However, Sorenson (1990) relates cisplatin's cytotoxicity to the DNA-intrastrand crosslinks, concluding that the relative contribution of each lesion to toxicity is still in contention. Nine years later (Go, 1999), the question on the types of DNA lesions responsible for the cytotoxicity of cisplatin has still not been elucidated.

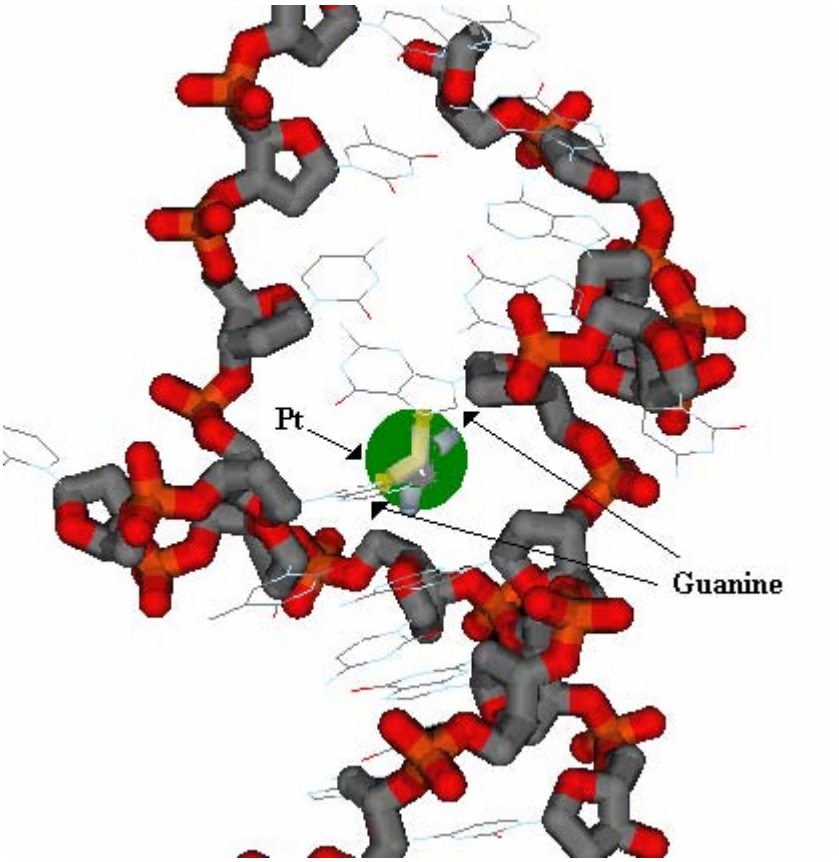

Figure 5.2. Cisplatin-DNA interstrand adduct.

5.2.3. Kinetics

The pharmacologic behaviour of cisplatin is determined by an initial aquation reaction consisting in the replacement of the chloride ligands by water molecules. This reaction is

driven by the high concentration of water and low concentration of chloride in tissue. The aquated platinum complex then covalently binds to macromolecules: DNA, RNA and proteins and forms cytotoxic adducts. The adduct formation is a fast process, as is the half-life of adducts (3.5 h). During a 24 h period after 1 h exposure to platinum compounds, most of the DNA adducts would have disappeared giving little effect on the tumour growth (Schwachöfer 1991). This might explain the total absence of an additive effect when cisplatin is given 24 h before irradiation.

The major mechanism of cisplatin-induced cell death is apoptosis. Cisplatin causes a slow-down of cells in S phase and initiates apoptosis (Ormerod 1996).

5.3. Literature review on chemotherapy models

5.3.1. General review

Several mathematical models of chemotherapy consider generalized analytical models for cycle-specific and cycle-non-specific therapies, respectively. The main differences between the above mentioned two categories lie on the parameters quantifying cycle specificity: change in loss factor and variation in growth fraction (Weldon 1988). Many such models assume that the growth fraction of the tumour cell population responds instantaneously to cell killing by chemotherapy. This is not realistic, as drug pharmacokinetics indicates the existence of a drug ‘binding time’ to achieve cell damage, which does not occur instantaneously. Some chemotherapeutic agents need several hours to form cytotoxic DNA adducts (Welters 1999). Moreover, numerous drugs express cytostatic properties, thus arresting the cells, before dying, into one of the cycle phases. Cell arrest can last for days (Sorenson 1990) therefore the instantaneous kill is not validated.

There are models studying the effect of various drug concentrations and exposure times on tumour control. Gardner (2000) proposes an exponential kill model to predict the shape of dose-response curves based on several parameters: cycle phase specificity of the drug, cycle time, drug concentration and exposure time. The analytical equations presented are able to predict the inhibitory concentration to achieve a certain percentage of cell kill.

Several studies have used the 'area under the time-concentration curve' (AUC) as an approach to model chemotherapy. The area under the curve is a commonly used measure of total drug exposure, and is obtained by plotting the concentration of the agent as a function of time. The AUC is obtained by integration. While for some drugs (like alkylating agents) the effect is proportional to the AUC (Tannock 1998), for others, the duration of exposure may be more important than concentration, therefore the relationship between AUC and tumour response is weaker. Studies with cisplatin show that AUC is a good predictor of response (Schellens 1996, Levasseur 1998, El-Kareh 2003). Moreover, since the magnitude of exposure to cisplatin is, through the DNA-adducts formation, the major determinant of the response rate, the AUA (area under the DNA adduct-time curve) also offers a reliable prediction in tumour response (Schellens 1996).

The AUC models are usually based on in vitro data regarding time-dependency of drug potency, slope of the concentration-effect curves, and relative degree of drug resistance. Levasseur et al (1998) have created a pharmacodynamic model to facilitate the quantitative assessment of the growth-inhibitory effect of anticancer agents as a function of concentration and exposure time. Empirical mathematical expressions were built into a global concentration-time-effect model which showed that it was possible to modulate drug effect, response heterogeneity, and drug resistance by altering the time of exposure to the agents.

A compartmental model of cisplatin cellular pharmacodynamics (El-Kareh 2003) considers transport reaction processes between extracellular and intracellular

compartments, with drug species classified in: extracellular concentration, intracellular concentration, concentration bound to DNA and concentration released from DNA as a result of DNA repair. The model is based on the assumption that cell kill depends on the peak level of DNA-bound intracellular platinum and for short exposure times it yields predictions similar to those resulting from AUC-type models.

5.3.2. Literature review on drug resistance models

Models of drug resistance started to be developed in the late 70s, with the Goldie-Coldman (1979) model on the theory of evolution of drug resistance by clonal selection. Their model was based on biological assumptions stating that drug resistance results from clonal selection of randomly occurring mutants which are completely impervious to the drug. The analytical model followed the development of the mutant cell population as well as the sensitive tumour cells, with the consideration that the same growth kinetics applies to both groups of cells. Clinically, such an assumption is not realistic, as sensitive cells are killed more easily than mutant resistant ones. Another oversimplification of their model was to consider drug resistance as all-or-none (mutants completely unreceptive to the drug) since mutations, which confer different levels of resistance, can occur. Therefore, progressively higher levels of resistance can be expected to emerge with continued treatment. The fact that drug resistance ‘cumulates’ in time is illustrated by the model developed in the current work.

Birkhead et al (1986) have designed a model that brings the principles of Goldie-Coldman model closer to the actual clinical practice. The modelled tumour includes three cell categories: cells presenting with intrinsic resistance, the second group characterized by acquired resistance and the sensitive population, responsive to the drug. Various drug concentrations are administered to study tumour response in time. The model relates to chemotherapy treatment in general, therefore, in order to simulate treatment strategies, specific values have to be used for cell-kill and resistance. This requirement is a

limitation to the model, due to the lack of biological data and the uncertainties in the existing values for larger groups of patients.

The literature on chemo-modelling shows that optimum treatment strategies are hard to derive mainly because of lack of quantitative knowledge of the biological parameters of cancer chemotherapy. This is one of the reasons the present work considers one specific drug only for modelling – cisplatin. By specifying the drug, the number of unknown parameters is reduced, and biologic data is easier obtained from specific *in vitro* experiments (Sorenson 1990).

5.4. Modelling of tumour response to chemotherapy: the effect of various schedules of cisplatin on a HNSSC

5.4.1. Introduction

Daily versus weekly administration of cisplatin is still trialed in clinics, although there are results showing better tumour control in favor of daily treatment (Marcu 2003) (Chapter 2).

As already described in §5.2.2 cisplatin can react with the DNA to form interstrand and intrastrand crosslinks. These adducts then inhibit DNA replication and RNA transcription, leading to DNA breaks that can be lethal for the affected cell. Rather than being arrested in the S phase of the cell cycle, as would be expected if DNA synthesis were inhibited, cells are arrested in the G2 phase before dying (Sorenson 1990). The major mechanism of cisplatin-induced cell death is apoptosis. The main property of cisplatin - the formation of DNA adducts that leads to cell cycle arrest and eventually apoptosis – is implemented into the model.

5.4.2. Methods

The effect of daily treatment with cisplatin as a sole treatment agent on tumour control has been simulated. The 'treated' tumour is the virtual head and neck cancer which has been grown in a previous model (Chapter 3) (Marcu 2002). The tumour is composed of stem cells, finitely proliferating cells (limited number of generations) and, finally, nonproliferating (quiescent) cells in a proportion of up to 80% of the total number of cells.

5.4.2.1. Experimental basis

The cisplatin model is based on the data resulting from experiments performed on L1210/0 cell lines by Sorenson et al (1990). After the administration of various doses of cisplatin they concluded that for intermediate/high toxicity concentration of cisplatin (2 μg/mL), more than 80% of the cells were arrested in the G2 phase by 2 days; after 4-6 days, approximately half of the cells were observed as debris. Higher concentrations of cisplatin led to virtually complete disintegration of cells by 6 days post administration. To make the equivalence to the *in vivo* situation, the current model defines as 'clinical dose' the dose that leads to 80% cell arrest. Furthermore, the arrested cells are enrolled from the cycling cells only, given that cisplatin, as chemotherapy in general, affects proliferating rather than quiescent cells.

5.4.2.2. Modelling treatment with cisplatin

The flow chart in Figure 5.3 shows the effect of cisplatin administration on the virtual tumour. Five hours after administration 80% of the cycling cells are 'marked'. Cell 'marking' in the model corresponds to biological DNA adducts formed by cisplatin. When reaching the G_2 phase, those cells which are 'marked' will be arrested. Two days after the 'marking', 50% of the arrested cells are released which would relate to damage repair, and the other half begins apoptosis. Cell kill will occur 72 hours after cell release.

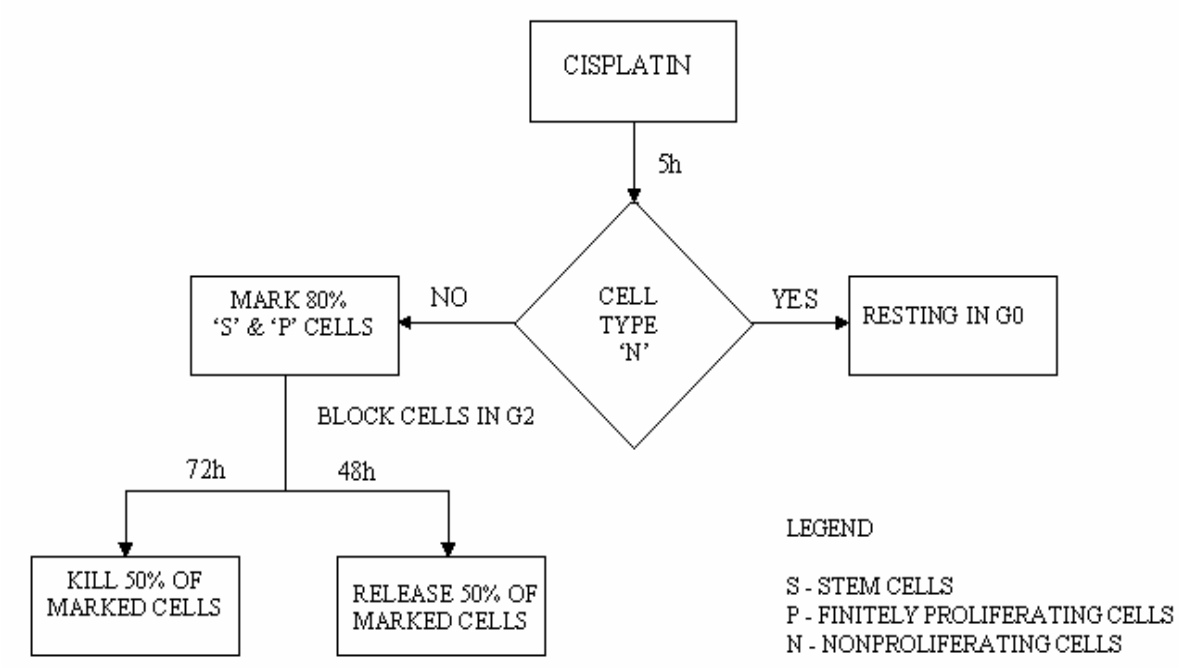

Figure 5.3. Cisplatin action flow chart

Weekly treatment with cisplatin is a very common schedule for head and neck cancers.

In order to model the weekly administration of cisplatin, when in clinics a larger dose is given compared to the daily one, the above described parameters have been changed accordingly. Larger drug doses lead to higher amounts of DNA adducts. It is also known that cell killing increases in direct proportion to lesion frequencies, i.e. DNA adducts, produced by cisplatin (Begg 1990). Therefore, the large dose has been expressed by higher 'marking' and, consequently, by higher killing. For weekly treatment simulation the following values for the three parameters have been used: 95% for cell mark, 40% for cell release and 60% for cell kill. Also, higher drug doses arrest the cells for longer periods in the G2 phase (Sorenson 1990). This fact was illustrated by lengthening the time the cells spend in G2 from the original 48 hours to 72 hours. A further length would be unrealistic, since cells blocked for longer than 72 hours before release, start to disintegrate, not being capable of repair (Sorenson 1990).

5.4.3. Results

5.4.3.1. Cisplatin on a daily schedule

A daily treatment with cisplatin has been simulated to illustrate the behaviour of the tumour population during and after treatment. The curve in Figure 5.4 represents the cell survival for the tumour as a whole. Figure 5.5 presents the survival curves for both cycling and non-cycling cells during daily cisplatin treatment. When comparing Figure 5.4 and Figure 5.5 it can be noticed that the shape of the survival curve for the whole tumour is dictated by the quiescent population, as they dominate in number. It can also be seen that the number of non-cycling cells increases due to natural cell production, while the number of cycling cells decreases as a result of cisplatin's kill. The initial fluctuations in the number of quiescent cells might be explained by the uneven production of individual types of cells during cisplatin treatment, resulting in fewer nonproliferating cells produced between fractions of chemotherapy to compensate natural cell loss. The parameters used to model daily treatment were the following: 80% cells 'marked', 50% cells released (of those marked) and the remaining 50% of cells killed.

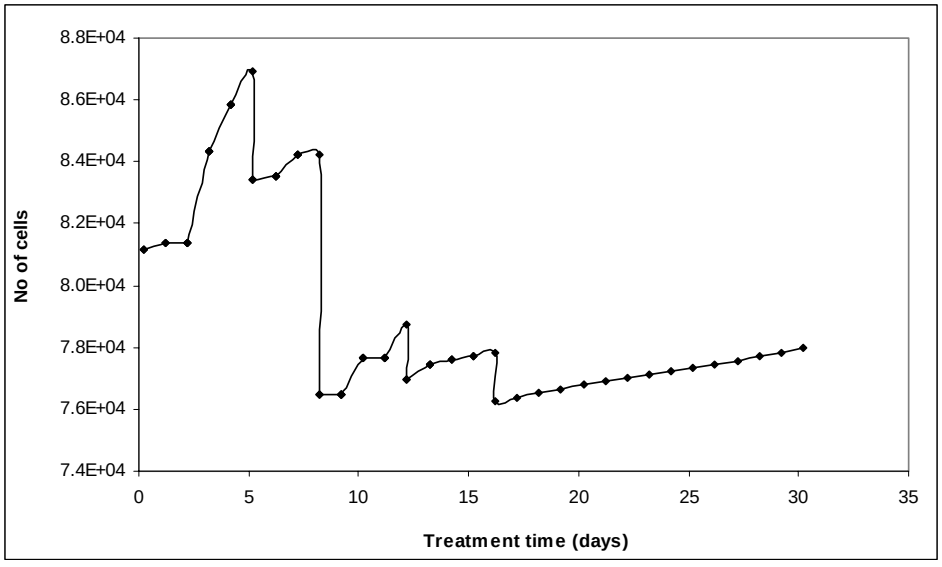

Figure 5.4. Survival curve for the tumour as a whole after 2 weeks of daily treatment with cisplatin.

After the treatment had completed, the tumour was left to grow unperturbed, from the surviving proliferative cells. The two graphs in Figure 5.5 show that, although the tumour growth as a whole increases after treatment, the increase is given by the production of nonproliferating cells originating from the surviving cycling cells. The proliferating population, though not eradicated, reaches a steady state maintained by the counteraction between cell production and natural cell kill.

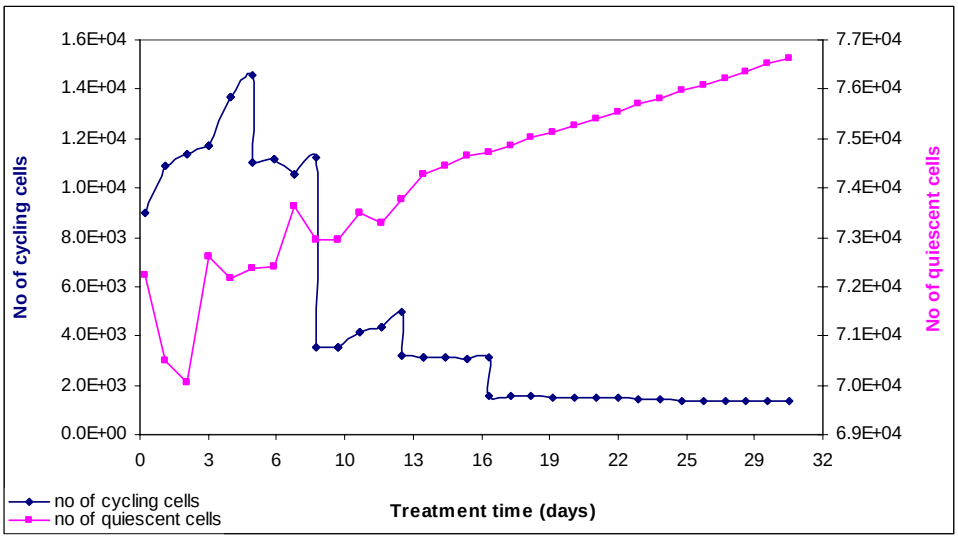

Figure 5.5. Survival curves for cycling and non-cycling cells during daily treatment.

Figure 5.6 shows the distribution of tumour cells along the four phases, illustrating the cell arrest in the G2 phase produced by cisplatin. It can be noticed that there are cells arrested even after the treatment has been completed, and redistribution of cells occurs once the cells are released from G2. Although the treatment that has been simulated over 2 weeks has finished with the last dose of cisplatin given on day 12, the effects of the treatment are present even after that time, since the 'kill' happens within 5 days after drug administration. This explains the still active part of the curves represented below up to day 17.

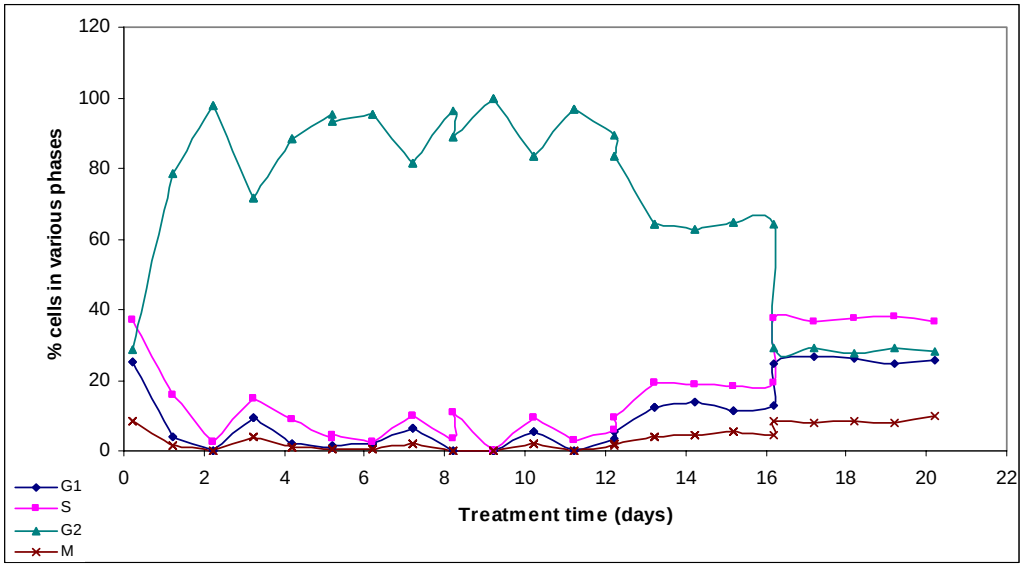

Figure 5.6. Cell distribution along the cell cycle during daily chemotherapy with cisplatin.

5.4.3.2. Cisplatin on a second and third-daily schedule: a novel approach in cisplatin's administration

In order to compare tumour control given by various schedules, cisplatin administration has been simulated on a daily basis, every second day and also every three days, for two weeks, and survival curves plotted. It should be noted from Figures 5.7 and 5.8 that when cisplatin is administered every 3 days, cell kill is higher than for cisplatin given every 2nd day. This paradoxical result is the effect of the intercalations within the temporal landmarks in cisplatin's action – administration, marking, release and kill – of consecutive treatment days. Therefore, cell block, release and kill are not correlated as efficiently in the second-daily treatment as they are in the third-daily treatment.

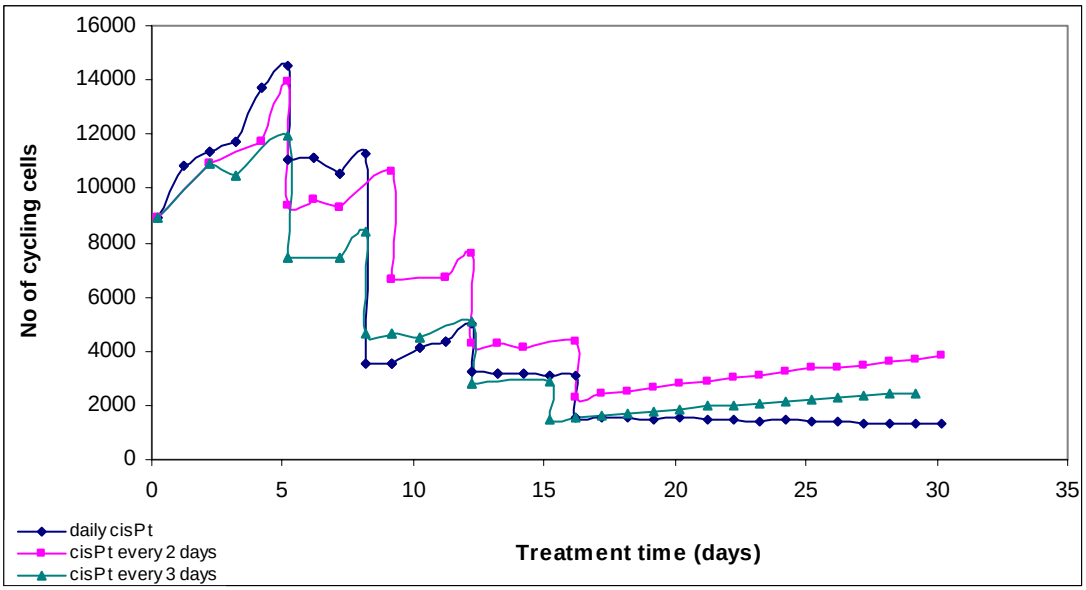

Figure 5.7. Comparative survival curves for cycling cells for daily, second daily and third daily treatment, respectively.

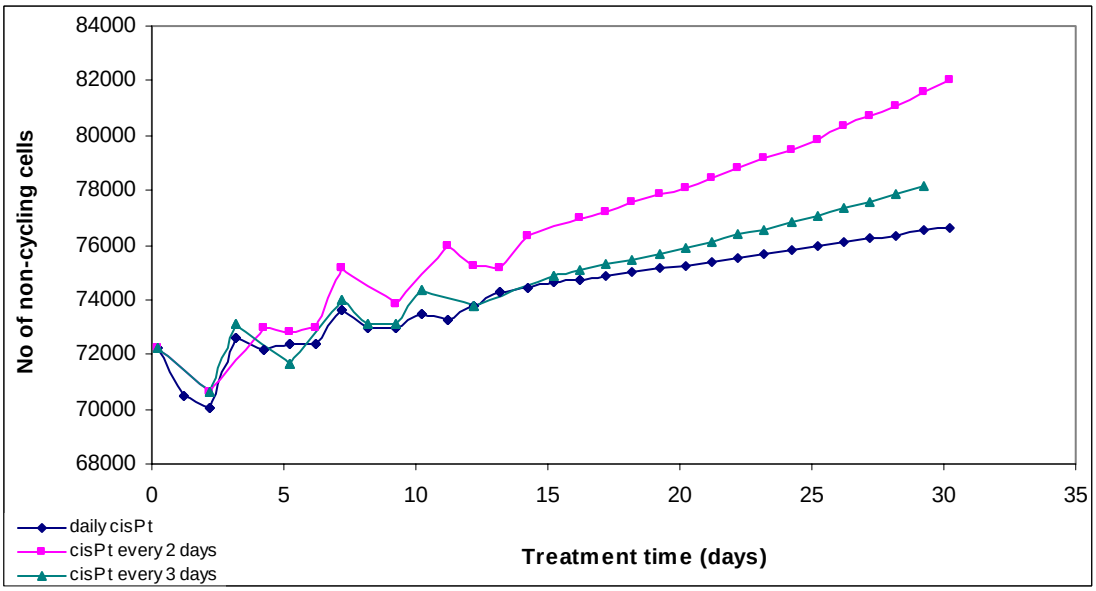

Figure 5.8. Comparative survival curves for non-cycling cells for daily, second daily and third daily treatment, respectively.

5.4.3.3. Cisplatin on a weekly schedule

For weekly treatment simulation the following values for the three parameters have been used: 95% for cell mark, 40% for cell release and 60% for cell kill due to higher drug doses administered. Also, cell arrest lasts for 72 hours, instead of 48 hours as it does for lower doses (daily administration).

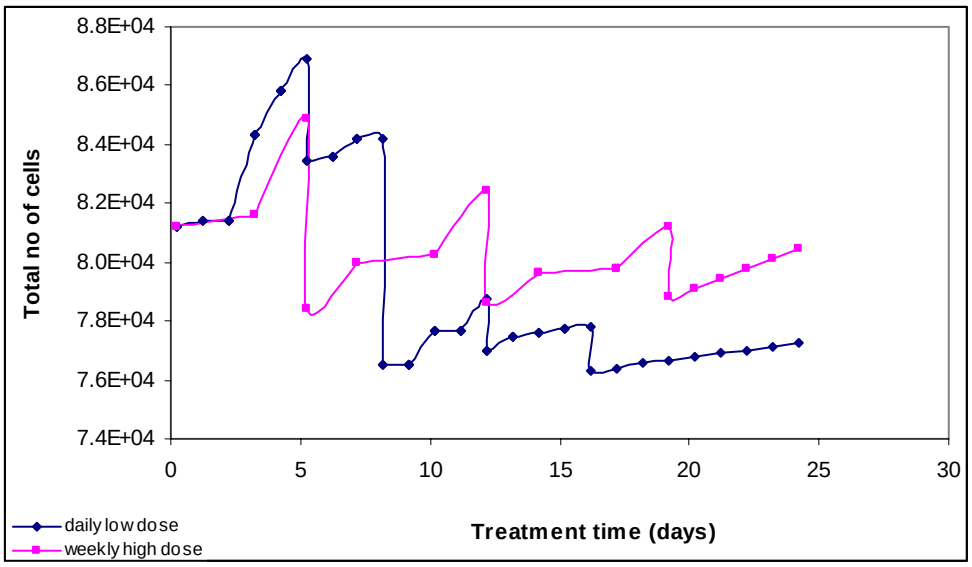

Figure 5.9. Daily versus weekly administration of cisplatin

Cell survival curves after low dose daily and high dose weekly cisplatin administration, respectively, are represented in Figure 5.9. It is to be observed that tumour control is superior for the daily administration, the result being in accordance with the latest literature review data (Marcu 2003). The poorer tumour control in the weekly schedule might be due to the inefficient cell killing relative to cell growth in between cycles of chemotherapy. Therefore repopulation overtakes cell kill, leading to inferior tumour response.

5.4.4. Conclusions

A daily treatment with cisplatin for two weeks has been simulated to illustrate the behaviour of the tumour population during and after treatment. It was noted that the

shape of the survival curve for the whole tumour is dictated by the quiescent population, as they dominate in number, but also they are not affected by cisplatin. It was seen that the number of non-cycling cells increases due to natural cell production, while the number of cycling cells decreases as a result of cisplatin's kill, reaching, after treatment, a steady state (assuming no change in kinetics in respect to treatment).

It was shown that cisplatin treatment every third day is comparable, in regards to tumour control, with a daily administration, and more effective than an every-second-day-treatment.

Also, tumour control is superior for the daily low dose administration as compared to weekly high dose.

The model shows that the optimal administration of cisplatin would be the every-third-day schedule, which would lead to similar tumour control as the daily treatment but to less normal tissue toxicity, allowing longer times between chemotherapy cycles for the normal tissue to repair the damage.

5.5. The model of drug resistance

5.5.1. Introduction

Drug resistance is a major factor in the failure of cisplatin-based chemotherapy (Andrews 1990, Ormerod 1996, Trimmer 1999, Welters 1997). Cisplatin resistance can be either intrinsic or acquired. Acquired resistance can emerge in tumours after an initial drug exposure. The literature shows up to a sevenfold increase in cisplatin resistance by various mechanisms (Welters 1999). Several mechanisms of cisplatin resistance have been identified:

- decreased DNA-adduct formation,
- enhanced DNA repair (Andrews 1990),
- decreased susceptibility to the induction of apoptosis (Ormerod 1996),
- increased drug inactivation by sulphur-containing molecules and
- altered expression of regulatory proteins (Trimmer 1999).

The outcomes of the above-mentioned mechanisms can be classified into two categories:

- mechanisms affecting the initial drug uptake (e.g. increased drug inactivation by sulphur-containing molecules, decreased DNA-adduct formation, and enhanced DNA repair) and
- mechanisms influencing the fate of the cell (e.g. decreased susceptibility to the induction of apoptosis, and altered expression of regulatory proteins).

Both the individual as well as the combined contribution of the two classes of mechanisms are studied in the current work.

5.5.2. Methods

Cellular resistance, substantiated by a decreased drug uptake, has been modelled by reducing the percentage of cells ‘marked’ by cisplatin. The initial value of 80% marked cells has been reduced and a sensitivity study undertaken for a range of values situated between 10% and 80%. The mechanisms of drug resistance that affect the fate of the exposed cell (like decreased susceptibility to the induction of apoptosis), have been also modelled by varying the percentage of killed cells within a range below the initial rate of 50%. Values from 5% to 50% cells killed have been selected for the sensitivity study.

The multi-mechanistic dependence of drug resistance has been modelled by combining the low drug uptake with the decreased susceptibility to the induction of apoptosis. The two mechanisms have been implemented into the model by reducing both the percentage

of ‘marked’ cells (low drug uptake) and the percentage of cells killed. A combination of 10% marking and 5% killing has been employed to investigate the extreme case.

5.5.3. Results and discussions

The results obtained from treatment simulation without drug resistance have been presented in §5.4.3.

5.5.3.1. Treatment simulation with drug resistance affecting drug uptake

The two classes of mechanisms responsible for acquired cellular resistance have been modelled by adjusting two independent parameters: percentage of marked cells and percentage of killed cells, respectively. The results of the two studies are shown below.

Cellular resistance, substantiated by a decreased drug uptake, has been modelled by reducing the percentage of cells ‘marked’ by cisplatin. The initial value of 80% marked cells has been reduced and a sensitivity study performed for a range of values situated between 10% and 80%.

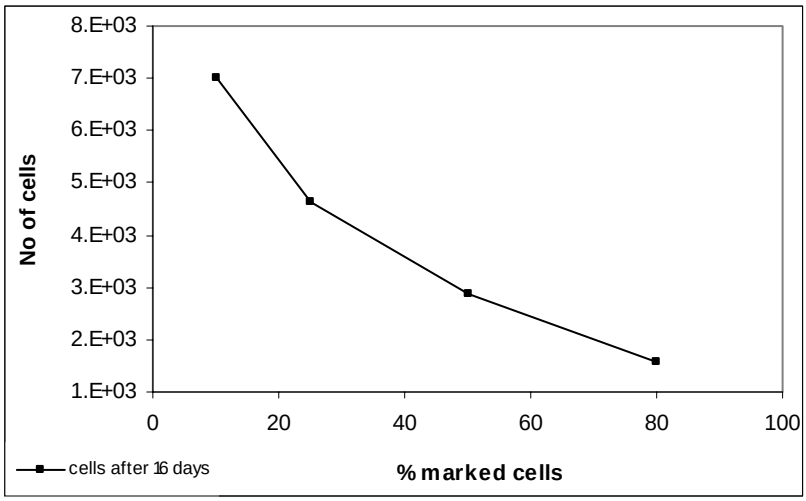

Figure 5.10. Number of surviving cells following 2 weeks of daily treatment with cisplatin for various percentages of ‘marked’ cells.

The graph in Figure 5.10 shows the surviving population of cells following 2 weeks of daily treatment with cisplatin, when various percentages of 'marked' cells have been considered. The 'default' value of 80% marked cells has been varied within the (10%-80%) range. The percentage of the marked cells in the resistant population, with each dose of cisplatin applied during the two-week treatment, is considered to be a constant fraction of the surviving cells (unmarked). The number of surviving cells after the same treatment period for the percentage of marked cells within the (10% - 80%) range has been plotted in Figure 5.10. The curve shows a logarithmic decrease of the surviving cell population with the increase in the percentage of cells marked by cisplatin. The percentage of cells killed has been kept at a 50% constant value.

To quantify the extent of drug resistance, the Cisplatin Resistance Factor (CRF) has been defined as the ratio between the number of surviving cells of the resistant population and the number of surviving cells of the sensitive population (the 'default' cell population), determined after the same treatment time.

Table 5.1 shows the CRF values for various percentages of 'marked' cells during treatment. A cumulative process of drug resistance is observed, which can be explained by the continuous growth of the resistant cells during treatment.

Table 5.1. Cisplatin Resistance Factor values during treatment as a function of percentage 'marked' cells.

% of marked cells / **CRF**	*80% (default)*	*50%*	*25%*	*10%*
CRF after 9 days	1.0	1.7	2.0	2.4
CRF after 12 days	1.0	1.7	2.3	2.7
CRF after 16 days	1.0	1.8	2.9	4.5

The results expressed in Table 5.1 are illustrated in Figure 5.11, where the accumulation of drug resistance during 2 weeks of daily treatment for various percentages of 'marked' cells is displayed.

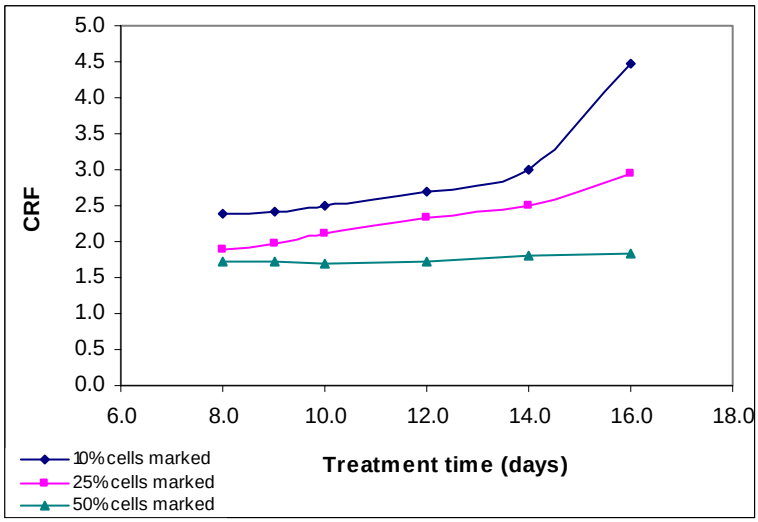

Figure 5.11. The cumulation of drug resistance during 2 weeks of daily treatment with cisplatin for various percentages of 'marked' cells.

The curves in Figure 5.11 show an almost constant curve of drug resistance in time when high percentages of cells (50% - 79%) are marked (i.e. the case of less resistant tumours), however more resistant than the 'original' one). When smaller percentages of cells are marked (i.e. the case of more resistant tumours) the increase of Cisplatin Resistance Factor in time becomes linear (25% cell mark) and even supra-linear (for 10% cell mark).

5.5.3.2. Treatment simulation with drug resistance affecting the fate of the cell

The mechanisms of drug resistance that affect the fate of the exposed cell (like decreased susceptibility to the induction of apoptosis), have been modelled by varying the percentage of killed cells within a range below the initial rate of 50%. Values from 5% to 50% cells killed have been selected for the sensitivity study. The standard value of 80% marking has been used for all cases.

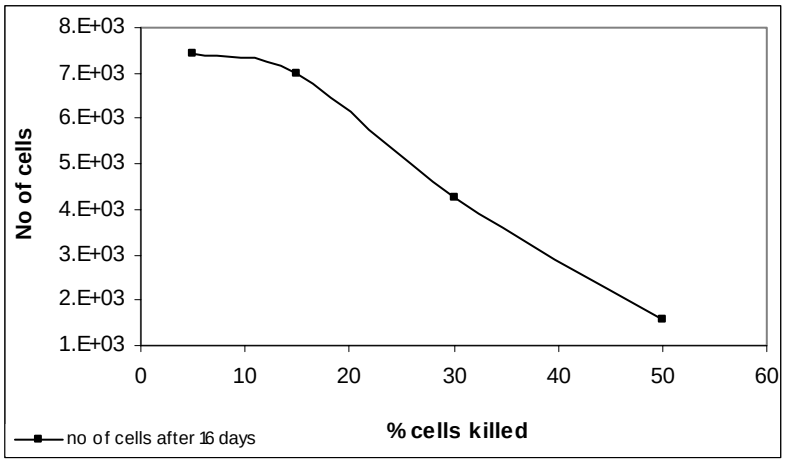

Figure 5.12. Number of surviving cells following 2 weeks of daily treatment with cisplatin for various percentages of killed cells.

The graph in Figure 5.12 shows the surviving population of cells following 2 weeks of daily treatment with cisplatin, when various percentages of cells killed per day have been considered. The 'default' value of 50% cells killed has been varied within the (5%-50%) range, and the number of surviving cells after the same treatment period plotted. The graph shows a close-to-linear dependence of the number of surviving tumour cells with the percentage of cells killed by cisplatin for values between 15% and 50% cell kill, with a bending in the curve for lower percentages of cell kill.

Similarly to the previous drug resistance study when the drug uptake has been changed by varying the percentages of 'marked' cells, the Cisplatin Resistance Factor has been determined for the decreased susceptibility to the induction of apoptosis.
Table 5.2 shows the CRF values for various percentages of cells killed during treatment. The cumulative process of drug resistance is observed once more.

Table 5.2. Cisplatin Resistance Factor values during cisplatin treatment as a function of percentage of killed cells.

% of killed cells / **CRF**	*50% (default)*	*30%*	*15%*	*5%*
CRF after 9 days	1.0	1.8	2.4	2.4
CRF after 12 days	1.0	2.7	4.1	4.4
CRF after 16 days	1.0	2.7	4.4	4.7

The cumulation of drug resistance indicated by the curves in Figure 5.13 shows a rapid increase of CRF with time, reaching saturation towards the end of the treatment. It is to be noted that the slope of the CRF curve increases with smaller percentages of cells being killed (higher resistance). The plateau area relates to the saturation of the cycling cells with cisplatin-DNA adducts (‘marking’).

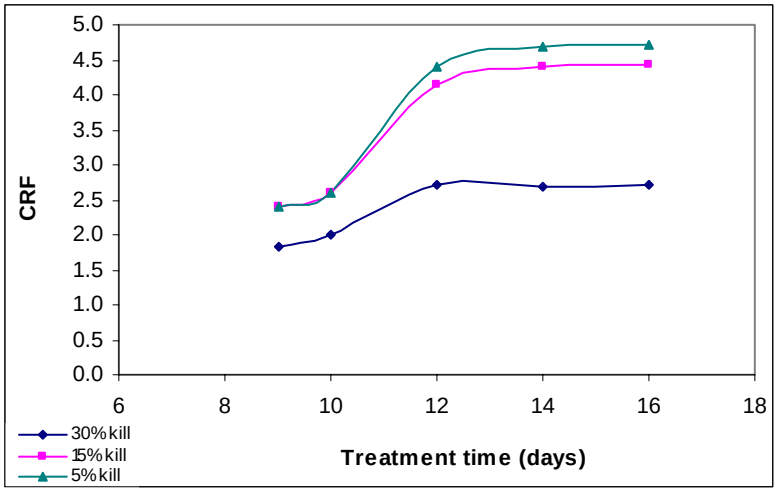

Figure 5.13. The cumulation of drug resistance during 2 weeks of daily treatment with cisplatin for various percentages of killed cells.

5.5.3.3. Treatment simulation with multi-mechanistic drug resistance

The multi-mechanistic dependence of drug resistance has been modelled by combining the low drug uptake with the decreased susceptibility to the induction of apoptosis. Therefore, a combination of 10% marking and 5% killing has been employed. The results are expressed by the graphs in Figure 5.14.

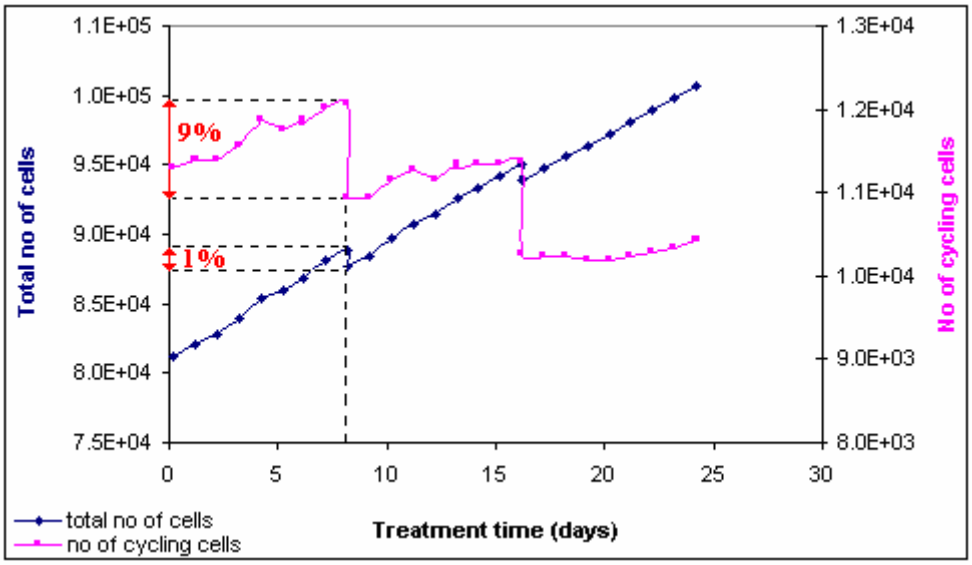

Figure 5.14. Survival curves after two weeks daily treatment with cisplatin of a drug resistant tumour.

A highly resistant tumour, as the one modelled with 10% marking and 5% kill, will overcome tumour regression and eventually overgrow the original size of the tumour. The continuously increasing curve in Figure 5.14 illustrates the ability of the resistant tumour to be non-responsive to treatment, therefore to grow similarly to an unperturbed tumour. The slight periodical decreases in cell numbers are due to drop offs in the number of cycling cells with each cell kill. It is shown that a 9% decrease in cycling cells will result in a 1% decrease only in the total population (see dotted line in Figure 5.14).

5.5.4. Conclusions

Drug resistance has been considered by modelling two classes of mechanisms: one leading to low drug uptake and the other considering the decreased susceptibility to the induction of apoptosis. Acquired cellular resistance, substantiated by a decreased drug uptake, has been modelled by reducing the percentage of cells ‘marked’ by cisplatin. A sensitivity study has been undertaken to study the various percentages of marked cells and their effect on cell survival. The curve shows a logarithmic decrease of the cell population with the increase in the percentage of cells affected by cisplatin. The mechanisms of drug resistance that affect the fate of the exposed cell have been modelled

by varying the percentage of killed cells. It has been shown that there is a supra-linear dependence (on a semi logarithmic scale) of the number of surviving tumour cells on the percentage of cells killed by cisplatin.

To quantify the extent of drug resistance, the Cisplatin Resistance Factor (CRF) has been defined. By determining CRF during treatment, drug resistance has been shown to be a cumulative process. For low drug uptake, resistance cumulates linearly or even supra-linearly for very low uptake. When decreased susceptibility to the induction of apoptosis is modelled, resistance cumulates over a sigmoid pattern.

The multi-mechanistic dependence of drug resistance has been modelled by combining the low drug uptake with the decreased susceptibility to the induction of apoptosis. It was shown that highly resistant tumours can overcome tumour regression leading to treatment failure (Figure 5.14).

5.6. The model of tumour repopulation during chemotherapy

5.6.1. Introduction

Repopulation of tumour cells between cycles of chemotherapy is usually a neglected factor (Davis 2000). Repopulation is a clinically observed phenomenon after radiotherapy. Several papers support the evidence that normal and cancerous squamous epithelia share the same behaviour in response to injury (Trott 1991, Trott 1999, Denham 1996). Also, in tissues with high turnover rate (e.g. bone marrow, intestinal mucosa) the mitotic rate increases greatly after cytotoxic treatment (Davis 2000). Furthermore, as the effect of both radiotherapy and chemotherapy on tumour cells is the same (eradication of cancer cells), the response of the tumour to injury and cell loss from the two treatment methods should consist of similar mechanisms. The large number of quiescent cells

resting in the G0 phase is an ‘available’ source of cancer cells able to repopulate the tumour. It was shown in the literature that recruitment is one of the possible mechanisms responsible for tumour regrowth after radiotherapy (Hansen 1996), or at least a contributor towards regrowth when combined with other mechanisms (accelerated stem cell division, change of symmetry) (Marcu 2004). The onset of repopulation due to chemotherapy is, however, poorly documented in the literature. Chemotherapy usually is administered at larger intervals than radiotherapy to facilitate recovery of the normal tissue with high cell turnover. As a result, weekly drug administration is more common than daily treatment. This schedule provides sufficient time intervals for the proliferating cancer cells to repopulate the tumour. There are limited experimental data suggesting that repopulation occurs at various rates after chemotherapy (Davis 2000). That might be attributable to the various recruitment rates of the quiescent cells as a response to the cell loss caused by chemotherapy.
Cell recruitment is considered in the current cisplatin model and the effect on cell kill and tumour repopulation studied.

The information about repopulation after chemotherapy in animal models is limited (Davis 2000). Nevertheless, the existent data suggest that there may be a delay in the onset of repopulation after treatment and that the rate of repopulation may increase with subsequent cycles of chemotherapy.

5.6.2. Methods

The principles used for implementing the properties of cisplatin into the model have been described in §5.4.2.2. The ‘default’ parameters are kept constant in the present study, therefore, 80% of cycling cells are ‘marked’ by cisplatin and eventually arrested in the G2 phase. Half of the marked cells will be released 48 hours after the adduct formation (‘marking’), while the other half will undergo apoptosis and become debris 72 hours later. The flow chart of cisplatin’s action is schematized in Figure 5.3. Cisplatin treatment is simulated on a daily basis, 5 days a week, over 2 weeks. The two weeks simulation of

cisplatin treatment is sufficient for achieving a trend in the behaviour of the tumour. Longer treatment schedules will be simulated later, when the combined cisplatin-radiotherapy is discussed (Chapter 6).

Cell recruitment during chemotherapy has been modelled similarly to recruitment during radiotherapy (Chapter 4). Therefore, after each act of cell kill, a certain percentage of quiescent cells are released into the cell cycle and regain their proliferative ability. Part of the recycled cells are stem cells and the other fraction consists of finitely proliferating cells. Initially 5% of the quiescent cells are recruited, with 4% being stem cells (referred to as 5/4), and in the second case studied, the recruitment affects 15% of the resting cells, also with 4% stem population (15/4). A large cell recruitment of 50% has also been modelled with the purpose of studying the effect of the extent of recruitment on tumour behaviour. There are no recruitment figures documented in the literature, therefore the values chosen started from very low (5%) to larger percentages (50%). The reason for selecting a very low percentage for the stem population (4% out of the total cells recruited) was to illustrate the high impact such a small amount of indefinitely proliferating cells can make on tumour regrowth.

Due to the uncertainties in regard with the start of tumour repopulation, both *immediate* onset of recruitment (after the first act of cell kill) and *late* recruitment (after the sixth cell kill action, in the second week of treatment) have been considered for modelling. While in the radiotherapy model the process of recruitment was ‘triggered’ after each dose of radiotherapy because of the ‘hit and kill’ effect of radiation, in the chemotherapy model, the first recruitment, in case of immediate onset after the first cell kill event, however, is assumed to happen five days after the administration of cisplatin (see §5.5.2.1).

5.6.3. Results and discussion

5.6.3.1. Cell recruitment

Cell survival curves after 2 weeks of treatment with cisplatin, without and with cell recruitment, respectively, are presented in Figure 5.15. The graphs also show an increase in total number of cells with larger percentages of cells recruited: 15% recruitment will lead to poorer tumour control than 5% cell recruitment, which is seen from the increasing tumour population during chemotherapy.

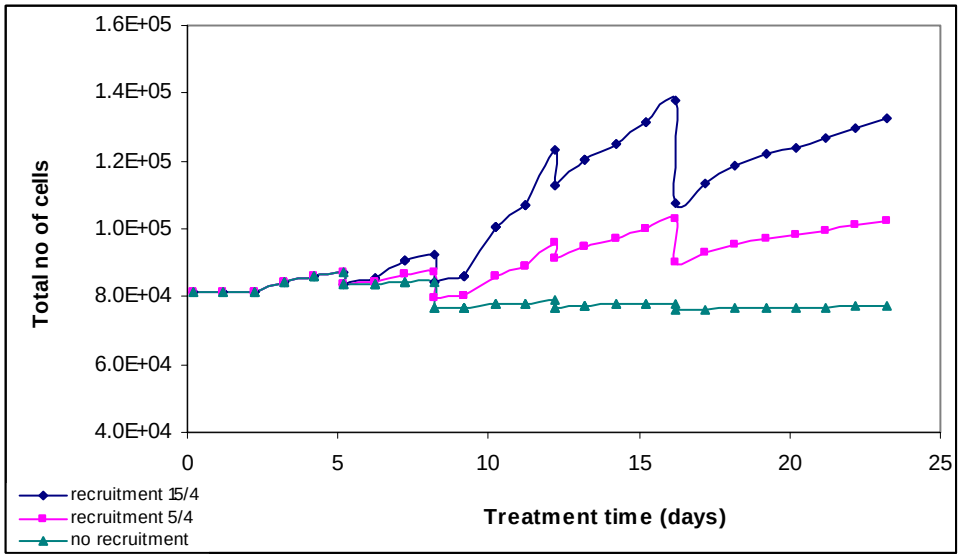

Figure 5.15. Cell survival curves with and without recruitment.

Beside the 5% and 15% recruitment, a 50% cell re-cycling has been also modelled, and the results obtained after the same treatment time (one week) have been plotted (Figure 5.16). The total number of cells is represented, on a linear scale, as a function of percentages of cells recruited. The graph shows a supra-linear dependence of the tumour growth during treatment on the extent of recruitment, which presents the process of recruitment as a potent mechanism in chemotherapy.

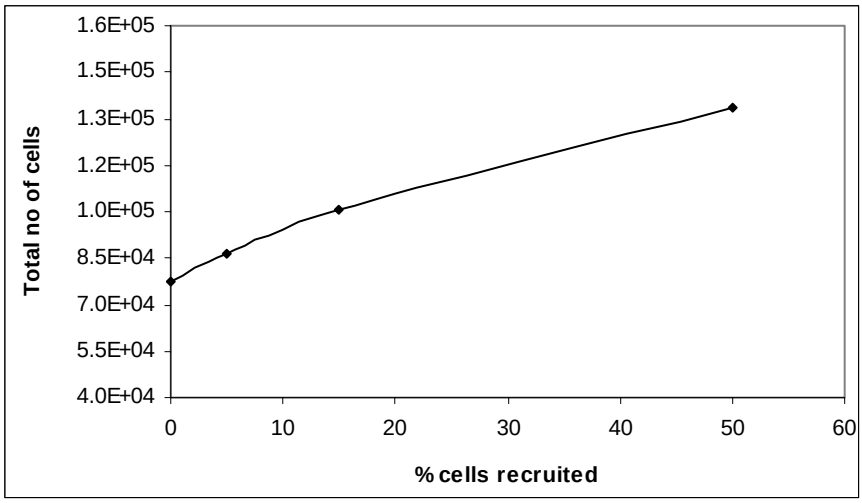

Figure 5.16. Total number of cells as a function of the percentage of cells recruited after 10 days of treatment with cisplatin.

For all the previous cell recruitment studies presented in the current work, the onset of repopulation has been considered to begin immediately after the first act of cell kill. However, it is hypothesized in the literature that repopulation would occur after a delay period. Therefore, a later onset of repopulation (after one week treatment) has also been modelled, and the cell survival curve compared to the curve obtained for the immediate onset of recruitment and the case when no recruitment was considered (Figure 5.17). As expected, a later onset of recruitment has led to poorer tumour regrowth, as a large percentage of proliferating cells has been already killed in the first week of treatment by the initial doses of cisplatin. Also, there has been less time for repopulation with a seven days delay in kick off.

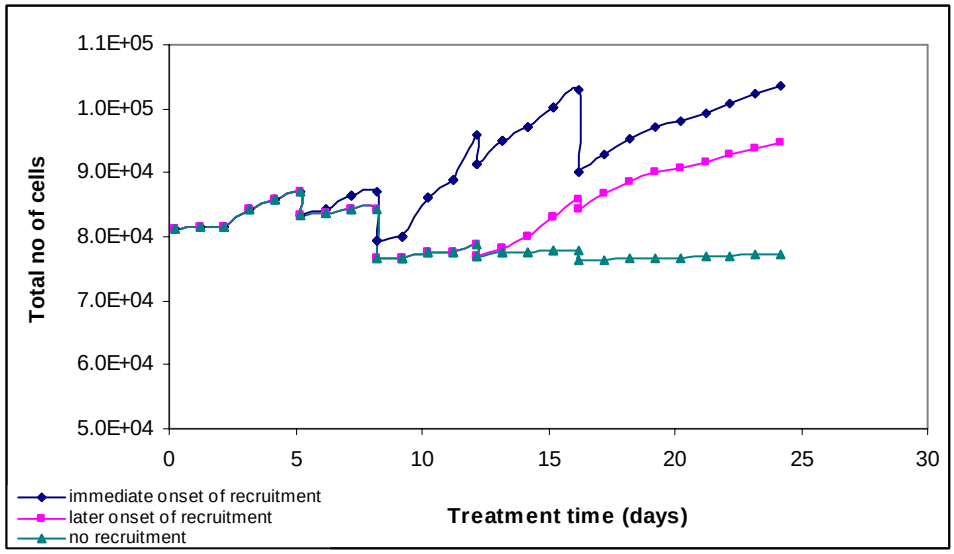

Figure 5.17. Cell survival curves without recruitment and with immediate and late onset of recruitment, respectively.

5.6.3.2. Tumour repopulation versus drug resistance

In order to illustrate the possible contribution of tumour repopulation during chemotherapy towards treatment failure, a comparative study of cell recruitment versus drug resistance has been undertaken.

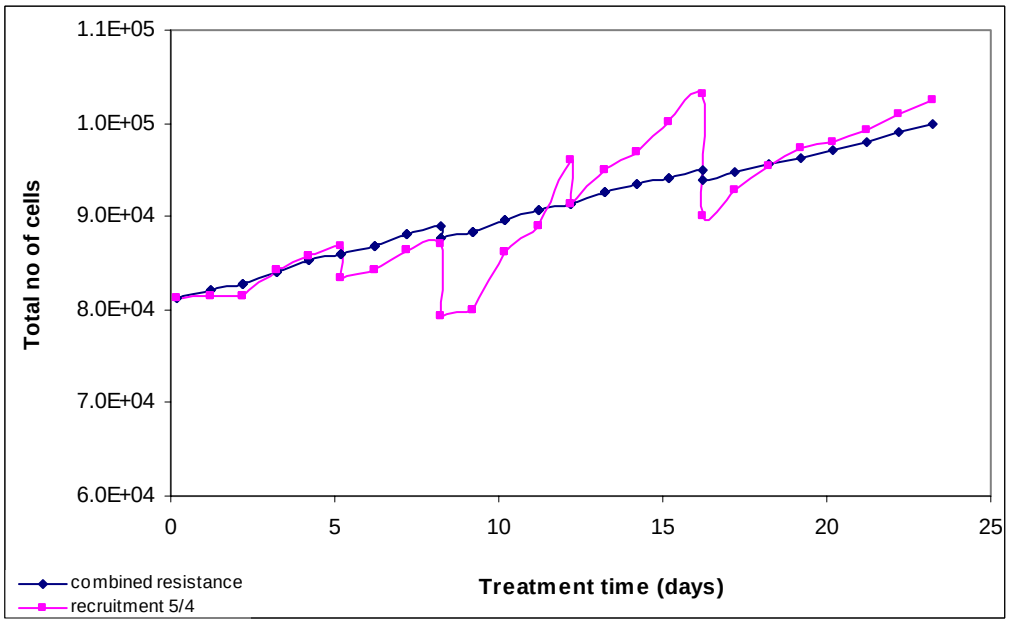

Figure 5.18. Drug resistance versus cell repopulation during chemotherapy.

The graphs in Figure 5.18 show survival curves for recruitment (5/4) and for combined drug resistance (10% mark and 5% kill), respectively. Comparing the two graphs it can be seen that even a small recruitment can lead to treatment failure (because of the poor tumour control) in the same way as high drug resistance does. The onset of cell recruitment has been modelled above after the first dose of chemotherapy. As mentioned before, there is no evidence that cell recruitment is triggered by the very first act of cell kill. Therefore, later onset of cell recruitment (after one week) during treatment with cisplatin is also considered.

Figure 5.19 compares survival curves for the multi-mechanistic drug resistant tumour, and the repopulated tumour by immediate and late recruitment, respectively, with 5% of cells re-cycled. While the immediate onset of recruitment leads to similarly poor tumour control as drug resistance, the later onset of recruitment result in a better controllable, however still regrowing tumour. Figure 5.20 compares the same three curves, this time with larger recruitment (15%). It is shown that even for late onset of recruitment the tumour can repopulate aggressively, and overtake drug resistance.

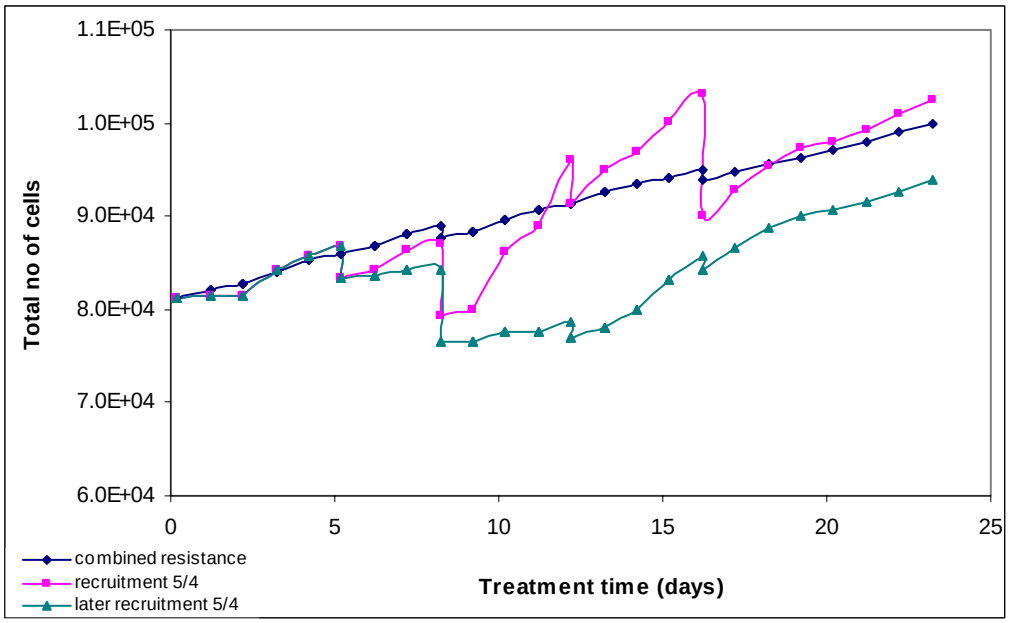

Figure 5.19. Late onset versus immediate onset of recruitment with chemotherapy, for 5/4 recruitment percentages.

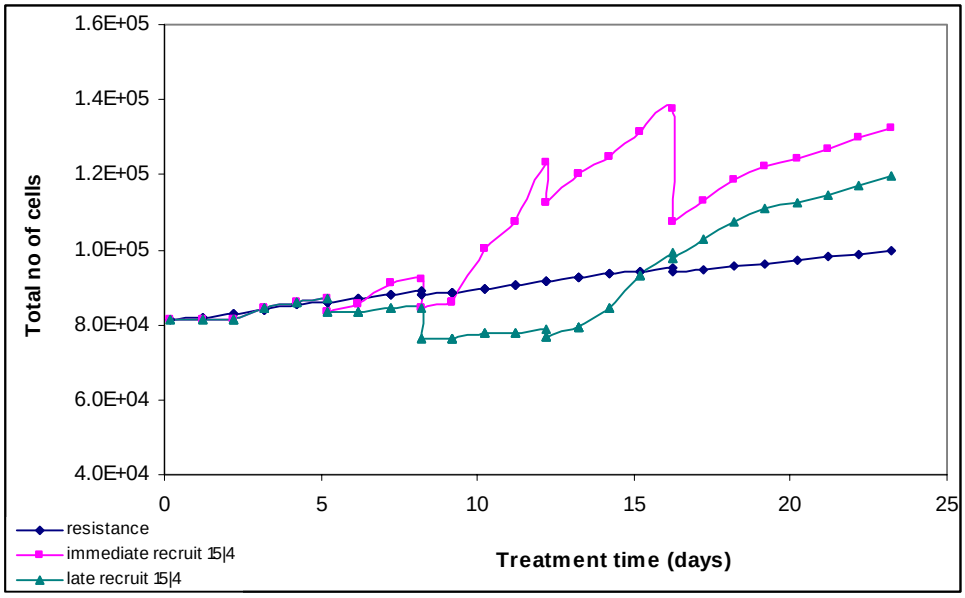

Figure 5.20. Late onset versus immediate onset of recruitment with chemotherapy, for 15/4 recruitment percentages.

Comparing the late recruitment curves from Figures 5.19 and 5.20, when 5/4 and 15/4 percentages of recruited cells have been, respectively, considered, it can be noted that a mid value of 10/4 recruitment with late onset would lead to similar outcome as the drug resistance curve. It can be concluded that a relatively small percentage of re-cycling cells (10%) can significantly increase the probability of treatment failure for cisplatin treatments.

The explanation for the above obtained results falls into the initial considerations for the tumour composition: 20% cycling cells and 80% quiescent cells, with cisplatin affecting only the cycling cells. Therefore, if 10% of quiescent cells are recruited, an additional 8% of the total cells will be re-cycled, which increases the cycling population by 40%. Since the effect of cisplatin as a sole cytotoxic agent on the tumour population after 2 weeks of treatment without recruitment consists of less than 10% cell kill (Figure 5.5), with a 40% increase in cycling cells it is expected that tumour regrowth would overcome cell kill, therefore leading to repopulation. The poor tumour response to cisplatin given alone corresponds with the results obtained by Joschko et al (1997) from human tumour

xenografts. Tumour response after cisplatin was comparable to that seen in controls (untreated tumours).

5.6.4. Conclusions

Tumour repopulation, a so far neglected factor in chemotherapy, has been modelled through the mechanism of recruitment. Percentages of cells recruited in the range of (5%-50%) have been plotted as a function of tumour population, and a supra-linear dependence observed, which indicates the potent effect of recruitment on tumour control.

Both immediate and late onset of recruitment have been studied, indicating a poorer tumour control in the first case.

When comparing cell survival curves after chemo treatment with cell recruitment and with drug resistance, respectively, it was shown that even small percentages of recruited cells (15%) with a late onset of repopulation will lead to treatment failure, similarly to drug resistance.

The study on cell recruitment shows that tumour repopulation due to chemotherapy should not be neglected.

Chapter 6

The combined model of cisplatin and radiotherapy

6.1. Introduction

It is an accepted fact that there is an enhanced cell killing when cisplatin is administered in combination with radiotherapy. This enhancement of tumour response is thought to be mediated through several mechanisms: enhanced formation of toxic platinum intermediates in the presence of radiation-induced free radicals, a radiation-induced increase in cellular platinum uptake, inhibition of DNA repair and cell cycle arrest.

The clinical trials described in Chapter 2 have indicated that there are survival benefits from the combined treatment in comparison to either cisplatin or radiation alone. However, it is not obvious whether the benefit is due to potentiation of radiation or to additional cell kill by cisplatin. The present chapter will bring some light on this question by comparing radiation cell survival curves resulted from the additional kill of cisplatin with survival curves obtained from the potentiation of radiation by cisplatin.

It was also evident from Chapter 2 that daily administration of cisplatin leads to a better tumour control in the head and neck cancer trials than the weekly scheduling of the drug. Therefore, daily as compared to weekly administration of cisplatin is simulated in the present chapter, the results discussed and weighed against the clinical data.

6.2. Literature review on chemo-radiotherapy models

The literature is very scarce on chemo-radiotherapy models. Therefore, this section will summarise the original model developed by Goldie and co-workers (1988). Their model simulates the alternated chemotherapy and radiation on a hepatoma, based on experimental data. The model was built on a previously developed tumour growth model with three discrete compartments: stem cells, differentiating cells and end cells. The main focus of the model was on stem cells, which have been classified into various resistant groups: cells resistant to chemotherapy but radiation sensitive, cells resistant to radiation but chemo sensitive, cells sensitive to both treatments and, the final group of cells, resistant to both therapies. The aim of the combined model was to alternate radiotherapy with chemotherapy (cyclophosphamide) in various protocols in order to achieve an optimal tumour control. They have concluded that the combined regimen is more effective in eliminating the stem cells than any of the two modality treatments alone.

6.3. Sequencing and timing cisplatin and radiotherapy: a modelling approach

6.3.1. Introduction

As already discussed in Chapters 1 and 2, there is no optimum timing identified between cisplatin and radiation when administered concurrently. Since the exact mechanisms of radiosensitization by cisplatin are still under investigation (Lawrence 2003), it becomes difficult to accurately model the optimal schedule. Due to the variety of cisplatin's properties, the timing between cisplatin and radiotherapy can also vary. Table 6.1 shows the rationale behind different timings as a function of cisplatin's characteristics.

Table 6.1 Rationale for different timings between radiation and cisplatin

Properties of cisplatin	Correlation of cisplatin and radiation
Radiosensitizer	Cisplatin should be in the tissue when RT is applied; *Timing*: *cisplatin before irradiation*
PLD & SLD repair inhibitor	To inhibit the repair of a sublethal damage caused by radiation, cisplatin should be administered very closely to RT, so the damage is not repaired meantime. Depending on drug pharmacokinetics, cisplatin should be given closely before or after RT; *Timing*: *cisplatin either before or after irradiation*
Hypoxic cell sensitizer	If cisplatin is administered before RT, more cells could be killed by RT due to cisplatin's action on hypoxic cells; When cisplatin is given after RT more cells could become oxygenated, as cisplatin can easier infuse the tumour because of the tumour shrinkage produced by RT. *Timing*: *cisplatin either before or after RT*
G2 phase arrester	Cisplatin can arrest the cells in G2 phase for a few days during which part of the cells are loosing their ability to proliferate others will repair the damage. Since G2 is almost as sensitive as M, the arrested cells are more prone to RT damage. *Timing*: *cisplatin could be administered anytime regarding RT*
DNA adduction	Cisplatin can be linked to the DNA through intrastrand and also interstrand adduction. This property confers the cytotoxic effect of cisplatin. If this property is linked to radiosensitisation, cisplatin should be present when irradiating; *Timing: cisplatin before RT* If the cytotoxicity is a stand-alone property, cisplatin could be administered anytime regarding RT. Because both RT & cisplatin are cytotoxic, a highly effective schedule could be a concurrent administration. *Timing*: *cisplatin concomitantly with RT*

The obvious question that arises is which of the above properties are more relevant and also more strongly manifested?

Several in vitro experiments have been designed to study the interaction between cisplatin and radiation. The controversial results obtained show the complexity of cisplatin's action on tumour cells. Korbelik and Skov (1989) have reported that cisplatin shows substantial preferential radiosensitisation of hypoxic cells in vitro at clinically used doses. On the other hand, Sun and Brown (1993) have demonstrated the lack of differential radiosensitization of hypoxic cells in murine RIF-1 tumours by cisplatin, showing, however, that there is a strong schedule-dependent interaction between the two cytotoxins. This observation is supported by Hoglmeier (1985) who found no elective radiosensitization of hypoxic cells due to cisplatin. The study undertaken on mouse fibrosarcoma concluded that the response of the tumour to the combined treatment is an independent addition of the two effects. The hypothesis of independent cell kill is also imparted by Dewit (1985) from crypt cell experiments.

In regards to time sequencing, a number of experiments support the advantage of cisplatin given before radiotherapy. Overgaard (1981) has shown that cisplatin 30 minutes before radiation enhanced the radiation response in the C3H mammary carcinoma in mice by a factor of 1.7, while the 'after' effect factor was only 1.2. The same mouse model system was used by Kanazawa (1988) for schedule-dependent therapeutic gain calculations. The highest degree of radiation enhancement was obtained when cisplatin was administered on a daily basis immediately before radiation. Bartelink (1985) has studied the therapeutic enhancement of cisplatin in mice, showing again, that the greatest enhancement was achieved with cisplatin administered daily immediately before irradiation. Two ample reviews of experimental and clinical data on cisplatin-radiation interaction (Dewit 1987, Kallman 1992) have shown that in most of the investigations the greater-than-additive effect caused by cisplatin occurred when the drug was given shortly before radiotherapy.

Nevertheless, a later study on rat yolk sac tumour cell lines (Nakamoto 1996) has concluded that cisplatin has synergistic effects independent of the time course and sequence with radiation, when given within 6 hours. Similar results have been obtained by Dewit (1985) from experiments on mouse duodenal crypt cells, concluding that the increased killing of crypt cells by cisplatin is the same irrespective of the sequence of administration, providing that cisplatin was given within 6 hours of radiation.

Some clinical trials with cisplatin and radiation, on unresectable head and neck cancers, have shown superior results when cisplatin was administered before radiotherapy. The outcome of the trial conducted by Slotman (1986) was described as 'impressive tumour reduction'. A highly successful trial has been conducted by Jeremic (2000) following a concurrent cisplatin-radiotherapy schedule with fractionated administration of both cisplatin and radiation. Cisplatin was administered on a daily basis, 30 minutes before irradiation.

Despite the superior results when given on a daily basis, cisplatin is still administered more commonly in weekly cycles (Marcu 2003), with no exact temporal relationship between the timing of drug and radiation.

Experimental data shows that the combined effect of cisplatin and radiation is maximal when cisplatin is given close in time to radiation fractions. Inhibition of SLDR by cisplatin is suggested to be the most reasonable mechanism to explain the radiation potentiation. Cisplatin has no potentiating effect when administered 24 h before irradiation (Schwachöfer 1991).

6.3.2. Methods

The effect of daily treatment with cisplatin-radiotherapy on tumour control has been simulated. The 'treated' tumour is the virtual head and neck cancer which has been grown in a previous model (Chapter 3) (Marcu 2002). The tumour is composed of stem

cells (indefinitely proliferating), finitely proliferating cells (limited number of generations) and, also nonproliferating (quiescent) cells. Cisplatin is modelled to affect the cycling cells (Chapter 5) while radiation acts on both quiescent and proliferating cells, as described in Chapter 4.

A conventionally fractionated radiotherapy treatment has been simulated for the tumour: daily dose of 2 Gy, 5 days a week, over 7 weeks (as described in Chapter 4). Cisplatin has been administered, on a daily basis (as described in Chapter 5), concurrently with radiotherapy.

The sequencing between the drug and radiation has been completed with cisplatin either before or after irradiation. The timing of the drug and radiation, has been kept, in both cases, very close (cisplatin immediately before, or immediately after radiotherapy).

Cell recruitment has been considered as a consequence of both chemotherapy and radiotherapy, with a constant percentage of cells recruited after each killing event. Moreover, to cover any biologically sensible value, a range of (5% – 90%) quiescent cells recruited has been considered. Similarly to previous recruitment methods (Chapters 4, 5) 4% of recruited cells were stem cells.

6.3.3. Results and discussions

6.3.3.1. Cisplatin-radiotherapy versus radiotherapy alone, without repopulation mechanisms

Simulating the combined radio-chemotherapy without considering cell recruitment, the radiation-cisplatin cell survival curve does not show any significant differences from the radiation survival curve (Figure 6.1). Figure 6.1 also shows no variation in survival between the two sequencing methods: cisplatin before or after radiotherapy. The negative region of the horizontal axis represents the unperturbed tumour growth curve. The

treatment starts at time '0' and the positive region shows the effect of radio-chemotherapy on tumour. Since cisplatin affects only part of the cycling cells, which are inferior in number to quiescent cells (20% cycling cells as opposed to 80% noncycling cells), the effect of cisplatin is significantly weaker than the effect of radiation on tumour cells. The killing due to radiotherapy is close to 50% (SF_2 = 54%), while the cell kill produced by cisplatin is only 8% when no recruitment is considered (50% cell kill, out of 80% cycling cells marked, from the total of 20% cycling cells) (see Figure 5.3).

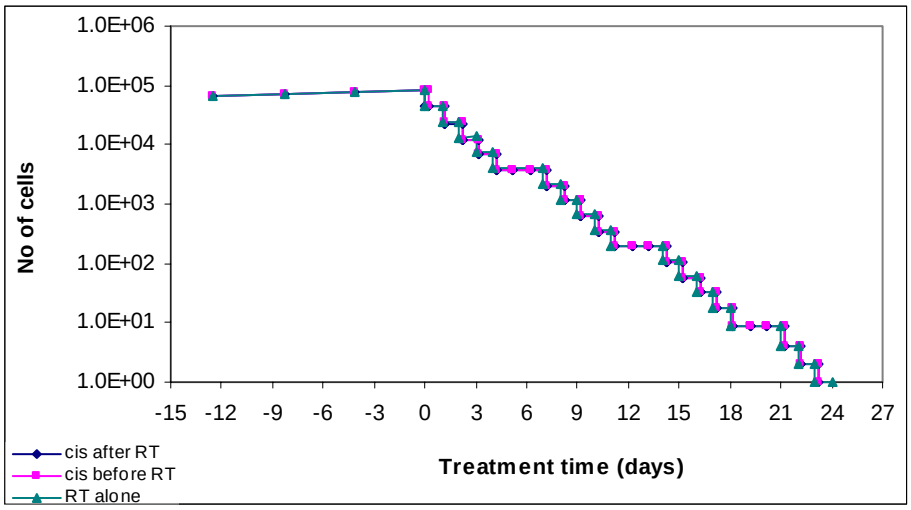

Figure 6.1. Cell survival curves for chemo-radiotherapy versus radiotherapy without recruitment

In order to obtain more sensible results, cell recruitment into the mitotic cycle (without other repopulation mechanisms) has been considered. The sequencing of cisplatin-radiation has been studied, and the combined modality treatment as opposed to radiotherapy alone has been analysed.

6.3.3.2. The sequencing of cisplatin and radiotherapy, when cell recruitment is considered

Two chemoradiotherapy simulations have been performed with cisplatin scheduled immediately before and also after radiotherapy. Figure 6.2 shows surviving curves with the two different sequencing methods of drug and radiation, for various percentages of cells recruited.

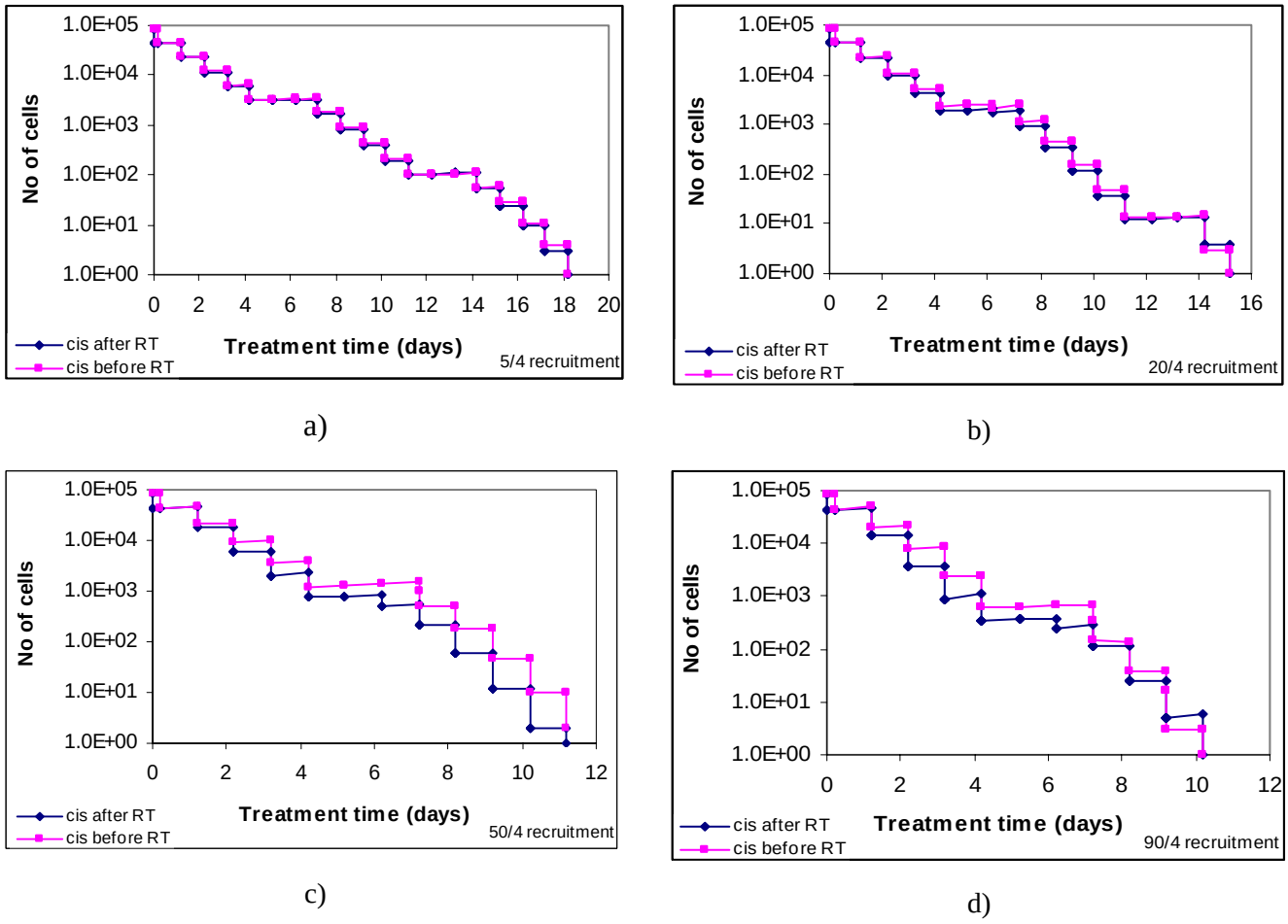

Figure 6.2. Cell survival curves obtained for different sequencing of cisplatin and radiation for various percentages of cells recruited.

It is to be noted that tumour control increases with the increase in recruitment (Figure 6.2 a-d). With more cells recruited into the cycle, the proportion of cycling to non-cycling cells increases, therefore the effect of cisplatin increases (since cisplatin affects the cycling cells). Also, radiotherapy is more effective, as cells in the G0 phase are more radioresistant than the majority of cycling cells (excepting cells in the DNA synthesis phase). Furthermore, cisplatin arrests the cells in the G2 phase, which is equally radiosensitive to mitosis (Sinclair 1969). As a consequence, the overall radioresistance of the cycling cells decreases significantly, hence contributing to radiation-produced cell kill.

This result is in agreement with the hypothesis raised by Steel (1992) by which the response to therapy might be improved if non-proliferating cells could be stimulated to enter the cycle. To support this statement, Figure 6.3a and 6.3b illustrate the increase in tumour control with increase in recruitment, for both cisplatin given immediately before radiotherapy and immediately after radiation. The graphs show that the larger the recruitment, the better the effect of the combined cisplatin-radiotherapy on tumour regression.

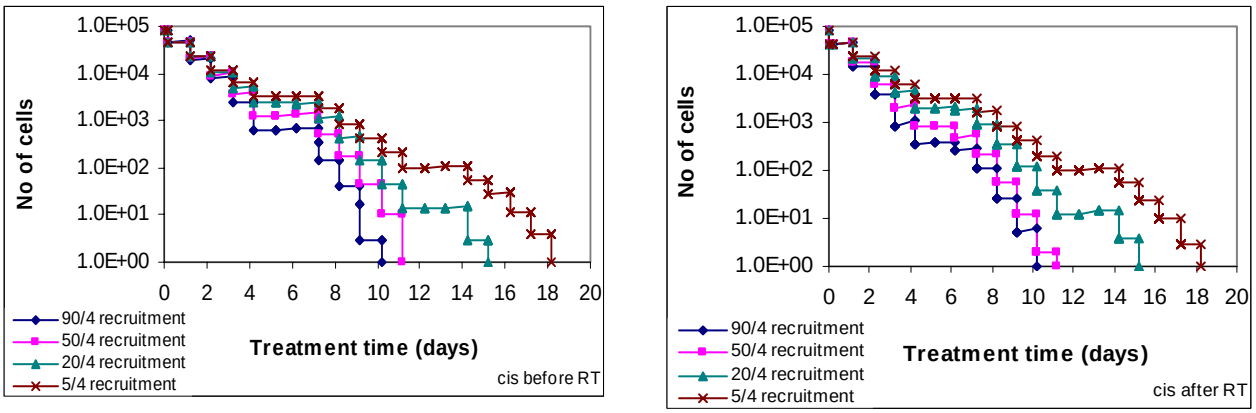

a) b)

Figure 6.3. Recruitment-dependence of tumour regression in the combined cisplatin-radiotherapy.

Figure 6.4 represents a logarithmic decrease of treatment length with the percentage of cells recruited, in order to drop the tumour population from 10^5 to 10^2 cells. The graph is valid for both cisplatin before and after radiotherapy. It can be seen that the larger the recruitment into the cycle, the better the effect of the combined cisplatin-radiotherapy on tumour regression, so shorter the treatment time for an isoeffect.

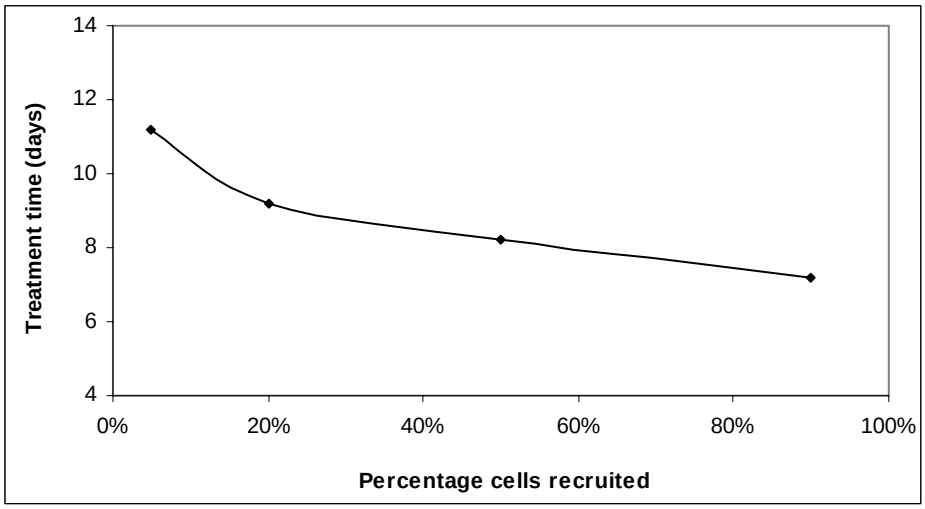

Figure 6.4. Treatment time dependence on the number of cells recruited in the combined cisplatin-radiotherapy leading to a drop in tumour cells from 10^5 to 10^2.

Consequently the interplay between cisplatin and radiation is stronger manifested for higher recruitment percentages.

Although the model incorporates the independent cell kill of cisplatin and radiation, the above described interplay between the two agents supports the idea of local cooperation. Yet, this interaction is not considered as a radiosensitization created by cisplatin, since no radiosensitizing property (like PLD, SLD repair inhibition, hypoxic cell sensitization) is applied in the model.

6.3.3.3. Cisplatin-radiotherapy versus radiotherapy alone, with cell recruitment

Figure 6.5 compares cell survival curves for chemo-radiotherapy, with cisplatin administered both before and after radiation, and radiation alone, with 50/4 recruitment. It is observed that cisplatin in combination with radiotherapy gives better tumour control than radiotherapy alone. The treatment time for isoeffect (in this work isoeffect is complete tumour eradication) in the combined cisplatin-radiation treatment has been reduced by 35% when compared to radiotherapy alone. This result is in accordance with the literature data showing that cisplatin concurrently with radiation leads to a better

outcome than radiotherapy alone. The first study that directly compared daily doses of cisplatin given concurrently with fractionated radiotherapy, with standard radiotherapy (2 Gy/day dose, 5 days/week for 7 weeks) alone was the prospective randomized trial conducted by Jeremic (1997). Their results show 51% local recurrence-free survival after 5 years in the cisplatin-radiotherapy group, and only 27% local recurrence-free survival after 5 years in the radiotherapy-only group.

However, the effect created by the combined modality treatment on tumour control, as shown by the graph, is additive only. It is to be mentioned that the cell killing processes of the two modality treatments have been implemented independently into the computer-model, as described in §6.3.2. Consequently, the results illustrated in Figure 6.5 are due to the independent cell kill produced by cisplatin and radiation, which did not lead to synergy. However, there is evidence in the literature supporting the synergistic effect of cisplatin when administered concurrently with radiation (Overgaard 1981, Dewit 1986, Kallman 1992, Nakamoto 1996). Since in the current study the individual cell kill has led to an additive effect only, in order to obtain the results observed in some of the in vitro experiments and also clinical trials, cisplatin must have radiosensitizing properties.

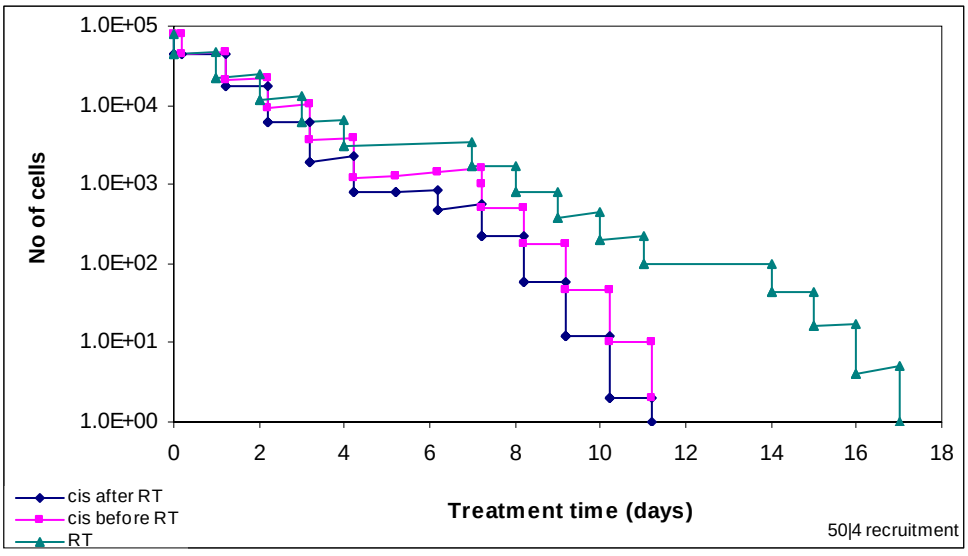

Figure 6.5. Cell survival curves for chemo-radiotherapy versus radiotherapy with recruitment

6.3.4. Conclusions

The model has shown that cisplatin administered before radiation gives similar tumour control to the post-radiation sequencing of the drug, if cisplatin is given very close in time to radiation. Furthermore, the killing effect of the combined modality treatment on tumour increases logarithmically with the increase in cell recruitment. The rationale behind this result originates from the variation of the radioresistivity parameter along the cell cycle. Since the quiescent cells present with a higher radioresistance than the majority of the cycling cells (excepting those in the S phase), by re-entering the mitotic cycle, the previously quiescent cells loose their radioresistance, and therefore they become more prone to radiation damage. Also, since cisplatin arrests the cells in the G2 phase, which is equally radiosensitive as mitosis, the overall radioresistance of the cycling cells decreases drastically, hence contributing to radiation-produced cell kill.

From the above exposed rationale, one can conclude that chemo-radiotherapy may be more beneficial for rapidly proliferating tumours, with high repopulation ability, than for slowly proliferating ones.

The current model has considered only the independent cell kill produced by cisplatin and radiation, respectively. When comparing radiation survival curves and cisplatin-radiation survival curves, no supra-additivity was indicated. These findings suggest that the individual cell kill produced by the two cytotoxins leads to an additive-only tumour response when the treatments are given concurrently. Therefore, it was suggested that for a synergistic effect, cisplatin must potentiate the effect of radiation, through the radiosensitizing mechanisms addressed in the literature.

It is, therefore, concluded, that the independent cell kill of cisplatin and radiation is independent on the time sequencing between the drug and radiotherapy. If some studies have shown that cisplatin administered before radiation has led to better results, this indicates that cisplatin should have radiosensitizing properties.

6.4. Potentiation of radiation by cisplatin

6.4.1. Introduction

Clinical trials have shown superior outcome from the combined modality treatment when using cisplatin, compared to radiation alone. However, it is not obvious whether the benefit is due to potentiation of radiation or to additional cell kill by cisplatin. As shown in the previous section (§6.3), the addition of the independent cell kill from cisplatin and radiotherapy has led to an additive-only effect. This observation leads to the conclusion that for a better outcome, cisplatin should potentiate the killing effect of radiation.

The proposed mechanisms of cisplatin's radiosensitizing effects and its supraaditivity with radiotherapy have been described by slow biochemical (inhibition of SLDR) and fast free-radical-mediated events (Sharma 1999). However, the exact mechanism of cisplatin radiosensitisation is still under investigation (Lawrence 2003).

An explanation for how cisplatin can increase the number of double strand breaks produced by radiation is given by Begg (1990). An adduct in the process of being excised in the vicinity of a Single Strand Break (SSB) will produce a temporary opposing SSB, resulting in the conversion of a SSB into DSB (Double Strand Break). Alternatively, an adduct may inhibit the repair of a radiation-induced SSB, leading to a lethal SSB event. It was experimentally determined that the approximate number of radiation-induced DNA breaks per Gy per mammalian cell is 1000 SSB and 40 DSB (Elkind 1977). Also, the number of cisplatin-DNA adducts was found close to 10^5 adducts per cell at a D_0 dose of drug (Roberts 1988). Calculations of interaction probabilities based on DNA lesion numbers suggest interactions can occur over distances up to 100 base pairs (Begg 1990), therefore the probability of interaction could be high.

In order to function appropriately, cells are checked along the mitotic cycle for DNA damage. There are two DNA damage-induced checkpoints along the cell cycle: one in G1

and another in G2 phase. Cells will arrest in these phases upon sensing DNA damage. This arrest is presumably induced to prevent the replication of damaged DNA. A response to unrepairable damage is the induction of apoptosis, or programmed death. A radiation-produced single strand break can be easily repaired during a cell arrest. However, when cisplatin binds to a radiation-damaged DNA, the probability for repair is extremely low, as the damage is similar to a double strand break. In this way, cisplatin 'sets' the damage, by transforming a sublethally damaged cell into a lethally damaged one.

6.4.2. Methods

In order to investigate the radiosensitizing effect of cisplatin by inhibition of sublethal damage repair, the radiosensitivity parameters along G1 and G2 phases, respectively, have been changed. This operation implies changes in the surviving fractions for the above-mentioned phases. To illustrate the dependence of the survival curves given by the combined modality treatment on the linear parameter of the LQ model, a large range of alpha values have been covered. The same changes (in percentage) have been implemented for both G1 and G2 phases.

The alpha parameter has been increased by 10%, 30% and 50%, respectively, equally for both G1 and G2 phases, and the survival curves plotted.

Cell recruitment into the cycle has been considered in all simulations, with 50% recruitment after each killing event (with 4% stem cells recruited out of the 50% total recruitment).

6.4.3. Results and discussions

Table 6.2 presents the values for the alpha parameter for radiotherapy alone (see Appendix C) and also the range of values, for G1 and G2 phases, considered for the

combined cisplatin-radiotherapy. In order to decrease the surviving fractions, as it would result from cisplatin's radiosensitization, the value of the alpha parameter has been increased by various percentages, equally for the G1 and G2 phases. The resulting survival curves are illustrated in Figure 6.6, together with the curve given by the initial alpha values (unchanged).

Table 6.2. Variation in the α parameter for G1 and G2 phases of the cell cycle

Treatment type	α value for G1	α value for G2
Radiotherapy	0.25	0.597
Cisplatin-radiotherapy	(0.25 – 0.375)	(0.597 – 0.895)

The graphs in Figure 6.6 show very small differences when the alpha parameter is changed within the indicated values (Table 6.2). Because of the exponential relationship between alpha and surviving fraction, the 50% increase in alpha was not enough to show considerable decrease in the surviving fraction. Furthermore, only the surviving fractions of G1 and G2 phases have been decreased, which did not contribute significantly to the overall change in survival. The G2 phase is known to be as sensitive as mitosis, so experiences already low survival. The G1 phase has an average sensitivity, however, compared to the 'unchanged' phases, S and G0, the sensitivity in G1 is still too high in order to alter the overall survival.

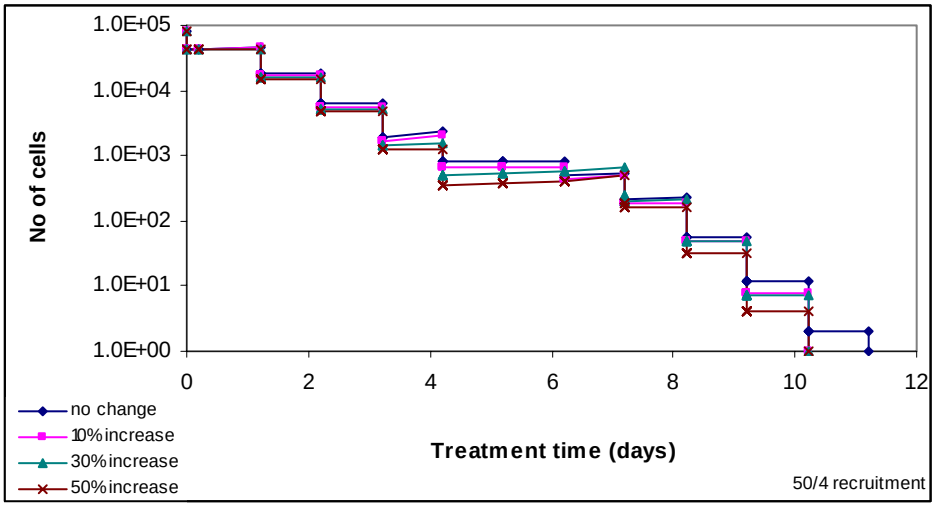

Figure 6.6. Cell survival curves given by cisplatin-radiotherapy when the α parameter for the G1 and G2 phases is increased.

The graphs in Figure 6.6 indicate that the overall survival decreases very slowly with the increase in the alpha parameter. Average surviving fractions have been calculated for the four cases when alpha has been changed, and plotted as a function of the percentage increase in alpha (Figure 6.7). The average surviving fraction during cisplatin-radiotherapy with 50/4 recruitment, with the initial (unchanged) alpha parameters, was 0.39. With an increase in alpha, as large as 50%, the overall survival has been decreased only to 0.34.

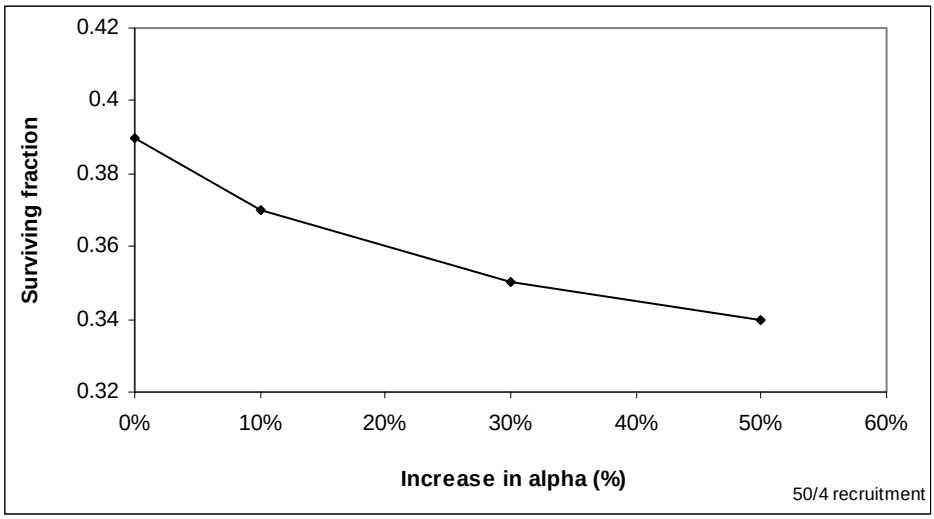

Figure 6.7. Surviving fraction as a function of α in the combined cisplatin-radiotherapy with cell recruitment.

These results suggest that radiosensitization due to cisplatin, if there is any, should occur through more complex biological mechanisms.

6.4.4. Conclusions

To demonstrate the radiosensitizing properties of cisplatin by sublethal damage repair inhibition, the surviving fractions have been changed. The increase in the alpha parameter along the G1 and G2 phases of the cycle has led to decrease in the surviving fraction. However, a 50% increase in alpha has altered the overall survival by only 12% (from 0.39 to 0.34), not leading to synergistic effects between cisplatin and radiation. Yet, higher increase in alpha might be unrealistic for head and neck cancers. These results

suggest that radiosensitization due to cisplatin, if there is any, should occur through complex biological mechanisms. Therefore, in order to model cisplatin as a radiosensitizer, the mechanisms behind the process of radiosensitization should be better understood.

6.5. Determination of the optimum schedule in the treatment of unresectable head and neck cancer with cisplatin-radiotherapy

6.5.1. Introduction

It was mentioned, several times in the present work, that the optimum schedule in the treatment of unresectable squamous cell carcinomas of the head and neck with cisplatin and radiation is still under investigation in clinics. As a step forward in the process of finding a better schedule, the results of the previous and also of the current chapter are summarized below:

- the review of a selected number of trials shows that treatment regimens that correlate better with the pharmacokinetics and the radiobiological properties of the therapeutic agents resulted in the achievement of better outcomes;
- cisplatin treatment every third day is comparable, in terms of tumour control, with a daily administration, reducing, therefore, normal tissue toxicity;
- tumour control is superior for the daily low dose administration as compared to weekly high dose;
- cisplatin administered before radiation gives similar tumour control to the post-radiation sequencing of the drug;

- the killing effect of the combined modality treatment on tumour increases with the increase in cell recruitment, assuming no associated repopulation from other mechanisms;
- the individual cell kill produced by cisplatin and radiation leads to an additive-only tumour response when the treatments are given concurrently;
- for a synergistic effect cisplatin must potentiate the effect of radiation;

6.5.2. Methods

Radiotherapy and chemotherapy have been simulated concurrently, by implementing the action of both radiation (as described in Chapter 4) and cisplatin (as described in Chapter 5) on the virtual head and neck cancer. Three different schedules for cisplatin combined with conventionally fractionated radiotherapy have been modelled: cisplatin on a daily basis, cisplatin every third day and also cisplatin on a weekly basis. Surviving curves resulting from the three simulations have been plotted and compared. For daily and third daily cisplatin, the 'default' values for cisplatin's action have been considered: 80% marking, 50% cell kill, while for the weekly simulation 95% of cycling cells have been marked, with a corresponding 60% cell kill (see Chapter 5). Cell recruitment of 50/4 has been considered after each kill event.

6.5.3. Results and discussions

It was shown in Chapter 5, that in single agent treatment, cisplatin administered every third day has led to similar tumour control to the daily administration. However, when cell recruitment was taken into account, the equivalence between the two treatments was not valid anymore, since tumour repopulation in between cisplatin treatments could not be effectively compensated by cell kill. The combination of cisplatin with radiotherapy has accentuated the divergence between the daily and third daily cisplatin (Figure 6.8).

Weekly administration of cisplatin concurrently with radiotherapy resulted into poorer tumour control than the daily dosage of cisplatin (Figure 6.8). This result is in accordance with laboratory investigations showing that the most profound effect of combined cisplatin-radiotherapy is expected from fractionated administration of both treatment modalities concurrently (Bartelink 1985, Bartelink 2000). The clinical trial conducted by Jeremic (2000) using cisplatin on a daily basis concurrently with fractionated radiotherapy resulted in 46% survival after 5 years, compared to 34% survival after 4 years (Fountzilas 1994) or 46% survival after 2 years (Gasparini 1991), just to mention some of the trials using weekly cisplatin with fractionated radiotherapy (see also Appendix B).

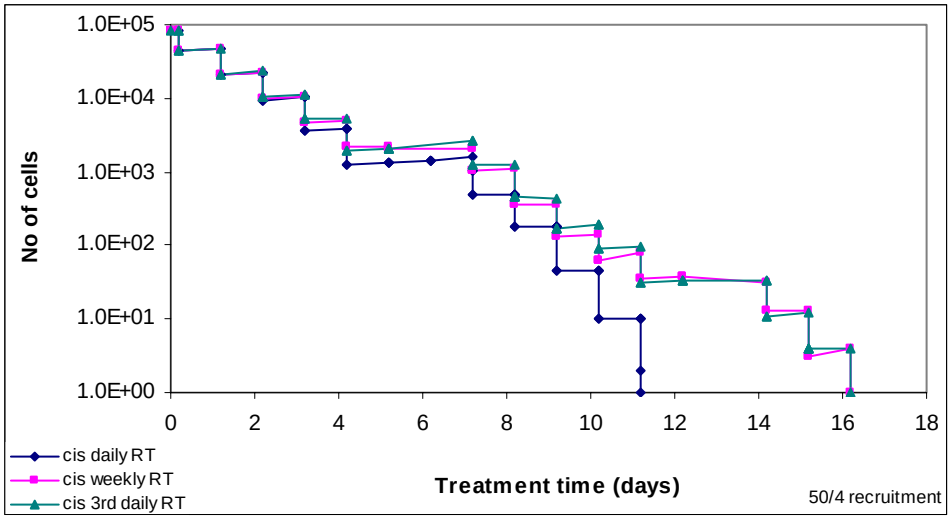

Figure 6.8. Survival curves for the combined cisplatin-radiotherapy with cisplatin administered daily (blue graph), third-daily (green graph) and weekly (pink graph).

Figure 6.9 compares the survival curves for radiotherapy as a sole treatment and for the combined radio-chemotherapy with cisplatin administered once a week during the course of treatment.

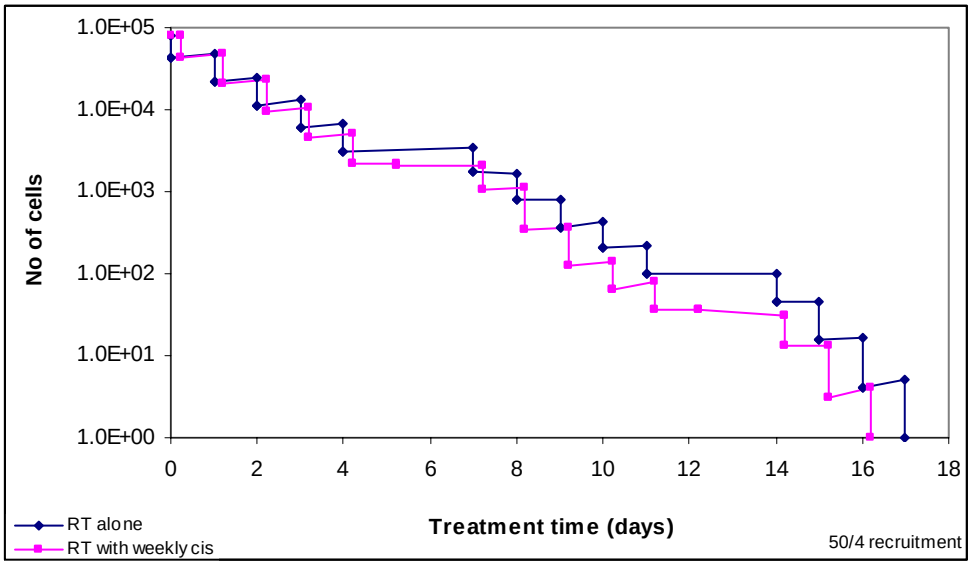

Figure 6.9. Cell survival curves for radiotherapy and for cisplatin-radiotherapy with cisplatin administered on a weekly basis.

The improvement in tumour control is only 6% for the weekly cisplatin, as compared to 35% enhancement for the daily cisplatin (see Figures 6.8 and 6.9).

These findings support the evidence given by pre-clinical studies showing that the combined effect of cisplatin and radiation is maximal when cisplatin is given close in time to radiation fractions. No cooperative effect is seen when cisplatin is administered 24 h before irradiation (Schwachöfer 1991). When cisplatin is given weekly, though in large doses, the combined treatment lacks of cooperation between cisplatin and radiation. A once-a-week administration of cisplatin has low potentiating effect on radiation since the drug is not present in the tumour along the whole radiotherapy. Furthermore, the cytostatic property of cisplatin is not used effectively in such schedule. With a once-a-week chemotherapy, there is no subsequent dose of cisplatin that would be able to renew cell arrest, therefore radiotherapy cannot enhance the cell kill along the sensitive G2 phase.

For the daily cisplatin schedule, the drug is actively present all the time during radiotherapy, since it is administered every day. During the weekend, there is still active drug present within the tumour, as the series of mechanisms consisting of adduct

formation-cell arrest in G2-release of the viable cells-apoptosis last for 5 days. As a consequence, the effect of cisplatin on the tumour cumulates, and the interplay between radiation and daily cisplatin leads to an efficient cell kill.

6.5.4. Conclusions

The model has shown that cisplatin administered immediately before radiation gives similar tumour control to the post-radiation sequencing of the drug. Furthermore, the killing effect of the combined modality treatment on tumour increases logarithmically with the increase in cell recruitment (Figure 6.3). The rationale behind this result originates from the variation of the radioresistivity parameter along the cell cycle. Since the quiescent cells present with higher radioresistance than the majority of the cycling cells (excepting those in the S phase), by re-entering the mitotic cycle, the previously quiescent cells loose their radioresistance, and therefore they become more prone to radiation damage. Also, since cisplatin arrests the cells in the G2 phase, which is equally radiosensitive to mitosis, the overall radioresistance of the cycling cells decreases drastically, hence contributing to radiation-produced cell kill.

From the above exposed rationale, one can conclude that chemo-radiotherapy may be more beneficial for rapidly proliferating tumours than for slowly proliferating ones.

The current model has considered only the independent cell kill produced by cisplatin and radiation, respectively. When comparing radiation survival curves and cisplatin-radiation survival curves no supra-additivity was indicated. These findings suggest that the individual cell kill produced by the two cytotoxins leads to an additive-only tumour response when the treatments are given concurrently. Therefore, it was suggested that for a synergistic effect, cisplatin must potentiate the effect of radiation, through the radiosensitizing mechanisms addressed in the literature.

When comparing weekly with daily administration of cisplatin, concurrently with radiotherapy, it was noted that the daily administration increases tumour control, by reducing the length of the radiotherapy treatment by 35% while the weekly cisplatin with radiotherapy enhances tumour control by only 6%.

Having a better knowledge about the mechanism of cell recruitment during chemo-radiotherapy and also on the amount of cells involved in the process, would allow a more comprehensive analysis of the optimal scheduling of radiation–drug therapies.

Chapter 7

Final conclusions

This work has encompassed the major challenges brought by the combined modality treatment: chemo-radiotherapy. The aims of the current investigation, as pointed out in Chapter 1, were the following:

- To expose the challenges in the combined modality treatment for head and neck cancers
- To develop a computer-based tumour model with realistic biological parameters, that would allow simulation of treatment with radiation and chemotherapy
- To simulate radiotherapy on the virtual tumour and analyse the effects of radiotherapy on tumour regression and regrowth
- To investigate the mechanisms responsible for tumour repopulation after radiotherapy
- To implement the mechanisms of action of cisplatin, to simulate and analyse the effect of cisplatin on the virtual tumour
- To investigate the effect of drug resistance on tumour response
- To examine the process of tumour repopulation after chemotherapy
- To simulate the combined modality treatment: cisplatin-radiotherapy on the virtual tumour and to analyse the effect of the treatment on tumour behaviour
- To investigate the optimal treatment sequencing between cisplatin and radiotherapy and also the optimal schedule for head and neck carcinomas.

The objective of the combined chemo-radiotherapy treatment is to achieve a higher therapeutic ratio compared to the single-agent therapy through either a better tumour response or reduced normal tissue damage. The present work has reviewed a selected

number of trials for unresectable squamous cell carcinoma of head and neck with cisplatin used as a single chemotherapeutic agent with and without irradiation. It was observed that treatment regimens that correlate better with the pharmacokinetics and the radiobiological properties of the therapeutic agents resulted in the achievement of better outcomes. However, at present, there is no optimal schedule for treating head and neck cancer and the most efficient sequencing of drug and radiation has still not been established. Optimisation of the treatment can be improved through further study and modelling of the pharmacokinetic and radiobiological interactions between cisplatin and radiotherapy.

The review of the head and neck trials has provided foundation for a computerised simulation of treatment schedules of a virtual head and neck tumour which, eventually, has served as a basis for a temporal study of the combined cisplatin-radiotherapy.

The biological growth of a tumour has been modelled through the application of probabilistic functions and cellular characteristics to a Monte Carlo methodology. The resultant cell population was compared with accepted biological tumour constitution and growth characteristics and agreement was achieved in terms of the exponential tumour growth, the volume doubling time and an exponential distribution of cells along the cell cycle. Three basic cellular types have been modelled: stem (S cell), proliferative (P cell) and non-proliferative (N). The S:P:N ratio for the head and neck tumour was considered to be 2:13:85. Stem cells were able to indefinitely proliferate while proliferating cells had been restricted to a finite number of cell divisions. Non-proliferative cells (N cell) were the non-dividing cells; after leaving the mitotic phase of the cell cycle, the N cell entered the resting phase (G_0). The cycle time had a mean value of 33 hours with a standard deviation of 13.7 hours, and presented with a truncated Gaussian distribution around the average value. Tumour volume doubling time was 52 days.

The development of the virtual population of tumour cells has offered a mechanism for further study and understanding of the impact of different factors on the tumour growth and behaviour under treatment.

Initially, a conventional fractionated radiotherapy treatment has been simulated for the virtual tumour: daily dose of 2 Gy, 5 days a week, over 7 weeks. The Linear Quadratic model has been used to determine values for α and β along the four cycle phases as well as the quiescent phase. The corresponding surviving fractions have also been determined according to the variation in intrinsic radiosensitivity along the cell cycle. With the implementation of phase-specific surviving fractions the process of repopulation during radiotherapy has been studied. The repopulation mechanisms the present work has considered for study were: cell recruitment, accelerated stem cell division and asymmetry loss in stem cell division.

Experiments on cell cultures were undertaken to examine the onset of repopulation. The experimental curves derived from data obtained from squamous cell line irradiation indicated the possibility of the immediate onset of repopulation with the start of the treatment. Furthermore, since there are no 'recruitable' cells in a monolayer cell culture, it was concluded that recruitment is not the key mechanism in tumour repopulation in the presented study. Therefore, accelerated repopulation was attributed to the other two mechanisms: accelerated stem cell division and loss of asymmetrical division of stem cells.

The experimental data has been compared with the results obtained from the theoretical model. Once again, cell recruitment was shown to not constitute a key mechanism in tumour repopulation after radiotherapy. However, when combined with accelerated stem cell division, cell recruitment has shown a contribution towards regrowth through the additive effect of the two mechanisms. The mechanism of accelerated stem cell division has presented with a twofold decrease in tumour control compared to cell recruitment. Nevertheless, tumour regrowth was shown to be more pronounced with recruitment *and* accelerated division than with accelerated stem division alone.

It was suggested that loss of asymmetry in stem cell division could be the key process in tumour regrowth. Further work has demonstrated that stem cells must be affected by the

loss of asymmetry only in small percentage (less than 10%), otherwise the repopulation of the tumour would reach unrealistic proportions in a very short time (within a week). The work shows, that even for small percentage of stems (5%) affected by successive symmetrical division during the whole treatment, tumour repopulation is so high that not even partial eradication is achieved. Furthermore, the process of symmetrical division should reach a saturation stage, similar to the unperturbed tumour growth. Moreover, the stems affected by this mechanism should follow a non-linear distribution function. With a linear implementation of asymmetry loss the tumour has grown continuously, despite the cell kill produced by radiation. A more appropriate description was given by a non-linear distribution, which reached 'saturation' and afterwards decreased as cell kill overcame repopulation. The percentages of the three cell types: stem, finitely proliferating and nonproliferating varied during radiotherapy, thus altering the initial composition of the tumour. Tumour repopulation involved a drastic change in the S:P:N ratio along the treatment.

The general conclusion in regards with tumour repopulation is that cell recruitment, accelerated stem cell division and the loss of asymmetrical division of stem cells, are all mechanisms determining, to a certain extent, tumour repopulation after radiotherapy.

The effect of cisplatin on the virtual head and neck tumour has also been modelled. The entire sequence of events caused by cisplatin's properties, i.e. DNA-adduct formation, cell arrest, cell release into the cycle and cell kill via apoptosis has been simulated. The main processes covered in regards with cisplatin's action were the following: scheduling of cisplatin, tumour resistance to cisplatin and the mechanism of repopulation in chemotherapy.

A daily treatment with cisplatin has been simulated to illustrate the behaviour of the tumour population during and after treatment. It was noted that the shape of the survival curve for the whole tumour is dictated by the quiescent population, as they dominate in number, but also they are not affected by cisplatin. It was seen that the number of non-cycling cells increases due to natural cell production, while the number of cycling cells

decreases as a result of cisplatin's kill, reaching, after treatment, a steady state. It was shown that cisplatin treatment every third day is comparable, in regards to tumour control, with a daily administration, and more effective than an every-second-day-treatment. Also, tumour control was superior for the daily low dose administration as compared to weekly high dose. The model has shown that the optimal administration of cisplatin, as a sole treatment, would be the every-third-day schedule, which would lead to similar tumour control as the daily treatment but to less normal tissue toxicity, allowing longer times between chemotherapy cycles for the normal tissue to repair the damage.

Drug resistance has been considered by modelling two classes of mechanisms: one leading to low drug uptake and the other considering the decreased susceptibility to the induction of apoptosis. Acquired cellular resistance, substantiated by a decreased drug uptake, has been modelled by reducing the percentage of cells 'marked' by cisplatin. A sensitivity study has been undertaken to study the various percentages of marked cells and their effect on cell survival. The curve has shown a logarithmic decrease of the cell population with the increase in the percentage of cells affected by cisplatin. The mechanisms of drug resistance that affect the fate of the exposed cell have been modelled by varying the percentage of killed cells. It has been shown that there is a close-to-linear dependence of the number of surviving tumour cells on the percentage of cells killed by cisplatin. To quantify the extent of drug resistance, the Cisplatin Resistance Factor (CRF) has been defined. By determining CRF during treatment, drug resistance has been shown to be a cumulative process. For low drug uptake, resistance cumulates linearly or even supra-linearly for very low uptake. When decreased susceptibility to the induction of apoptosis is modelled, resistance cumulates over a sigmoid pattern. The multi-mechanistic dependence of drug resistance has been modelled by combining the low drug uptake with the decreased susceptibility to the induction of apoptosis. It was shown that resistant tumours can overcome tumour regression leading to treatment failure.

Tumour repopulation, a so far neglected factor in chemotherapy, has been modelled through the mechanism of recruitment. Percentages of cells recruited in the range of (5%-50%) have been plotted as a function of tumour population, and a supra-linear

dependence observed, which indicates the potent effect of recruitment on tumour control. Both immediate and late onset of recruitment have been studied, indicating a poorer tumour control in the first case. When comparing cell survival curves after chemo treatment with cell recruitment and with drug resistance, respectively, it was shown that even small percentages of recruited cells (15%) with a late onset of repopulation will lead to treatment failure, similarly to drug resistance. The study on cell recruitment, even as the only factor in tumour response to depopulation shows that tumour regrowth due to chemotherapy should not be neglected.

Finally, the combined effect of cisplatin-radiotherapy was set under investigation. A conventionally fractionated radiotherapy treatment has been simulated for the tumour: daily dose of 2Gy, 5 days a week, over 7 weeks. Cisplatin has been administered, on a daily basis, concurrently with radiotherapy. The sequencing between the drug and radiation has been studied with cisplatin either before or after irradiation. The timing of the drug and radiation, has been kept, in both cases, very close (cisplatin immediately before, or immediately after radiotherapy). Cell recruitment has been considered as a consequence of both chemotherapy and radiotherapy, with a constant percentage of cells recruited after each killing event. To cover any biologically sensible value, and also an early or delayed onset of recruitment, a range of (5% – 90%) quiescent cells recruited has been considered.

The model has shown that cisplatin administered before radiation gives similar tumour control to the post-radiation sequencing of the drug, if cisplatin is given very close in time to radiation. Furthermore, the killing effect of the combined modality treatment on tumour increases logarithmically with the increase in cell recruitment.

It was demonstrated in the present work that the effect of cisplatin, as a single cytotoxic agent, decreases with the increase in cell recruitment, since repopulation overcomes cell kill. Therefore, it was concluded that in chemotherapy, repopulation should not be a neglected factor as it can lead, similarly to drug resistance, to treatment failure. On the other hand, cell recruitment alone during radiotherapy, in the absence of a change in

symmetry of stem cell production, has not been found as a key mechanism leading to accelerated repopulation. The rationale behind this result originates from the variation along the cell cycle of the surviving fraction. Since the quiescent cells present with a higher radioresistance than the majority of the cycling cells (excepting those in the S phase), by re-entering the mitotic cycle, the previous quiescent cells loose their radioresistance, therefore they become more prone to radiation damage. Also, since cisplatin arrests the cells in the G2 phase, which is equally radiosensitive to mitosis, the overall radioresistance of the cycling cells decreases drastically, hence contributing to radiation-produced cell kill. These effects make the combined cisplatin-radiotherapy more effective than either cisplatin-treatment or radiotherapy alone, on account of cooperation between the drug and radiation.

When comparing radiation survival curves and cisplatin-radiation survival curves, no supra-additivity was indicated. These findings have indicated that the individual cell kill produced by the two cytotoxins leads to an additive-only tumour response when the treatments are given concurrently. Therefore, it was suggested that for a synergistic effect, cisplatin must potentiate the effect of radiation, through the radiosensitizing mechanisms addressed in the literature.

To demonstrate the radiosensitizing properties of cisplatin by sublethal damage repair inhibition, the surviving fractions have been changed. The increase in the alpha parameter along the G1 and G2 phases of the cycle has led to decrease in the surviving fraction. However, a 50% increase in alpha has altered the overall survival by only 12% (from 0.39 to 0.34), not leading to synergistic effects between cisplatin and radiation. Therefore, it was concluded that radiosensitization due to cisplatin, if there is any, should occur through more complex biological mechanisms.

It was shown by the current work that in single agent treatment, cisplatin administered every third day has led to similar tumour control to the daily administration. However, when cell recruitment was taken into account, the equivalence between the two treatments was not valid anymore, since tumour repopulation in between cisplatin

treatments could not be effectively compensated by cell kill. The combination of cisplatin with radiotherapy has accentuated the divergence between the daily and third daily cisplatin. When comparing weekly with daily administration of cisplatin, concurrently with radiotherapy, it was noted that the daily administration increases tumour control, by reducing the length of the radiotherapy treatment by 35% while the weekly cisplatin with radiotherapy enhances tumour control by only 6%.

To summarize, the major results of the current work are highlighted in the following paragraph:

- A virtual tumour of the head and neck has been grown using stochastic methods
- The tumour is described by well-founded biological parameters
- The effect of both radiation and cisplatin on the virtual tumour, either as sole treatments or in combination, has been investigated
- Cell recruitment is not the key mechanism leading to repopulation after radiotherapy
- Asymmetry loss in stem cell division is suggested to be the main repopulation mechanism in squamous cell carcinomas
- Tumour repopulation should not be neglected during chemotherapy treatment as could lead to similar outcome as drug resistance
- Cisplatin should be administered close in time (immediately before, or immediately after) in regards with radiotherapy
- Daily administration of cisplatin is superior, as tumour control, to weekly administration, when given concurrently with radiotherapy.

The review of the trials presented in Chapter 2 has shown that treatment regimens that correlate better with the pharmacokinetics and the radiobiological properties of the therapeutic agents resulted in the achievement of better outcomes. Those were the trials using fractionated schedule for both cisplatin (daily administration) and radiation. However, weekly scheduling of the drug is still more common than the low-dose daily administration of cisplatin. The present work has proven, by implementing the radiobiological properties of radiation, and kinetics of cisplatin that daily administration,

with cisplatin administered close in time to radiation is a definite step towards optimisation of the current treatments for the unresectable head and neck cancers.

Future directions

Models in cancer treatment are useful tools to reproduce the biological world. Nevertheless, due to the complexity of the biological reality, there is always scope for improvement. The present work has covered a vast area of cancer research, with an individual analysis of the effect of radiotherapy and also cisplatin on tumour behaviour, as well as the effect of the combined cisplatin-radiotherapy on head and neck tumours. All the processes described and analysed in the current work were modelled around the 'time' parameter only.

Also, the key factor in studying the effect of the two treatments was tumour control. There was no consideration of normal tissue toxicity, simply because the doses used in both treatment types were either conventionally used (for radiotherapy) or having a medium toxicity (as for cisplatin). However, modelling a variety of schedules for the combined cisplatin-radiotherapy, with focus on both tumour control and normal tissue toxicity, the therapeutic ratio could be improved not only by increasing tumour control, but also by decreasing normal tissue complication.

Therefore, some of the future directions resulting from the present work are:

- To model the spatial components of tumour growth (hypoxia, angiogenesis, tumour invasion) and to incorporate them into the temporal model
- To model normal tissue toxicity, especially in the case of chemotherapy
- To model the effect of tirapazamine (a currently used hypoxic cell sensitizer) in combination with cisplatin and radiotherapy for head and neck cancers, a protocol presently under trial, and to compare the theoretical results with the outcome of the trial

- To undertake cell line studies with the aim of investigating the repopulation mechanisms in tumours with high cell turnover
- To generalize the model for the treatment of other rapidly proliferating tumours by considering their specific tumour kinetic parameters.

A complex tumour model, incorporating the biological parameters of a particular neoplasm, the spatio-temporal characteristics of the tumour, and also tumour behaviour during therapy, becomes a vital tool in the area of individualized patient treatment, which is a central aspect in today's cancer research.

Appendix A. Cisplatin as a single agent for advanced head and neck cancers

Trial or study	*No. patients & patient selection*	*Treatment type*	*Chemotherapy schedule*	*End points*		
				Complete response[1]	*Partial and/or overall response*	*Toxicity (side effects)*
Jacobs et al 1978 Phase II	18 advanced SCC H&N	24 h infusion	80mg/m^2 every 3 wks	5.5%	PR[2] - 33% overall response 72%	minimal toxicity: renal 6% hematologic: 9% gastrointestinal: 76%
Creagan et al 1982 Phase II	33 advanced SCC H&N (oral cavity, paranasal sinus, larynx, pharynx,)	24 h infusion	90mg/m^2/24 h every 3 to 4 wks; intravenously (IV)	-	overall response rate (OR) 12% with the duration between 15-56 wks	gastrointestinal, hematologic moderate to severe nausea & vomiting
Sako et al 1978 Phase III	30 advanced SCC H&N	high dose (HD) versus low dose (LD) cisplatin	HD: 120mg/m^2 in 15 min LD: 20mg/m^2 in 15 min every 3 wks in 6 cycles	HD: 13% LD: 6.6%	overall response (OR): HD: 33% LD: 26.6%	significant gastrointestinal toxicity- almost all patients; renal toxicity: HD: 66.6%, LD: 58%; ototoxicity with high frequency

						hearing loss: HD: 87%, LD: 47%
Veronesi et al 1985 Phase III (randomised study)	62 advanced SCC H&N (III&IV) (oral cavity, oropharynx, hypopharynx, rhinopharynx)	high dose (HD) versus low dose (LD) cisplatin	HD (33pts) 120mg/m^2 IV infusion for 30-45 min LD (29 patients) 60mg/m^2 IV for 30-45 min every 3 wks for 2 cycles	insignificant (HD) & zero (LD)	PR: HD: 16.1% PR: LD: 17.8% median survival 34 wks	tolerable toxicity HD more severe vomiting but no significant differences in rest

WHO definitions for response evaluation:

[1]Complete response (CR) of a tumour is considered to be the complete clinical disappearance of the tumour, determined by two observations not less than 4 weeks apart

[2] Partial response (PR) involves at least 50% disappearance of the tumour, determined by two observations not less than 4 weeks apart.

Abbreviations: SCC H&N – squamous cell carcinoma of the head and neck; HD – high dose (cisplatin); LD – low dose (cisplatin); min – minutes; h – hours; wks – weeks; mo – months; yrs – years.

Appendix B. Cisplatin / radiotherapy schedules for head and neck cancer

Trial or study	*No of patients and patient selection*	*Chemotherapy schedule*	*Radiotherapy schedule*	*Total dose CT*	*Total dose RT*	*End points*		
						Complete response	*Partial and/or overall response*	*Toxicity (side effects)*
Clamon et al 1995 Phase I	14 stage III & IV all sites, no nasopharynx	1-3mg/m^2/day	1.1Gy twice a day	35-105mg/m^2	70.4-75.9Gy	21%	PR: 64%	severe toxicities; central nervous system toxicity became dose-limiting
Leipzig 1983 Phase II	14 advanced SCC H&N	15mg/m^2 IV d. 1->5 d. 21->25 0.2-2 h before RT	conventional RT 6-7 wks	150mg/m^2	60-66Gy	78.5%	18 wks without evidence of recurrence	renal toxicity (1 patient died from renal failure); rare nausea

Al-Sarraf et al 1987 (RTOG study) updated by *Marcial et al* 1990 Phase II (with 2 control arms) RTOG 81-17 study	124 22% of patients nasopharyngeal	100mg/m^2 rapid IV bolus every 3 wks, on days 1, 22 & 43	1.8-2Gy/day 5 days/week 7 wks	300mg/m^2	66-73.8Gy	71% (best response: 89% nasopharynx worst response: 37% hypopharynx	PR: 30% 60% patients finished the complete treatment; survival rate: 1 yr : 68% 4 yrs : 34% (all patients) 4 yrs : 12% (when nasopharynx is excluded)	severe toxicities: hematologic: 19% stomatitis: 31%; renal: 6% 1patient-renal failure; The adequate CRT was delivered in 58% of patients
Harrison et al 1991 Phase II (prospective study)	24 12.5% nasopharyngeal patients (stage IV)	100mg/m^2 on days 1 & 22	1.8Gy/day for 4 wks followed by BID-RT for 2 wks: am fraction: 1.8Gy given to the entire area of risk & p.m. fraction: 1.6Gy given to the	200mg/m^2	70Gy (1.8Gy for 4 wks +3.4Gy for 2 wks = 36Gy + 34Gy)	64% no different results when excluding nasopharynx	PR: 32%; local disease-free survival at 1 yr- 56%; overall survival at 1 yr- 69%;	well tolerated treatment despite its intensity; 1 treatment related death; 100%pts – mucositis; 17%pts did not receive their day 22

			gross disease alone. Fractions were separated by 4-6 h. Total: 6 wks					cisplatin because of decreased renal function.
Fontanesi et al 1991 Phase II	30 stage III & IV all sites	100mg/m^2 IV infusion over 6 h on days 1, 21 & 42	1.11Gy twice a day, 4-6 h interfractions initiated within 12 h of the first course of cisplatin. 6-8 wks	300mg/m^2	60-76.35Gy	89%	survival without evidence of disease at 19 mo - 66%;	acceptable toxicity; 1 death from renal failure; 23% patients-severe xerostomia; significant weight-loss (4%-20% of body weight)
Gasparini et al 1991 Phase II	35 stage II (unresectable), III & IV all sites	80mg/m^2 IV infusion of 30min, 2 h after the beginning of RT, every 3 wks: days 1, 21&42	2Gy/day 6-8 wks	240mg/m^2	60-70Gy	75%	PR: 25% estimated 1 yr survival-58%; estimated 2 yrs survival- 46%;	moderate renal & hematologic toxicities (<= grade2); 87% patients-stomatitis (37% severe stomatitis-grade4, which led to a split of 10-15 days after 30Gy of RT for 34% patients; these

								patients did not receive the last course of CT).
Glaser et al 1993 Phase II	36 all sites (oral cavity, oropharynx, larynx, hypopharynx0 no nasopharyngeal	single weekly dose: 35mg/ m^2 over 1 h, 3-4 h before irradiation.	2Gy daily over 6 wks	210mg/ m^2	60Gy	75%	PR: 25% disease free survival 64% at 1 yr 52% at 2 yrs; overall survival 81% at 1 yr 47% at 2 yrs	no renal toxicity; well tolerated treatment; 86% patients received the full schedule of weekly cisplatin
Fountzilas et al 1994 Phase II	48 16% nasopharyngeal	100mg/ m^2 on days 2, 22 & 42	1.8Gy/day 5 days/week 7 wks	300mg/m^2	70Gy	72% (87.5% nasopharynx 87.5% oropharynx; 79% larynx) less for other sites	PR 10%; survival after 4 yrs 34%	no severe nephrotoxicity; 80% patients received the total dose; more than 50% patients had considerable weight loss; quite serious side effects.

Arias et al 1995 Phase II (pilot study)	40 stages III & IV 7.5% nasopharyngeal	20mg/m^2/day days 1->5 in continuous perfusion	1.6Gy twice a day; 4-6 h interval; 2+2 wks with 2 wks gap	100mg/m^2	64-67.2Gy	92.5% (100% nasopharynx 100% larynx)	2 yrs overall survival-64%; 3 yrs overall survival-47%; 2 yrs local control-65%.	The protocol was completed for all patients; mucositis-75% no other severe acute toxicities; late toxicity-xerostomia-45%;
Robbins et al 1997 Phase II (Radplat protocol-Memphis experiment.)	60 stage III & IV all sites, no nasopharynx	150mg/ m^2 weekly (days 1, 8, 15&22), intraarterial rapid delivery 3-5 min	1.8-2Gy once daily 5 days/week	600mg/ m^2	66-74Gy 7-8 weeks	75% (91% primary site; 67% lymph nodes)	85% completion rate; 1 yr overall survival 67%; 3 yrs overall survival 60%	42% patients grade III-IV toxicity; 25% patients have died of disease;
Bachaud et al 1997 Phase II	11 (curative intent) stage IV oropharynx & hypopharynx	5-7mg/m^2/day	1.8Gy/day 8 wks	200-280mg/m^2	72Gy	66%	PR-16%; overall survival-16 mo; 33% patients-disease-free for 12-33 mo;	Hematologic toxicity was the dose limiting factor (at the 7mg/m^2/day no patient completed the chemo protocol); There was no nephro-

								, oto-, or neurotoxicity
Choi et al 1997 Phase II (prospective study)	21 17-currative intent (59% nasopharynx); 4-palliative intent	5-10mg/m^2/day (continuous infusion) 3 courses of 2 wks (1 wk break between)	1.2-1.25Gy twice a day (4-6 h interval) 3 courses of 2 wks (1 wk break between)	150-300mg/m^2	64.8-70.8Gy	94%	47% patients survived >3 yrs	acceptable acute reactions in spite of concomitant infusion;
Huguenin et al 1998 Phase II (pilot study)	64 stage III & IV all sites, no nasopharynx	20mg/m^2/day 5 days in wks 1&5	1.2Gy twice a day - 6 h interval	200mg/m^2	74.4Gy	LC – 74%	local control at 5 yrs - 74%; overall survival at 5 yrs - 37%	27% patients >= grade3 toxicity; 50% patients with permanent xerostomy.
Serin et al 1999 Phase II	70 advanced nasopharynx	30mg/m^2 /wk	conventional RT	180-210mg/m^2	60-70Gy	CR-locoregional 90% patients	overall survival at 3 yrs - 63%; locoregional failure-free survival at 3 yrs - 79%;	14% patients grade3 toxicity
Jeremic et al 1997 Phase III	53 RT 53 RT + cisplatin stage III & IV all	6mg/m^2/day IV bolus 30 min before	1.8-2Gy daily 5days/wk 7-7.5 wks	210-225mg/m^2 (7-7.5 wks)	70Gy	CRT 72% RT 38%	5 yr survival CRT 32% RT 18%	CRT patients had more treatment interruptions than RT

	sites nasopharynx: 11% -RT group 9% - CRT group	irradiation						patients due to acute toxicity (9% versus 4%); Overall, the differences in toxicity were not significant;
Jeremic et al 2000 Phase III (prospective randomised trial)	65 stage III & IV all sites, 10% nasopharynx	6mg/m^2 IV bolus 3-4 h after the first RT fraction	1.1Gy twice a day, 4.5-6h interfractions	210mg/m^2	77Gy 7 wks	75%	survival at 2 yrs 68%; survival at 5 yrs-46%; locoregional progression free survival at 5 yrs-50%; distant metastasis. -free survival at 5 yrs- 86%	14% patients >10% weight loss; 11% patients – treatment interruptions because of acute toxicity; 5%-nephrotoxicity 12%-leukopenia; 25%-esophagitis; 49%-stomatitis

Abbreviations: CT – chemotherapy; RT – radiotherapy; CRT – chemoradiotherapy; CR -complete response; PR – partial response

Appendix C. Derivation of cell cycle phase-related surviving fractions

Consider the Linear Quadratic equation:

$$N = N_0 \exp[n(-\alpha d - \beta d^2)],$$

where:

- N_0 represents the initial number of cells in the cycle;
- N is the number of remaining cells after *n* fractions of *d* doses of radiotherapy;
- n is the number of fractions;
- d is the radiation dose given in one fraction;
- α is the linear parameter;
- β is the quadratic parameter.

As the literature considers the α/β ratio constant, we relate to this ratio as *k*.

The surviving fraction is defined as: $SF = \frac{N}{N_0}$.

To distinguish between the literature-given parameters and those given by the model, all the above quantities will wear the average (*av*) subscript. Also, n = 1 as the surviving fraction is determined after one radiation dose of 2Gy. Therefore, the linear quadratic equation can be rewritten as:

$$SF_{av} = \exp(-\alpha_{av} d - \frac{\alpha_{av}}{k} d^2) = \exp[\alpha_{av}(-d - \frac{d^2}{k})] \quad (1)$$

Total cell population before and after radiotherapy is expressed as a function of the individual populations in the five phases of the cycle:

$$\begin{aligned} N_0 &= N_{0G0} + N_{0G1} + N_{0S} + N_{0G2} + N_{0M} \quad , \\ N &= N_{G0} + N_{G1} + N_S + N_{G2} + N_M \, . \end{aligned} \tag{2}$$

Applying the linear quadratic formulation to each individual phase, the following system of equations is obtained:

$$\begin{cases} N_{G0} = N_{0G0} \exp[\alpha_{G0}(-d - \dfrac{d^2}{k})] \\ N_{G1} = N_{0G1} \exp[\alpha_{G1}(-d - \dfrac{d^2}{k})] \\ N_S = N_{0S} \exp[\alpha_S(-d - \dfrac{d^2}{k})] \\ N_{G2} = N_{0G2} \exp[\alpha_{G2}(-d - \dfrac{d^2}{k})] \\ N_M = N_{0M} \exp[\alpha_M(-d - \dfrac{d^2}{k})] \end{cases} , \quad \text{where} \quad \begin{cases} \dfrac{N_{G0}}{N_{0G0}} = SF_{G0} \\ \dfrac{N_{G1}}{N_{0G1}} = SF_{G1} \\ \dfrac{N_S}{N_{0S}} = SF_S \\ \dfrac{N_{G2}}{N_{0G2}} = SF_{G2} \\ \dfrac{N_M}{N_{0M}} = SF_M \end{cases} \tag{3}$$

Thus the total number of cells after radiation is:

$$N = N_{0G0}SF_{G0} + N_{0G1}SF_{G1} + N_{0S}SF_S + N_{0G2}SF_{G2} + N_{0M}SF_M \, , \tag{4}$$

which is equivalent with:

$$N_0 SF_{av} = N_{0G0}SF_{G0} + N_{0G1}SF_{G1} + N_{0S}SF_S + N_{0G2}SF_{G2} + N_{0M}SF_M \quad \big| : \mathrm{N_0}$$

$$\therefore \quad SF_{av} = \frac{N_{0G0}}{N_0} SF_{G0} + \frac{N_{0G1}}{N_0} SF_{G1} + \frac{N_{0S}}{N_0} SF_S + \frac{N_{0G2}}{N_0} SF_{G2} + \frac{N_{0M}}{N_0} SF_M \, . \tag{5}$$

Considering the literature data, the following assumptions have been made in regard with the sensitivity ratios for various phases of the cell cycle:

$$\begin{cases} SF_S = 3SF_M = 3SF_{G2} = 1.1SF_{G0} \\ SF_{G1} = SF_{av} \end{cases} \quad (6)$$

Taking (6) into account, equation (5) can be rewritten as:

$$SF_{av} = \frac{N_{0G0}}{N_0} \cdot \frac{1}{1.1} SF_S + \frac{N_{0G1}}{N_0} SF_{av} + \frac{N_{0S}}{N_0} SF_S + \frac{N_{0G2}}{N_0} \cdot \frac{1}{3} SF_S + \frac{N_{0M}}{N_0} \cdot \frac{1}{3} SF_S \quad (7)$$

therefore:

$$SF_S = SF_{av} \frac{N_0 - N_{0G1}}{\frac{N_{0G0}}{1.1} + N_{0S} + \frac{N_{0G2}}{3} + \frac{N_{0M}}{3}} \quad (8)$$

Using the linear quadratic formula (1) in equation (8) the relation below is obtained:

$$\exp[\alpha_S(-d - \frac{d^2}{k})] = \exp[\alpha_{av}(-d - \frac{d^2}{k})] \cdot \frac{N_0 - N_{0G1}}{\frac{N_{0G0}}{1.1} + N_{0S} + \frac{N_{0G2}}{3} + \frac{N_{0M}}{3}} \quad (9)$$

Applying the logarithmic function to (9), α_S can be determined:

$$\alpha_S = \alpha_{av} + \frac{1}{(-d - \frac{d^2}{k})} \cdot \ln \frac{N_0 - N_{0G1}}{\frac{N_{0G0}}{1.1} + N_{0S} + \frac{N_{0G2}}{3} + \frac{N_{0M}}{3}} \quad (10)$$

or

$$\alpha_S = \alpha_{av} - \frac{1}{(d + \frac{d^2}{k})} \ln P \tag{11}$$

where

$$P = \frac{N_0 - N_{0G1}}{\frac{N_{0G0}}{1.1} + N_{0S} + \frac{N_{0G2}}{3} + \frac{N_{0M}}{3}} \tag{12}$$

To express the α parameters for the remaining phases, the assumptions made in (6) are considered. Therefore:

$$\begin{cases} \alpha_M = \alpha_{av} + \dfrac{\ln 3 - \ln P}{(d + \frac{d^2}{k})}; \\ \alpha_{G0} = \alpha_{av} - \dfrac{\ln 1.1 - \ln P}{(d + \frac{d^2}{k})}; \\ \alpha_{G1} = \alpha_{av}; \\ \alpha_{G2} = \alpha_M \end{cases} \tag{13}$$

Appendix D. Derivation of the number of cycling stem cells after cell recruitment

Let N_{t0} be the total number of surviving cells after the first dose of radiotherapy but before recruitment. Also, let's consider N_{q0} the number of surviving quiescent cells consisting of both stem and proliferating subgroups, and N_{c0} the number of surviving cycling cells. Thus:

$$N_{t0} = N_{q0} + N_{c0}$$

If q is the percentage of the total number of surviving cells which are in the quiescent phase (G_0), then $N_{q0} = qN_{t0}$.

After radiotherapy, cells are recruited from G_0. Let's consider t_r the percentage of the total number of cells recruited (stem & finitely proliferating). Consequently, the amount of cycling cells will be:

$$N_c = N_{c0} + t_r N_{q0}$$

Consider also that s_r is the percentage of stems recruited. If the total number of stems before recruitment was N_{s0}, then after recruitment the number of cycling stems is changed into:

$$N_s = N_{s0} + s_r t_r q N_{to}$$

Since $N_{s0} = s_0 N_{t0}$, where s_0 is the percentage of cycling stems before recruitment, the above relation can be expressed as:

$$N_s = s_0 N_{t0} + s_r t_r q N_{to}$$

$$\therefore \qquad N_s = (s_0 + s_r t_r q) N_{t0}$$

Example: for $s_0 = 2\%$, $s_r = 4\%$, $t_r = 50\%$ and $q = 85\%$, the total number of cycling stems is $N_s = (2\% + 4\%*50\%*85\%)\ N_{t0} = 3.7\% N_{t0}$.

References

1. Al-Sarraf M, Pajak T, Marcial V, et al. *Concurrent radiotherapy and chemotherapy with cisplatin in inoperable squamous cell carcinoma of the head and neck. An RTOG study*. Cancer 59:259-265, 1987.
2. Andrews PA, Howell SB, Cellular *pharmacology of cisplatin, perspectives on mechanisms of acquired resistance*, Cancer Cells 2:35, 1990.
3. Arias F, Dominguez M, Illarramendi J, et al. *Split hyperfractionated accelerated radiation therapy and concomitant cisplatin for locally advanced head and neck carcinomas: a preliminary report*. Int J Radiat Oncol Biol Phys 33:675-682, 1995.
4. Aroesty, J., Lincoln, T., Shapiro, N., Boccia, G., *Tumour growth and chemotherapy: mathematical methods, computer simulations, and experimental foundations*, Math Biosc. 17:243-300, 1973.
5. Bachaud JM, Chatelut E, Canal P, et al. *Radiotherapy with concomitant continuous cisplatin infusion for unresectable tumors of the upper aerodigestive tract: results of a phase I study*. Am J Clin Oncol 20:1-5, 1997.
6. Bartelink H, Kallman RF, Rapacchietta D, Hart GAM, *Therapeutic enhancement in mice by clinically relevant dose and fractionation schedules of cis-diamminedichloroplatinum (II) and irradiation*. Radiother Oncol 6:61-74, 1985.
7. Bartelink H, Begg A, Martin JC, et al. *Towards prediction and modulation of treatment response.* Radiother Oncol 50:1-11, 1999.
8. Bartelink H, Begg A, Martin JC, et al. *Translational research offers individually tailored treatments for cancer patients*, The Cancer Journal 1:2-10, 2000.
9. Begg AC, *Cisplatin and radiation: interaction probabilities and therapeutic possibilities*, Int J Radiat Oncol Biol Phys. 19:1183-1189, 1990.
10. Begg, A.C., *Cell proliferation in tumours*. In: Steel, G.G. editor, Basic clinical radiobiology, 2nd ed., Oxford University Press, New York, 14-23, 1997.

11. Begg AC, Haustermans K, Hart AAM, et al. *The value of pre-treatment cell kinetic parameters as predictors for radiotherapy outcome in head and neck cancer: a multicenter analysis*. Radiother Oncol 50:13-23, 1999.
12. Biade S, Stobbe CC, Chapman JD, The intrinsic radiosensitivity of some human tumor cells throughout their cell cycles. Radiat. Res. 147:416-421, 1997.
13. Birkhead BG, Gregory WM, Slevin ML, Harvey VJ, *Evaluating and designing cancer chemotherapy treatment using mathematical models,* Eur J Clin Oncol. 22(1):3-8, 1986.
14. Brown JM, *Tumour radiosensitivity: it's the subpopulations that count*. Int. J. Radiat. Oncol. Biol. Phys. 47:549-550, 2000.
15. Choi KN, Rotman M, Aziz H, et al. *Concomitant infusion cisplatin and hyperfractionated radiotherapy for locally advanced nasopharyngeal and paranasal sinus tumors*. Int J Radiat Oncol Biol Phys 39:823-829, 1997.
16. Clamon G, Baatz L, Hoffman H, et al. *Neurotoxicity in a phase I trial of continuous-infusion cisplatin with hyperfractionated radiotherapy for locally advanced head and neck cancer.* Head Neck May/June:236-241, 1996.
17. Coldman AJ, Goldie JH. *Role of mathematical modeling in protocol formulation in cancer chemotherapy*. Cancer Treat Rep 69:1041-1045, 1985.
18. Coughlin CT, Richmond RC. *Biologic and clinical developments of cisplatin combined with radiation: concepts, utility, projections for new trials, and the emergence of carboplatin.* Semin Oncol 16: 31S -43S, 1989.
19. Creagan E, O'Fallon J, Woods J, et al. *Cis-diamminedichloroplatinum (II) administered by 24-hour infusion in the treatment of patients with advanced upper aerodigestive cancer.* Cancer 51:2020-2023, 1983.
20. Crissman J, Pajak T, Zarbo R, et al. *Improved response and survival to combined cisplatin and radiation in non-keratinized squamous cell carcinoma of the head and neck. An RTOG study of 114 advanced stage tumors.* Cancer 59:1397, 1987.
21. Davis AJ, Tannock IF, Repopulation of tumour cells between cycles of chemotherapy: a neglected factor, Lancet Oncol. 1:86-93, 2000.

22. de Graeff A, Slebos RJ, Rodenhuis S. *Resistance to cisplatin and analogues: mechanisms and potential clinical implications*. Cancer Chemother Pharmacol 22:325-332, 1988.
23. Denham J, Walker Q, Lamb D, Hamilton C *et al, Mucosal regeneration during radiotherapy,* Radiother. Oncol. 41:109-118, 1996.
24. Dewit L, Oussoren Y, Bartelink H, *Dose and time effects of cis-diamminedichloroplatinum (II) and radiation on mouse duodenal crypts*. Radiother Oncol 4:363-371, 1985.
25. Dewit L, *Combined treatment of radiation and cis-diamminedichloroplatinum (II): a review of experimental and clinical data,* Int J Radiat Oncol Biol Phys 13:403-426, 1987.
26. Dillehay LE, *A model of cell killing by low-dose-rate radiation including repair of sublethal damage, G_2 block and cell division.* Radiat. Res. 124:201-207, 1990.
27. Donaghey, C.E., *Cell cycle simulation made easy*, Int Rew Cytol. 66:171-211, 1980.
28. Dorie MJ, Kovacs MS, Gabalski EC, et al. *DNA damage measured by the comet assay in head and neck cancer patients treated with tirapazamine*. Neoplasia 1:461-467, 1999.
29. Dörr W, *Three A's of repopulation during fractionated irradiation of squamous epithelia: Asymmetry loss, Acceleration of stem-cell divisions and Abortive divisions*, Int. J. Radiat. Biol. 72:635-643, 1977.
30. Douple EB, Richmond RC, *A review of platinum complex biochemistry suggests a rationale for combined platinum-radiotherapy,* Int J Radiat Oncol Biol Phys. 5:1335-1339, 1979.
31. Douple EB, Richmond RC, *Radiosensitization of hypoxic tumour cells by cis- and trans-dichlorodiammineplatinum (II),* Int J Radiat Oncol Biol Phys 5:1369-1372, 1979.
32. El-Kareh AW, Secomb TW, *A mathematical model for cisplatin cellular pharmacodynamics,* Neoplasia 5(2):161-169, 2003.
33. Elkind MM, Redpath L, *Molecular and cellular biology of radiation lethality*. In: Becker, Ed. Cancer, vol 6. New York: Plennum Press: 51-99, 1977.

34. Ferguson PJ, Currie C, Vincent MD. *Enhancement of platinum-drug cytotoxicity in a human head and neck squamous cell carcinoma line and its platinum-resistant variant by liposomal amphotericin B and phospholipase A2-II.* Mol Pharmacol 27:1399-1405, 1999.

35. Fontanesi J, Beckford NS, Lester EP, et al. *Concomitant cisplatin and hyperfractionated external beam irradiation for advanced malignancy of the head and neck.* Am J Surg 162:393-396, 1991.

36. Fountzilas G, Skarlos D, Kosmidis P, et al. *Radiation therapy and concurrent cisplatin administration in locally advanced head and neck cancer. A Hellenic co-operative oncology group study*. Acta Oncol 33(7):825-830, 1994.

37. Gasparini G, Pozza F, Recher G, et al. *Simultaneous cis-platinum and radiotherapy in inoperable or locally advanced squamous cell carcinoma of the head and neck.* Oncology 48:270-276, 1991.

38. Glaser MG, Leslie MD, O'Reilly SM, et al. *Weekly cisplatinum concomitant with radical radiotherapy in the treatment of advanced head and neck cancer*. Clin Oncol 5:286-289, 1993.

39. Glynne-Jones R, Sebag-Montefiore D. *Chemoradiation schedules – what radiotherapy?* Eur J Cancer 38:258-269, 2002.

40. Go SR, Adjei AA, *Review of the comparative pharmacology and clinical activity of cisplatin and carboplatin*, J Clin Oncol. 17(1):409-422, 1999.

41. Goldie JH, Coldman AJ, *A mathematic model for relating the drug sensitivity of tumours to their spontaneous mutation rate*, Cancer Treat Rep 63:1727, 1979.

42. Goldie JH, Coldman AJ, Ng V, Hopkins HA, et al A mathematical and computer-based model of alternating chemotherapy and radiation therapy in experimental neoplasm, Antibiot Chemother, 41:11-20, 1988.

43. Gyllenberg, M., Webb, G.F., *Quiescence as an explanation of Gompertzian tumour growth,* Growth Dev Aging. 53(1-2):25-33, 1989.

44. Gyllenberg, M., Webb, G.F., *A nonlinear structured population model of tumour growth with quiescence*, J Math Biol. 28(6):671-94, 1990.

45. Hall, E.J., *Radiobiology for the radiologist*, 5th ed., Lippincott Williams & Wilkins, 382-386, 2000.

46. Hansen O, Grau C, Bentzen S, Overgaard J, *Repopulation in the SCCVII squamous cell carcinoma assessed by an in vivo-in vitro excision assay*, Radiother. Oncol. 39:137-144, 1996.

47. Harari PM, Mehta MP, Ritter MA, Petereit DG, *Clinical promise tempered by reality in the delivery of combined chemoradiation for common solid tumours*, Sem Radiat Oncol. 13(1):3-12, 2003.

48. Harrison L, Pfister D, Fass D, et al. *Concomitant chemotherapy-radiation therapy followed by hyperfractionated radiation therapy for advanced unresectable head and neck cancer*. Int J Radiat Oncol Biol Phys 21:703-708, 1991.

49. Hoglmeier F, Kummermehr J, Trott KR, *Effect of a combination therapy of cisplatin and local irradiation on a mouse fibrosarcoma*. Strahlentherapie 161: 362-366, 1985.

50. Hopewell JW, Nyman J, Turesson I, *Time factor for acute tissue reactions following fractionated irradiation: a balance between repopulation and enhanced radiosensitivity.* Int. J Radiat. Biol. 79:513-524, 2003.

51. Huguenin P, Glanzmann C, Taussky D, et al. *Hyperfractionated radiotherapy and simultaneous cisplatin for stage-III and –IV carcinomas of the head and neck. Long-term results including functional outcome*. Strahlenther Onkol 174:397-402, 1998.

52. Jacobs C, Bertino JR, Goffinet DR, et al. *24-hour infusion of cis-platinum in head and neck cancers.* Cancer 42:2135-2140, 1978.

53. Jakobsen A, Mortensen LS. *On the importance of sensitivity to the dose-effect relationship in chemotherapy*. Acta Oncol 36:375-381, 1997.

54. Jeremic B, Shibamoto Y, Stanisavljevic B, et al. *Radiation therapy alone or with concurrent low-dose daily either cisplatin or carboplatin in locally advanced unresectable squamous cell carcinoma of the head and neck: a prospective randomized trial.* Radiother Oncol 43:29-37, 1997.

55. Jeremic B, Shibamoto Y, Milicic B, et al. *Hyperfractionated radiation therapy with or without concurrent low-dose daily cisplatin in locally advanced squamous cell carcinoma of the head and neck: a prospective randomized trial.* J Clin Oncol 18:1458-1464, 2000.

56. Joschko MA, Webster LK, Bishop JF, Groves J et al, *Radioenhancement by cisplatin with accelerated fractionated radiotherapy in a human tumour xenograft,* Cancer Chemother Pharmacol. 40:534-539, 1997.

57. Kallman RF, Bedarida G, Rapacchietta D, *Experimental studies on schedule dependence in the treatment of cancer with combinations of chemotherapy and radiotherapy.* In Radiotherapy/chemotherapy interactions in cancer therapy, edited by J.L. Meyer and J.M. Vaeth, Basel: Karger, 1992.

58. Kanazawa H, Rapacchietta D, Kallman RF, *Schedule-dependent therapeutic gain from the combination of fractionated irradiation and cis-diammine-dichloroplatinum in C3H/Km mouse model system.* Cancer Res 48: 3158-3164, 1988.

59. Korbelik M, Skov KA, *Inactivation of hypoxic cells by cisplatin and radiation at clinically relevant doses.* Radiat Res 119:145-156, 1989.

60. Kummermehr, J.C., *Tumour stem cells - the evidence and the ambiguity,* Acta Oncol. 40(8):981-988, 2001.

61. Lartigau E, Stern S, Guichard M. *In vitro oxygen-dependent survival of 2 human cell lines after radiation combined with tirapazamine and cisplatin.* Cancer Radiother 4:217-222, 2000.

62. Lawrence TS, Blackstock AW, McGinn C, *The mechanism of action of radiosensitization of conventional chemotherapeutic agents,* Sem Radiat Oncol. 13(1):13-21, 2003.

63. Leipzig B. *Cisplatin sensitization to radiotherapy of squamous cell carcinomas of the head and neck.* Am J Surg 146:462-465, 1983.

64. Levasseur LM, Slocum HK, Rustum YM, Greco WR, *Modeling of the time-dependency of in vitro drug cytotoxicity and resistance,* Cancer Res. 58(24):5749-5761, 1998.

65. Lippert B (ed), *Cisplatin – chemistry and biochemistry of a leading anticancer drug,* Wiley-VCH, Zürich, 1999.

66. Malaise EP, Fertil B, Chavaudra N, Guichard M, *Distribution of radiation sensitivities for human tumor cells of specific histological types: Comparison of in vitro to in vivo data.* Int. J. Radiat. Oncol. 12:617-624, 1986.

67. Marcial V, Pajak T, Mohiuddin M, et al. *Concomitant cisplatin chemotherapy and radiotherapy in advanced mucosal squamous cell carcinoma of the head and neck.* Cancer 66:1861-1868, 1990.

68. Marcu L, van Doorn T, Zavgorodni S, et al. *Growth of a virtual tumour using probabilistic methods of cell generation.* Australas Phys Eng Sci Med 25:155-161, 2002.

69. Marcu L, van Doorn T, Olver I, *Cisplatin and radiotherapy in the treatment of locally advanced head and neck cancer,* Acta Oncol. 42(4):315-325, 2003.

70. Marcu L, van Doorn T, Olver I, Modelling of post irradiation accelerated repopulation in squamous cell carcinomas, Phys Med Biol. 49:3767-3779, 2004.

71. Nakamoto S, Mitsuhashi N, Takahashi T, Sakurai H, Niibe H, *An interaction of cisplatin and radiation in two rat yolk sac tumour cell lines with different radiosensitivities in vitro.* Int J of Radiat Biol, 70:747-753, 1996.

72. National Cancer Institute board of scientific advisors. Report of National cancer Institute clinical trials implementation committee, Bethesda, USA.

73. Nias AHW, *An introduction to radiobiology*. Wiley, England, 2000.

74. Ormerod MG, O'Neill C, Robertson D, Kelland LR et al: *cis-Diamminedichloroplatinum(II)-induced cell death through apoptosis in sensitive and resistant human ovarian carcinoma cell lines,* Cancer Chemother Pharmacol. 37:463-471, 1996.

75. Overgaard J, Khan AR, *Selective enhancement of radiation response in a C3H mammary carcinoma by cisplatin*. Cancer Treat Rep 65:501-503, 1981.

76. Perez RP. *Cellular and molecular determinants of cisplatin resistance*. Eur J Cancer 34:1535-1542, 1998.

77. Peters L, Withers HR, Thames HD, et al. *The problem: tumor radioresistance in clinical radiotherapy*. Int J Radiat Oncol Biol Phys 8:101-108, 1982.

78. Peters L, Withers HR. *Applying radiobiological principles to combined modality treatment of head and neck cancer-the time factor.* Int J Radiat Oncol Biol Phys 39:831-836, 1997.

79. Planting AS, de Mulder PH, de Graeff A, et al. *Phase II study of weekly high-dose cisplatin for six cycles in patients with locally advanced squamous cell carcinoma of the head and neck.* Eur J Cancer 33:61-65, 1997.

80. Prestayko AW, Crooke ST, Carter SK. *Cisplatin – current status and new developments*. Academic Press 1980.

81. Reed E, Kohn KW, *Platinum analogues*, in Chabner B, Collins JM (ed): Cancer chemotherapy-principles and practice. Philadelphia: Lippincott, 1990.

82. Retsky, M.W., Swartzendruber, D.E., Wardwell, R.H., Bame, P.D., *Is Gompertzian or exponential kinetics a valid description of individual human cancer growth?* Med Hypotheses. 33(2):95-106, 1990.

83. Reya, T., Morrison S.J., Clarke M.F., Weissman I.L., *Stem cells, cancer, and cancer stem cells*, Nature 414:105-111, 2001.

84. Rischin D, Peters L, Hicks R, Hughes P et al. *Phase I trial of concurrent tirapazamine, cisplatin, and radiotherapy in patients with advanced head and neck cancer*. J Clin Oncol. 19(2):535-42, 2001.

85. Robbins KT, Storniolo AM, Hryniuk WM, et al. *"Decadose" effects of cisplatin on squamous cell carcinoma of the upper aerodigestive tract. II Clinical studies.* Laryngoscope 106:37-42, 1996.

86. Robbins KT, Kumar P, Regine W, et al. *Efficacy of targeted supradose cisplatin and concomitant radiation therapy for advanced head and neck cancer: The Memphis experience*. Int J Radiat Oncol Biol Phys 38:263-271, 1997.

87. Roberts JJ, Knox RJ, Pera MF, Friedlos F, et al. *The role of platinum-DNA interactions in the cellular toxicity and anti-tumour effects of platinum coordination compounds.* In: Nicolini M, Ed. Platinum and other metal coordination compounds in cancer chemotherapy, Boston: 16-31, 1988.

88. Rosenberg B, Van Camp L, Krigas T., *Inhibition of cell division in Escherichia Coli by electrolysis products from a platinum electrode,* Nature 205:698, 1965.

89. Sako K, Razack MS, Kalnins I. *Chemotherapy for advanced and recurrent squamous cell carcinoma of the head and neck with high and low dose cis-diamminedichloroplatinum.* Am J Surg 136:529-533, 1978.

90. Schellens JH, Ma J, Planting AS, van der Burg ME et al, *Relationship between the exposure to cisplatin, DNA-adduct formation in leucocytes and tumour response in patients with solid tumours*, Br J Cancer. 73(12):1569-1575, 1996.

91. Schwachöfer JH, Crooijmans RP, Hoogenhout J, Kal HB et al *Effectiveness in inhibition of recovery of cell survival by cisplatin and carboplatin: influence of treatment sequence*, Int J Radiat Oncol Biol Phys, 20:1235-1241, 1991.

92. Serin M, Erkal HS, Cakmak A. *Radiation therapy and concurrent cisplatin in management of locoregionally advanced nasopharyngeal carcinomas.* Acta Oncol 38:1031-1035, 1999.

93. Sharma VM, Wilson WR, *Radiosensitization of advanced squamous cell carcinoma of the head and neck with cisplatin during concomitant radiation therapy*, Eur Arch Otorhinolaryngol 256(9):462-465, 1999.

94. Sinclair WK, *Dependence of radiosensitivity upon cell age.* In Proceedings of the Carmel Conference on Time and Dose relationships in Radiation Biology as Applied to Radiotherapy, pp 97-107. BNL Report 50203. Upton, NY, 1969.

95. Slotman GJ, Cummings FJ, Glicksman AR, Doolittle CL, et al, Preoperative simultaneously administered cis-platinum plus radiation therapy for advanced squamous cell carcinoma of the head and neck. Head Neck Surg, 8:159-164, 1986.

96. Sorenson CM, Eastman A. *Influence of cis-diamminedichloroplatinum (II) on DNA synthesis and cell cycle progression in excision repair proficient and deficient Chinese hamster ovary cells*. Cancer Res 48: 6703-6707, 1988.

97. Sorenson CM, Eastman A. *Mechanism of cis-diamminedichloroplatinum (II)-induced cytotoxicity: role of G2 arrest and DNA double-strand breaks.* Cancer Res 48: 4484-4488, 1988.

98. Sorenson CM, Barry MA, Eastman A. *Analysis of events associated with cell cycle arrest at G2 phase and cell death induced by cisplatin*. J Natl Cancer Inst 82:749-754, 1990.

99. Steel, G.G., *The growth kinetic of tumours*, Oxford University Press, Oxford, 1977.

100. Steel GG, *The search for therapeutic gain in the combination of radiotherapy and chemotherapy*, Radiother Oncol 11:31-53, 1988.
101. Steel GG, *Principles for the combination of radiotherapy and chemotherapy*. In Combined radiotherapy and chemotherapy in clinical oncology, edited by A. Horwich Oxford University Press, Canada, 1992.
102. Steel, G.G., *The growth rate of tumours*. In: Steel, G.G. editor, Basic clinical radiobiology, 2nd ed., Oxford University Press, New York, 8-13, 1997.
103. Sun JR, Brown JM, *Lack of differential radiosensitization of hypoxic cells in a mouse tumor at low radiation doses per fraction by cisplatin*. Radiat Res 133: 252-256, 1993.
104. Swan, G.W., *Role of optimal control theory in cancer chemotherapy*, Math Biosc. 101:237-284, 1990.
105. Tannock, I.F., Hill, R.P., *The basic science of oncology*, 2nd ed., McGraw-Hill, 155-176, 1992.
106. Tannock, I.F., Hill, R.P., *The basic science of oncology*, 3rd ed., McGraw-Hill, 135-165, 1998.
107. Trimmer EE, Essigmann JM, *Cisplatin*, Essays Biochem 34:191-211, 1999.
108. Trott K, Kummermehr J, *Accelerated repopulation in tumours and normal tissues*, Radiother. Oncol. 22:159-160, 1991.
109. Trott K, *The mechanisms of acceleration of repopulation in squamous epithelia during daily irradiation* Acta Oncol. 38 153-157, 1999.
110. Trotti A. *Update on toxicity in head and neck cancer: mechanism, grading,interventions*.Http://www.medscape.com/Medscape/oncology/TreatmentUpdate/2000/tu04/tu04-02.html
111. Tubiana M., *The growth and progression of human tumours: implications for management strategy*, Radiother Oncol. 6:167-184, 1986.
112. Tubiana M, *Repopulation in human tumours*, Acta Oncol. 27:83-88, 1988.
113. Turesson I, Carlsson J, Brahme A, Glimelius B *et al*, *Biological response to radiation therapy* Acta Oncol. 42:92-106, 2003.

114. Vermorken JB, Kapteijn TS, Hart AA, et al. *Ototoxicity of cis-diamminedichloroplatinum (II): influence of dose, schedule and mode of administration.* Eur J Cancer Clin Oncol 19: 53-58, 1983.
115. Veronesi A, Zagonel V, Tirelli U, et al. *High-dose versus low-dose cisplatin in advanced head and neck squamous carcinoma: a randomized study.* J Clin Oncol 3:1105-1108, 1985.
116. Vikram B, Strong EW, Shah J.P., et al. *Failure at distant sites following multimodality treatment for advanced head and neck cancer,* Head Neck Surg. 6:730-733, 1984.
117. von der Maase H, *Complications of combined radiotherapy and chemotherapy,* Sem Rad Oncol 4:81-94, 1994.
118. Wallner KE, Li GC. *Effect of cisplatin resistance on cellular radiation response.* Int J Radiat Oncol Biol Phys 13:587-591, 1987.
119. Weldon T, *Mathematical Models in Cancer Research,* Institute of Physics Publishing, Bristol and Philadelphia, 1988.
120. Welters MJP, Fichtinger-Shepman AM, Baan RA, Hermsen MA, van der Vijgh et al, *Relationship between the parameters cellular differentiation, doubling time and platinum accumulation and cisplatin sensitivity in a panel of head and neck cancer cell lines,* Int J Cancer 71:410-415, 1997.
121. Welters MJ, Fichtinger-Shepman AM, Baan RA, Jacobs-Bergmans AJ, et al, *Pharmacodynamics of cisplatin in human head and neck cancer: correlation between platinum content, DNA adduct levels and drug sensitivity in vitro and in vivo,* Br J Cancer 79:82-88, 1999.
122. Wheldon, T.E., *Mathematical models in cancer research,* Adam Hilger Publ., Philadelphia, 1988.
123. Wigg DR, *Applied radiobiology and bioeffect planning,* PhD thesis, Royal Adelaide Hospital, 2000.
124. Withers HR, Elkind MM, *Radiosensitivity and fractionation response of crypt cells of mouse jejunum.* Radiat Res 38:598-613, 1969.
125. Withers HR, Taylor JMG, Maciejewski B. *The hazard of accelerated tumor clonogen repopulation during radiotherapy.* Acta Oncol 27:131-146, 1988.

126. Withers HR, *Treatment-induced accelerated human tumour growth*, Semin. Radiat. Oncol. 3:135-143, 1993.

127. Yoshikawa A, Saura R, Matsubara T, et al. *A mechanism of cisplatin action: antineoplastic effect through inhibition of neovascularization*. Kobe J Med Sci 43:109-120, 1997.

128. Zaider M, Wuu CS, Minerbo GN, *The combined effects of sublethal damage repair, cellular repopulation and redistribution in the mitotic cycle. I. Survival probabilities after exposure to radiation.* Radiat. Res. 145:457-466, 1996.

129. Zak M, Drobnik J, *Effects of cis-dichlorodiammineplatinum (II) on the post irradiation lethality in mice after irradiation with X rays*, Strahlentherapie 142:112-115, 1971.